



저작자표시-비영리-변경금지 2.0 대한민국

이용자는 아래의 조건을 따르는 경우에 한하여 자유롭게

- 이 저작물을 복제, 배포, 전송, 전시, 공연 및 방송할 수 있습니다.

다음과 같은 조건을 따라야 합니다:



저작자표시. 귀하는 원저작자를 표시하여야 합니다.



비영리. 귀하는 이 저작물을 영리 목적으로 이용할 수 없습니다.



변경금지. 귀하는 이 저작물을 개작, 변형 또는 가공할 수 없습니다.

- 귀하는, 이 저작물의 재이용이나 배포의 경우, 이 저작물에 적용된 이용허락조건을 명확하게 나타내어야 합니다.
- 저작권자로부터 별도의 허가를 받으면 이러한 조건들은 적용되지 않습니다.

저작권법에 따른 이용자의 권리는 위의 내용에 의하여 영향을 받지 않습니다.

이것은 [이용허락규약\(Legal Code\)](#)을 이해하기 쉽게 요약한 것입니다.

[Disclaimer](#)

이 학 박 사 학 위 논 문

Studies on Cyclopolymerization of Diynes
with Unprecedented Regioselectivity and
Ring Size Using Ruthenium-Based Olefin
Metathesis Catalysts

루테늄 기반의 올레핀 복분해 촉매를 이용한
특이한 위치선택성과 고리 크기를 생성하는
다이하인의 고리화 중합에 관한 연구

2019년 2월

서울대학교 대학원

화학부 유기화학 전공

정 기 정

Abstract

Studies on Cyclopolymerization of Diynes with Unprecedented Regioselectivity and Ring Size Using Ruthenium–Based Olefin Metathesis Catalysts

Kijung Jung

Department of Chemistry

The Graduate School

Seoul National University

Cyclopolymerization (CP) of terminal diynes via olefin metathesis is a powerful method for preparing conjugated polymers containing cycloalkene repeat units. In this reaction, a metal carbene catalyst can react with a terminal alkyne in both manner of α - and β -additions. Extensive studies on CP using Ru-based olefin metathesis catalysts have shown that Grubbs type catalysts promote CP with exclusive α -addition, rather than β -addition. Although some attempts were made to rationalize this strong regioselectivity, there is currently no theory that allows for understanding the regiocontrol in CP based on intuitive guiding principles.

This research describes the β -selective CP of 1,6-heptadiynes with comprehensive investigations on the determining factors for the regioselectivity of Ru-based olefin metathesis catalysts.

Chapter 2 describes the first example of a β -selective addition to alkynes using Grubbs Z -selective catalyst. We found that this catalyst promoted the CP of 1,6-heptadiyne derivatives to give conjugated polyenes containing a six-membered ring as a major repeat unit. Through a model study using ring-closing enyne metathesis, we proposed a stereochemical model for the unprecedented selectivity.

Chapter 3 demonstrates a perfect regiocontrol for β -selective CP using a Ru dithiolate catalyst with a broader monomer scope and improved reaction efficiency. By elucidating the origin of the regioselectivity in CP using a conceptual theory based on electrophilic Fischer carbene model, we achieved excellent β -selectivity. Furthermore, the use of weakly coordinating ligands as additives led to improved polymerization efficiency, by stabilizing the propagating carbene.

Chapter 4 addresses the living β -selective CP using Ru dithiolate catalysts. Rational engineering of the steric factor on monomer or catalyst structures enabled the synthesis of PAs with controlled molecular weight and narrow dispersity, as well as the successful diblock and triblock copolymerizations. Observation on the propagating carbene revealed the effect of the pyridine additives with various binding affinities.

Chapter 5 shows the CP of 1,5-hexadiynes to prepare the conjugated polyenes containing four-membered rings as a repeat unit. Extensive screening of the monomers and catalytic systems enabled the incorporation of four-membered rings into the main chain of PAs, which is the first example for Ru catalyst system.

Key words : Cyclopolymerization, Polyacetylene, Grubbs catalyst, Ru alkylidene, Regioselective polymerization, Living polymerization

Student Number : 2013-20281

Table of Contents

Abstract	1
Table of Contents	4

Chapter 1. Introduction

1.1 Research Background	8
1.2 Thesis Research	13
1.3 References	14

Chapter 2. Highly β -Selective Ring-Closing Enyne Metathesis and Cyclopolymerization of 1,6-Heptadiyne Derivatives Using Grubbs *Z*-Selective Catalyst

2.1 Abstract	18
2.2 Introduction	19
2.3 Results and Discussion	21
2.4 Conclusion	36
2.5 Experimental Section	37
2.6 Supporting Information	45
2.7 References	56

Chapter 3. Toward Perfect Regiocontrol for β -Selective Cyclopolymerization of 1,6-Heptadiyne Derivatives Using a Ru Dithiolate Catalyst

3.1 Abstract	60
3.2 Introduction	61
3.3 Results and Discussion	63
3.4 Conclusion	78
3.5 Experimental Section	79
3.6 Supporting Information	86
3.7 References	94

Chapter 4. Living β -Selective Cyclopolymerization of 1,6-Heptadiyne Derivatives Using Ru Dithiolate Catalysts

4.1 Abstract	97
4.2 Introduction	98
4.3 Results and Discussion	100
4.4 Conclusion	120
4.5 Experimental Section	121
4.6 Supporting Information	128
4.7 References	152

Chapter 5. Cyclopolymerization of 1,5-Hexadiyne Derivatives to Form Four-Membered Rings

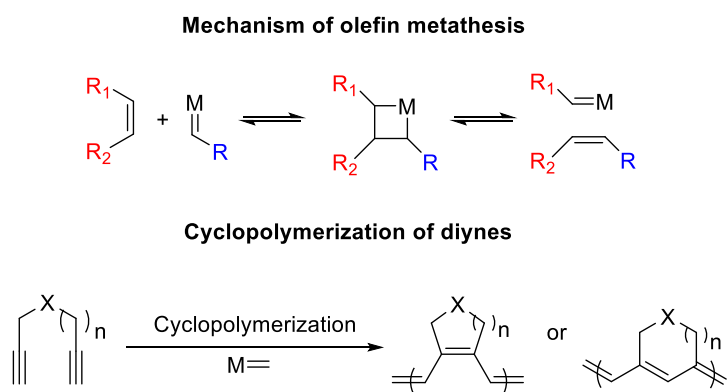
5.1 Abstract	154
5.2 Introduction	154
5.3 Results and Discussion	156
5.4 Conclusion	165
5.5 References	165
 Abstract (Korean)	 167

Chapter 1. Introduction

1.1 Research Background

Olefin metathesis

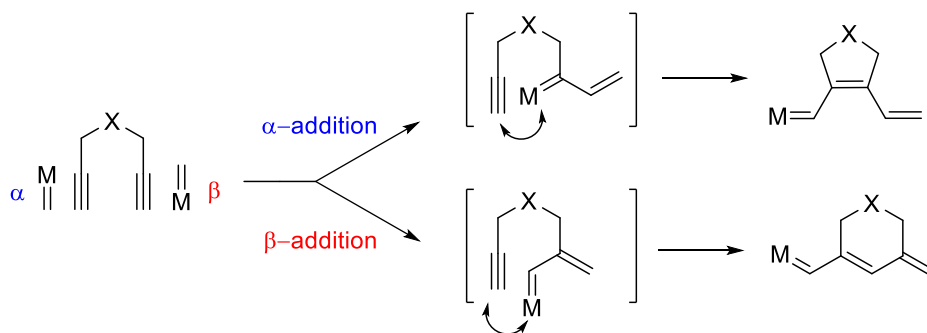
Olefin metathesis ('metathesis' from the Greek meaning 'change of position, transposition') rearranges the carbon atoms of two C=C bonds, generating two new ones (Scheme 1.1).¹ This process plays a prominent role in the development of useful synthetic transformations because of their mildness, high atom economy, and tolerance of functional groups. Although olefin metathesis can be classified into three main variations; ring-opening metathesis (ROM),² ring-closing metathesis (RCM),³ and cross-metathesis (CM),⁴ but the utility of olefin metathesis has been expanded to polymer chemistry, such as in ring-opening metathesis polymerization (ROMP)⁵ and cyclopolymerization (CP).⁶



Scheme 1.1 Olefin metathesis and cyclopolymerization (CP)

Cyclopolymerization

Cyclopolymerization (CP) of diynes using olefin metathesis reaction is a chain-growth polymerization forming conjugated polyacetylene (PA) containing cycloalkene repeat units (Scheme 1.1).⁶ The conjugated polymers obtained by CP are highly stable in air, and soluble in common organic solvents depending on their side chains. These properties make the polymers have the potential for use in organic electronics and optics.⁷ Studies on CP, using many transition-metal catalyst systems, have been conducted for more than three decades, and successfully prepared various functionalized PAs exerting high processability and enhanced properties, with controlled molecular weight and narrow dispersity (\mathcal{D}).⁸



Scheme 1.2 Regioselectivity for CP of 1,6-heptadiynes

Precisely controlling the regiochemistry in CP is challenging, because it is difficult for the catalyst to discriminate between the α - and β -positions of a terminal alkyne substrate, such as 1,6-heptadiyne. As highlighted in Scheme 1.2, the α -addition of the metal carbene to alkynes results in conjugated polymers containing five-membered rings, whereas the β -addition gives six-membered rings. In early days, ill-defined catalysts such as Ziegler–Natta,^{7a, 9} MoCl_5 , and WCl_6 catalysts¹⁰ showed no selectivity and produced regiorandom polyenes with mixtures of five- and six-membered rings.⁹ The development of well-defined Mo catalysts from the Schrock¹¹ and Buchmeiser¹² group enabled investigation on mechanisms of CP and polymer microstructures, demonstrating a regioselective living CP (Figure 1.1). Subsequently, the Buchmeiser group successfully achieved CP in an exclusively α -selective fashion, employing Ru catalysts by modifying air- and moisture-stable Hoveyda–Grubbs catalyst with electron-withdrawing groups (Figure 1.1).^{7d, 13}

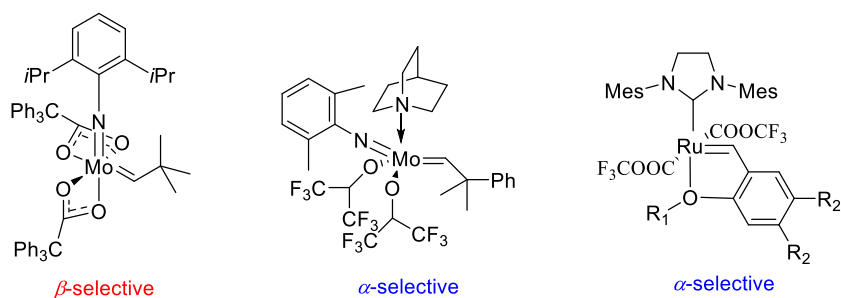


Figure 1.1 Schrock catalysts and Buchmeiser catalysts for regioselective CP

Later, our group reported highly efficient, α -selective living CP of 1,6-

heptadiyne derivatives using a fast-initiating third-generation Grubbs catalyst¹⁴ (**GI**, Figure 1.2) both in THF¹⁵ and DCM, by the aid of 3,5-dichloropyridine stabilizing the propagating species.¹⁶ Particularly in DCM, we discovered that lower reactivity in DCM was due to lower propagating carbene stability¹⁶ and competing [2+2+2] cycloaddition.¹⁷ We also demonstrated α -selective CP using a Grubbs 1st generation catalyst (**GI**, Figure 1.2), which is relatively less reactive toward CP than the catalysts containing *N*-heterocyclic carbene (NHC) ligands, by employing benzoic acid and sodium benzoate additives.¹⁸

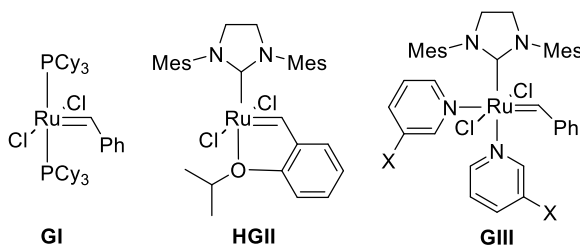


Figure 1.2 Ru-based Grubbs catalysts

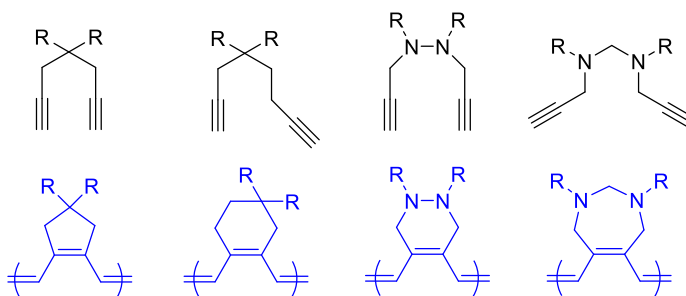


Figure 1.3 Various diyne monomers and the corresponding polymers generated by α -selective CP

As shown in Figure 1.3, we broadened the scope of monomers for CP, by

designing various 1,7-octadiynes¹⁹ and 1,8-nonadiynes²⁰ to successfully generate the conjugated polyenes containing six- and seven-membered ring repeat units, respectively. A limitation entailing with these monomers was slow polymerization rate due to longer distance between two alkynes compared to 1,6-heptadiynes. In 1,7-octadiyne case, this problem was solved by increasing the number and size of the substituents at the 4,4-^{19a, 19b} or 4,5-position of the side chains,^{19c} by the enhanced Thorpe-Ingold effect. We achieved the controlled CP of 1,7-octadiynes by using **GIII**, and living polymerization by the introduction of hydrazide group having a short C-N bond and enhanced Thorpe-Ingold effect.^{19d} Furthermore, we reported a CP of 1,8-nonadiyne derivatives to generate new conjugated PAs containing seven-membered ring repeat unit via α -addition by the introduction of amination and acetal groups.²⁰

Extensive studies on CP using Ru-based olefin metathesis catalysts have shown that Grubbs type catalysts promote CP with exclusive α -addition, rather than β -addition. Although some attempts were made to rationalize this strong regioselectivity,²¹ there is currently no theory that allows for understanding the regiocontrol in CP based on intuitive guiding principles.

1.2 Thesis Research

As there had been no investigations in β -selective CP since the last reports 20 years ago from Schrock's group using Mo catalysts, we became interested in tuning the regioselectivity toward β -addition to form six-membered rings in the polymer backbone using Ru catalysts. This research describes the β -selective CP of 1,6-heptadiynes with comprehensive investigations on the determining factors for the regioselectivity of Ru catalysts.

Chapter 2 describes the first example of a β -selective addition to alkynes in the Ru catalysts system, using Grubbs *Z*-selective catalyst. We found that this catalyst promoted the CP of 1,6-heptadiyne derivatives to give conjugated polyenes containing a six-membered ring as a major repeat unit. Through a model study using ring-closing enyne metathesis, we proposed a stereochemical model for the unprecedented selectivity.

Chapter 3 demonstrates a perfect regiocontrol for β -selective CP using a Ru dithiolate catalyst with a broader monomer scope and improved reaction efficiency. By elucidating the origin of the regioselectivity in CP using a conceptual theory based on electrophilic Fischer carbene model, we achieved excellent β -selectivity in CP. Furthermore, the use of weakly coordinating ligands as additives led to improved polymerization efficiency, by stabilizing the propagating carbene.

Chapter 4 addresses the living β -selective CP using Ru dithiolate catalysts. Rational engineering of the steric factor on monomer or catalyst structures enabled the synthesis of PAs with controlled molecular weight and narrow

dispersity (\mathcal{D}), as well as the successful diblock and triblock copolymerizations. Observation on the propagating carbene revealed the effect of the pyridine additives with various binding affinities.

Chapter 5 shows the CP of 1,5-hexadiynes to prepare the conjugated polyenes containing four-membered ring as a repeat unit. Extensive screening of the monomers and catalytic systems enabled the incorporation of four-membered rings into the main chain of PAs, which is the first example for Ru catalyst system.

1.3 References

1. (a) Grubbs, R. H.; Chang, S., *Tetrahedron* **1998**, *54*, 4413; (b) Fürstner, A., *Angew. Chem., Int. Ed.* **2000**, *39*, 3012; (c) Grubbs, R. H., *Tetrahedron* **2004**, *60*, 7117.
2. Buchmeiser, M. R., *Chem. Rev.* **2000**, *100*, 1565.
3. Grubbs, R. H.; Miller, S. J.; Fu, G. C., *Acc. Chem. Res.* **1995**, *28*, 446.
4. Schuster, M.; Blechert, S., *Angewandte Chemie International Edition in English* **1997**, *36*, 2036.
5. Novak, B. M.; Grubbs, R. H., *J. Am. Chem. Soc* **1988**, *110*, 960.
6. Choi, S. K.; Gal, Y. S.; Jin, S. H.; Kim, H. K., *Chem. Rev.* **2000**, *100*, 1645.
7. (a) Gibson, H. W.; Bailey, F. C.; Epstein, A. J.; Rommelmann, H.; Kaplan, S.; Harbour, J.; Yang, X. Q.; Tanner, D. B.; Pochan, J. M., *J. Am. Chem. Soc.* **1983**, *105*, 4417; (b) Samuel, I. D. W.; Ledoux, I.; Dhenaut, C.; Zyss, J.; Fox, H. H.; Schrock, R. R.; Silbey, R. J., *Science* **1994**, *265*, 1070; (c) Gal, Y. S.; Jin, S. H.; Choi, S. K., *J. Mol. Catal. A: Chem.* **2004**, *213*, 115; (d) Vygodskii, Y. S.; Shaplov,

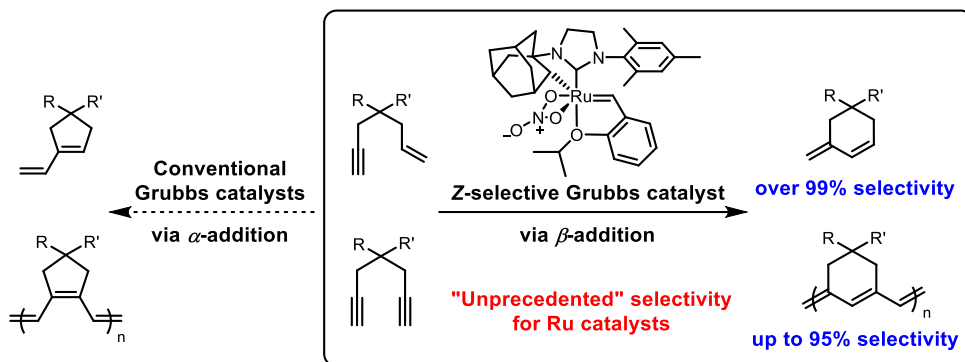
- A. S.; Lozinskaya, E. I.; Vlasov, P. S.; Malyshkina, I. A.; Gavrilova, N. D.; Kumar, P. S.; Buchmeiser, M. R., *Macromolecules* **2008**, *41*, 1919; (e) Sudheendran, M.; Horecha, M.; Kiriya, A.; Gevorgyan, S. A.; Krebs, F. C.; Buchmeiser, M. R., *Polym. Chem.* **2013**, *4*, 1590; (f) Guo, M.; Sun, R.; Han, H.; Wu, J.; Xie, M.; Liao, X., *Macromolecules* **2015**, *48*, 2378; (g) Wang, J.; Li, H.; Liao, X.; Xie, M.; Sun, R., *Polym. Chem.* **2016**, *7*, 4912; (h) Wu, J.; Li, H.; Zhou, D.; Liao, X.; Xie, M.; Sun, R., *J. Polym. Sci. A* **2017**, *55*, 485; (i) Li, H.; Wang, J.; Han, H.; Wu, J.; Xie, M., *React. Funct. Polym.* **2018**, *127*, 20.
8. Buchmeiser, M. R., *Polym. Rev.* **2017**, *57*, 15.
 9. Stille, J. K.; Frey, D. A., *J. Am. Chem. Soc.* **1961**, *83*, 1697.
 10. (a) Kim, Y. H.; Gal, Y. S.; Kim, U. Y.; Choi, S. K., *Macromolecules* **1988**, *21*, 1991; (b) Ryoo, M. S.; Lee, W. C.; Choi, S. K., *Macromolecules* **1990**, *23*, 3029; (c) Jang, M. S.; Kwon, S. K.; Choi, S. K., *Macromolecules* **1990**, *23*, 4135; (d) Kang, K. L.; Kim, S. H.; Cho, H. N.; Choi, K. Y.; Choi, S. K., *Macromolecules* **1993**, *26*, 4539; (e) Gal, Y. S.; Jin, S. H.; Park, J. W.; Lee, W. C.; Lee, H. S.; Kim, S. Y., *J. Polym. Sci. A* **2001**, *39*, 4101.
 11. (a) Fox, H. H.; Wolf, M. O.; O'Dell, R.; Lin, B. L.; Schrock, R. R.; Wrighton, M. S., *J. Am. Chem. Soc.* **1994**, *116*, 2827; (b) Schattenmann, F. J.; Schrock, R. R., *Macromolecules* **1996**, *29*, 8990.
 12. (a) Anders, U.; Nuyken, O.; Buchmeiser, M. R.; Wurst, K., *Angew. Chem., Int. Ed.* **2002**, *41*, 4044; (b) Anders, U.; Nuyken, O.; Buchmeiser, M. R.; Wurst, K., *Macromolecules* **2002**, *35*, 9029; (c) Anders, U.; Wagner, M.; Nuyken, O.; Buchmeiser, M. R., *Macromolecules* **2003**, *36*, 2668; (d) Mayershofer, M. G.; Nuyken, O.; Buchmeiser, M. R., *Macromolecules* **2006**, *39*, 3484.
 13. (a) Krause, J. O.; Zarka, M. T.; Anders, U.; Weberskirch, R.; Nuyken, O.; Buchmeiser, M. R., *Angew. Chem., Int. Ed.* **2003**, *42*, 5965; (b) Krause, J. O.; Nuyken, O.; Buchmeiser, M. R., *Chem. Eur. J.* **2004**, *10*, 2029; (c) Halbach, T. S.;

- Krause, J. O.; Nuyken, O.; Buchmeiser, M. R., *Macromol. Rapid Commun.* **2005**, *26*, 784; (d) Kumar, P. S.; Wurst, K.; Buchmeiser, M. R., *J. Am. Chem. Soc.* **2009**, *131*, 387; (e) Autenrieth, B.; Anderson, E. B.; Wang, D.; Buchmeiser, M. R., *Macromol. Chem. Phys.* **2013**, *214*, 33.
14. Choi, T. L.; Grubbs, R. H., *Angew. Chem., Int. Ed.* **2003**, *42*, 1743.
 15. (a) Kang, E.-H.; Lee, I. H.; Choi, T.-L., *ACS Macro Lett.* **2012**, *1*, 1098;
(b) Kim, J.; Kang, E.-H.; Choi, T.-L., *ACS Macro Lett.* **2012**, *1*, 1090.
 16. Kang, E.-H.; Yu, S. Y.; Lee, I. S.; Park, S. E.; Choi, T.-L., *J. Am. Chem. Soc.* **2014**, *136*, 10508.
 17. Kang, E.-H.; Kang, C.; Yang, S.; Oks, E.; Choi, T.-L., *Macromolecules* **2016**, *49*, 6240.
 18. Kang, C.; Kang, E.-H.; Choi, T.-L., *Macromolecules* **2017**, *50*, 3153.
 19. (a) Lee, I. S.; Kang, E.-H.; Park, H.; Choi, T.-L., *Chem. Sci.* **2012**, *3*, 761;
(b) Park, H.; Lee, H. K.; Choi, T. L., *Polym. Chem.* **2013**, *4*, 4676; (c) Park, H.; Lee, H.-K.; Kang, E.-H.; Choi, T.-L., *J. Polym. Sci. A* **2015**, *53*, 274; (d) Song, J. A.; Park, S. E.; Kim, T. S.; Choi, T. L., *ACS Macro Lett.* **2014**, *3*, 795.
 20. Song, J. A.; Choi, T.-L., *Macromolecules* **2017**, *50*, 2724.
 21. (a) Kumar, P. S.; Wurst, K.; Buchmeiser, M. R., *J. Am. Chem. Soc.* **2009**, *131*, 387; (b) Naumov, S.; Buchmeiser, M. R., *Organometallics* **2012**, *31*, 847.

Chapter 2. Highly β -Selective Ring-Closing Enyne
Metathesis and Cyclopolymerization of 1,6-
Heptadiyne Derivatives Using Grubbs Z -Selective
Catalyst

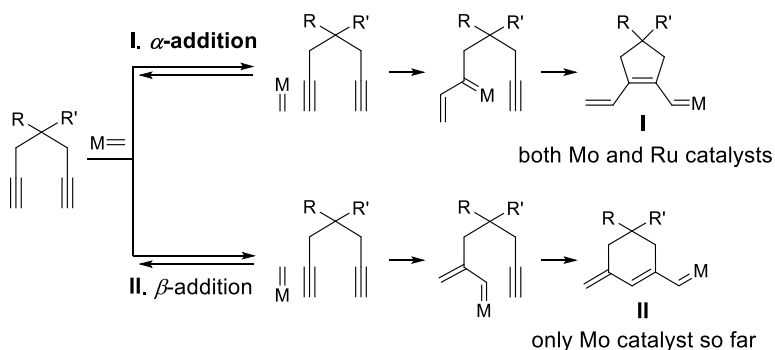
2.1 Abstract

It is well-known that Ru-based Grubbs catalysts undergo a highly selective α -addition to alkynes to promote *exo*-cyclization during ring-closing enyne metathesis (RCEYM) or to produce conjugated polyenes containing five-membered rings during the cyclopolymerization (CP) of 1,6-heptadiynes. There are a few reports of β -selective addition to alkynes using Schrock catalysts based on Mo, but none for Ru-based catalysts. In this chapter, we report the first example of β -selective addition to alkynes using readily accessible Ru-based catalyst, the Grubbs *Z*-selective catalyst, which produces only *endo* products during RCEYM reaction of terminal enynes and promotes CP of 1,6-heptadiyne derivatives to give conjugated polyenes containing a six-membered ring as a major repeat unit. This unique preference for β -selectivity originated from the side-bound approach of alkynes to the catalyst, where the steric hindrance between the chelating *N*-heterocyclic carbene ligand of the catalyst and the alkynes disfavored α -addition. To enhance the β -selectivity for CP further, one could increase the size of the substrates on the monomers and lower the reaction temperature to obtain conjugated polyenes containing up to 95% six-membered rings. Moreover, the physical properties of the resulting polymer were analyzed in detail and compared with those of the conjugated polyenes containing only five-membered rings, prepared from the same monomer but with a conventional Grubbs catalyst.



2.2 Introduction

Previously, our group reported a highly efficient living CP of 1,6–heptadiyne derivatives using third-generation Grubbs catalyst to produce conjugated polyenes containing five-membered ring backbones exclusively, with excellent control of the molecular weight and narrow dispersity (\mathcal{D}).^{14b, 15, 21} However, the formation of conjugated polyenes with six-membered rings by selective β -addition using Ru catalysts has not been achieved. Instead, Ru catalysts could only produce polyenes with six-membered rings from various 1,7–octadiyne monomers by selective α -addition.¹⁸ Hence, we became interested in the selective β -addition using Ru catalysts because there had been no investigations in this area since the last reports from the Schrock group 20 years ago (Scheme 2.1).^{10b, 22}

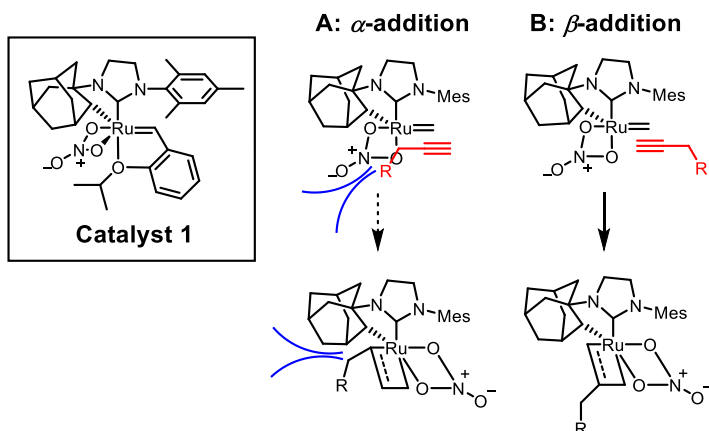


Scheme 2.1 Two possible pathways for CP of 1,6-heptadiyne derivatives

In this chapter, we discuss the preference of β -addition to alkynes using a new Ru-based catalyst containing a chelating *N*-heterocyclic carbene (NHC) ligand, also known as Grubbs *Z*-selective catalyst (**Catalyst 1**),²³ and demonstrate the first example of RCEYM to produce a six-membered *endo* product exclusively from terminal enynes. Also, β -selective CP of 1,6-heptadiyne derivatives is reported to produce conjugated polyenes containing predominantly six-membered ring repeat units, with up to 95% selectivity. We developed a plausible model to explain this unprecedented regioselectivity for **Catalyst 1** in both RCEYM and CP and provided strategies to enhance the β -selectivity. Lastly, we conducted several characterizations to compare the physical and electronic properties of the polyenes containing five- and six-membered ring microstructures.

2.3 Results and Discussion

In 2011, Grubbs and co-workers developed a new family of Ru-based catalysts containing chelating NHC ligands that promoted olefin metathesis reactions with high *Z*-selectivities.^{23–24} In particular, the introduction of adamantyl and nitrate ligands dramatically enhanced both the catalytic activity and *Z*-selectivity in various olefin metathesis reactions, such as cross metathesis,²⁵ macrocyclic ring-closing metathesis,²⁶ asymmetric ring-opening cross metathesis,²⁷ ethenolysis,²⁸ and ring-opening metathesis polymerization reactions.²⁹ Interestingly, DFT calculations revealed that **Catalyst 1** preferred the side-bound approach to olefins,³⁰ which was in sharp contrast to the conventional Grubbs catalysts, which favored the bottom-bound approach.³¹ As a result, this new approach caused steric repulsions between the substituents on the olefin and chelating NHC ligand, leading to a high *Z*-selectivity.^{30a} With these reports, we envisioned that **Catalyst 1** might react with the alkynes via β -addition rather than α -addition, because the substituents of the side-bound alkynes would experience a severe steric hindrance with the adamantyl and nitrate ligands during α -addition (Scheme 2.2A). However, the substituent on the alkynes could approach **Catalyst 1** away from the bulky ligands by β -addition, resulting in the least steric hindrance (Scheme 2.2B).

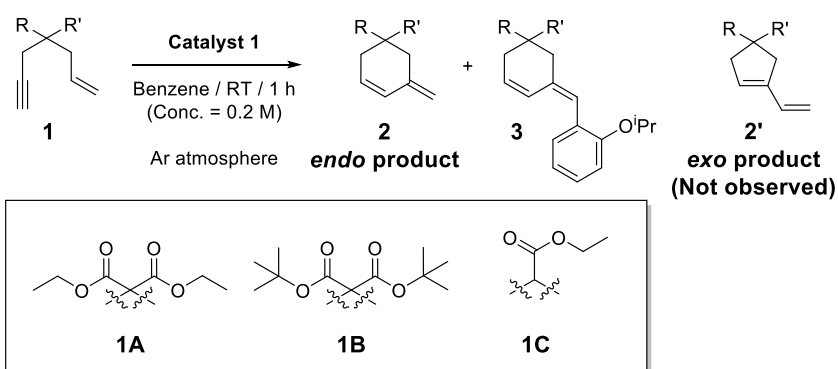


Scheme 2.2 Proposed model for the β -addition preference of Catalyst 1

Based on the proposed model for selective β -addition, our investigations began with the idea that this unique selectivity of Catalyst 1 would undergo the ring-closing enyne metathesis (RCEYM) reaction from substrate 1 to selectively produce *endo* product 2 (from α -addition of catalysts to the alkyne), not *exo* product 2' (from β -addition). RCEYM reaction is one of the most useful olefin metathesis reactions that gives cyclic dienes from substrates bearing both alkene and alkyne moieties.³² Ru-based Grubbs catalysts showed a strong preference for α -addition to give *exo* products;^{32,33} in particular, 4,4-substituted hept-1-en-6-yne (1) exclusively produced the five-membered *exo* product.³⁴ One notable exception was a special Mo catalyst developed by Hoveyda and Schrock that selectively produced *endo* products.³⁵

We employed three substituted enynes (1A–1C, Table 2.1) to determine whether the RCEYM of terminal enynes using **Catalyst 1** would show any regio-selectivity. From the ^1H NMR spectra of the crude reaction mixtures, we observed that only six-membered *endo* products (**2**) were obtained in all cases, without any signals corresponding to the five-membered *exo* products (**2'**) (Figure 2.1). In addition, a small amount of benzyldiene-attached products (**3**) containing the six-membered *endo* ring were also obtained (Table 2.1). This result was in sharp contrast to the previous RCEYM, yielding only five-membered *exo* ring products.^{34,35b}

Table 2.1 RCEYM using **Catalyst 1** to give *endo* product exclusively



entry	substrate	cat. loading (mol%)	conv (%) ^a	isolated yield (%) (2+3)
1	1A	10	51	38 (32+6)
2		20	>99	64 (56+8)
3	1B	10	67	51 (45+6)
4		20	>99	72 (64+8)
5	1C	10	36	16 (10+6)
6		20	60	24 (16+8)

^aCalculated from the ^1H NMR spectrum of a crude reaction mixture.

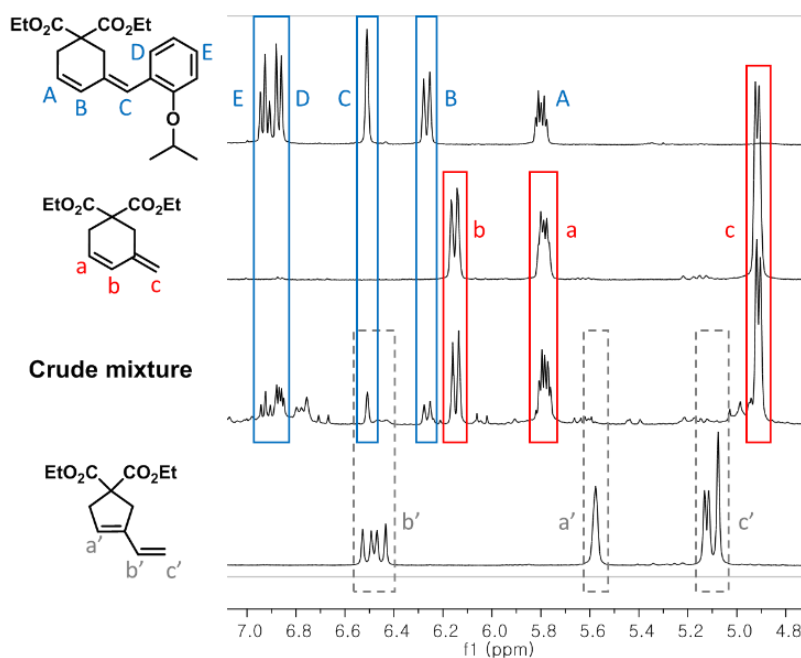
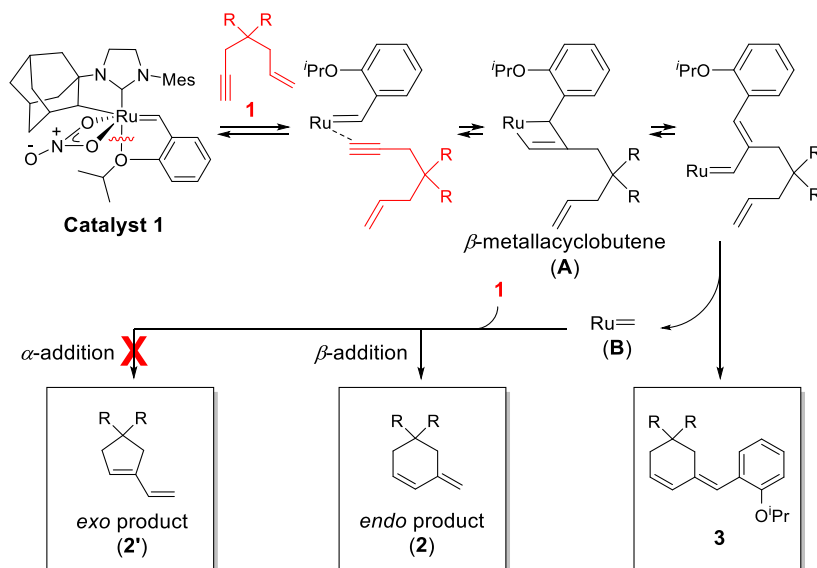


Figure 2.1 ^1H NMR spectra of 3A, 2A (top), reaction mixture from entry 2 (middle), and 2'A (bottom)



Scheme 2.3 Proposed mechanism of RCEYM using Catalyst 1

Scheme 2.3 describes the formation of *endo* products 2 and 3 using Catalyst

1. **Catalyst 1** preferentially reacted with the alkyne via β -addition to form the initial β -metallacyclobutene intermediate of **A** (Scheme 2.3). Then, the new alkylidene initially cyclized to give **3**, a six-membered *endo* product containing benzylidene transferred from **Catalyst 1**. After this first cycle, Ru methylidene became the active species (**B**), and catalyzed the formation of *endo* product **2**. Although the formation of **3** was inevitable because of the intrinsic structure of **Catalyst 1**, it is important to note that both **2** and **3** originated from the β -addition of **Catalyst 1**.

Initially, the ethyl malonate-type enyne (**1A**) showed a 51% conversion in benzene with 10 mol% of **Catalyst 1** in 1 h, and we isolated a total of 38% of the *endo* products, including 32% of the pure *endo* product (**2A**) and 6% of the benzylidene-coupled product (**3A**, Table 2.1, entry 1). Increasing the catalyst loading to 20 mol% further increased the total isolated yield to 69% for the *endo* product (entry 2). When a sterically bulkier *tert*-butyl group was introduced to the substrate (**1B**), the isolated yield of both of the *endo* products increased up to 72% (entries 3 and 4), presumably due to Thorpe–Ingold effects, which facilitated the ring-closing reactions.³⁶ In contrast, the RCEYM of **1C** with a smaller mono-substituent showed a much lower efficiency. The conversion of **1C** was only 36%, and the isolated yield of the total *endo* product was only 16% (entry 5) when treated with 10 mol% of **Catalyst 1**. Even with 20 mol% of the catalyst, the conversion and the yield of the total *endo* product were 60% and 24%, respectively (entry 6). By in-depth analysis of the crude mixtures, we realized that **1C** also underwent side reactions of undesired alkyne polymerization to generate substituted polyacetylene at an 11% isolated yield.^{12d, 37} This polymerization was

supported by NMR and matrix-assisted laser desorption/ionization time-of-flight (MALDI-TOF) analyses, and the M_n (number-average molecular weight) of 1.9 kDa was estimated by size-exclusion chromatography (SEC) (see Section 2.5 and 2.6). This result suggests that there were competing reaction pathways for intramolecular enyne cyclization and intermolecular alkyne polymerization. The former might be disfavored when the substituent is small (Thorpe-Ingold effect), such as in **1C**, and also because alkynes are more reactive than alkenes.³⁸ Despite this side reaction, *endo* selectivity was still retained without any *exo* products in all cases. All of the results reflected that **Catalyst 1** underwent exclusive β -addition, regardless of the size of the substituents, even though the efficiency of RCEYM depended on the size of the substituents. In short, we successfully achieved the first *endo*-selective RCEYM of terminal enynes using the user-friendly and commercially available Ru-based **Catalyst 1** after the pioneering achievement of Hoveyda and Schrock using a Mo catalyst system.³⁵

Based on the exclusive formation of the *endo* product from **Catalyst 1**, we pursued β -selective CP to give conjugated polyenes containing six-membered rings from 1,6-heptadiyne derivatives. Notably, there was only one example of such CP, again from Schrock's group who developed Mo alkylidene-containing sterically bulky carboxylate ligands to enforce β -addition.³⁹ However, there was no report of such CP using readily accessible Ru-based catalysts. Initially, we examined the reactivity and selectivity of **Catalyst 1** for the CP of diethyl dipropargylmalonate (DEDPM, **4**) with 2 mol% catalyst loading (or [M]:[C]=50) at room temperature. We were delighted to find that the conversion to the conjugated polyene after 3 h was

91%. More importantly, the ratio between the five- and six-membered rings on the polymer backbone was 1:3.4 (77% six-membered rings, entry 1, Table 2.2), determined by ^{13}C NMR, which showed well-resolved chemical shifts for the carbonyl carbon and the quaternary carbon depending on the ring sizes, i.e., five- or six-membered rings.^{10a} We used the ratio obtained from the signals for the carbonyl carbon as a lower limit (Table 2.2). Interestingly, this result was in sharp contrast to the previous CP results from the conventional Ru catalysts that produced the conjugated polyenes with only five-membered rings by α -addition.^{14b, 15, 21} According to our proposed model, α -addition would be further suppressed with increasing steric repulsions between the substituent on the alkynes and the adamantyl NHC ligand on the catalyst (Figure 2.2).

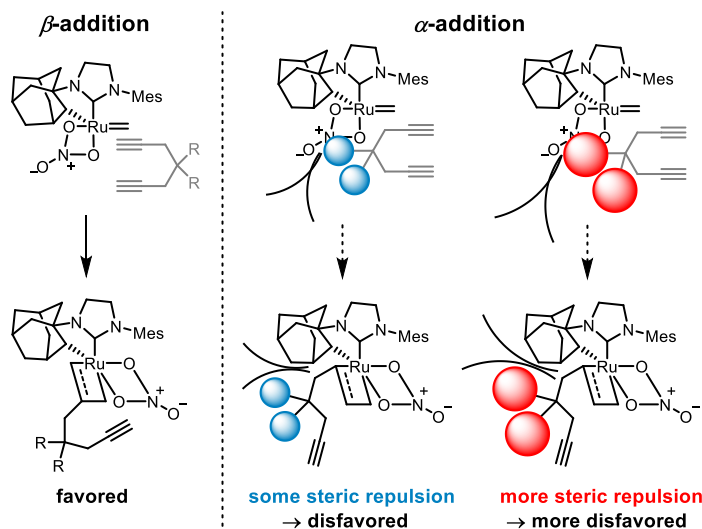


Figure 2.2 Proposed model for the preference of β -addition in CP using Catalyst 1

Table 2.2 CP of malonate-type monomers

Catalyst 1
 $[M]:[C]^g=50$
 Toluene 0.25 M
 RT (3 h), -40 °C (36-72 h)

4 **5** **6** **7** **8**

entry	monomer	temp	conv (%) ^b	yield (%) ^c	M_n (kDa) ^d	\bar{P}^d	5:6 ^e	5:6 ^f
1	4	RT	91	57	8.6	1.61	1:3.4	1:4.3
2	5	RT	79	41	6.6	1.56	1:2.0	nd
3	6	RT	95	80	13.1	1.60	1:4.9	1:5.6
4	7	RT	88	43	15.6	1.54	1:6.5	1:8.9
5	8	RT	82	78	6.9	1.49	1:6.1	nd
6	4	-40 °C	81	53	8.0	1.69	1:6.4	1:7.6
7	5	-40 °C	77	49	7.9	1.96	1:2.4	nd
8	6	-40 °C	92	87	16.4	1.69	1:11.4	1:11.6
9	7	-40 °C	78	50	12.5	1.52	1:13.8	1:15.6
10 ^g	7	-40 °C	>99	55	8.9	1.53	1:17.8	1:21.0

^aMonomer-to-catalyst ratio. ^bCalculated from ¹H NMR spectra. ^cPrecipitated in hexane at -78 °C. ^dDetermined by THF SEC calibrated using polystyrene (PS) standards. ^eCalculated from ¹³C NMR spectra based on the carbonyl carbon signals. ^fCalculated from ¹³C NMR spectra based on the quaternary carbon signals. ^g[M]:[C]=15, Conducted at 0.1 M, 4 h reaction.

To test this idea, various monomers containing substituents of different sizes at 4-position were synthesized and examined for the CP (Table 2.2). Mono-substituted diyne **5** bearing the smallest substituent showed a much lower six-membered ring selectivity (5:6-ring=1:2.0, entry 2), presumably because the steric repulsion was insufficient for selective β -addition. In contrast, when introducing two isopropyl groups (bulkier than the ethyl group in **4**) to monomer **6**, the six-membered ring selectivity of the resulting polymer increased significantly to 1:4.9 (entry 3). Finally, the introduction of even bulkier *tert*-butyl (**7**) and *N,N*-diethyl amide group (**8**) further increased the selectivity to 1:6.5 and 1:6.1, respectively (entries 4 and 5). In all cases, molecular weights of the polymers determined by SEC showed reasonable correlation with their theoretical values. The conjugated polyenes were isolated with moderate yields, and their *D*s were relatively broad, presumably due to the slow initiation and some termination. In short, these results demonstrate that the steric factor of the monomers obviously influenced the approach of the alkynes to **Catalyst 1** and altered the microstructure of the resulting polyenes. Furthermore, this validated our proposed model that the monomers with larger substituents, such as the *tert*-butyl group, effectively induced β -addition to produce six-membered ring-rich conjugated polyenes.

We repeated the CP at lower reaction temperatures down to $-40\text{ }^{\circ}\text{C}$ (Table 2.2, entries 6–10) to further increase the selectivity for β -addition and six-membered ring formation. In the case of monomer **4**, the five- to six-membered ring ratio of the resulting polyenes increased significantly from 1:3.4 to 1:6.4 when compared to the RT case (entry 1 vs. entry 6). Meanwhile, the polymerization of the smallest monomer (**5**) gave only a small enhancement of the ratio to 1:2.4, even at $-40\text{ }^{\circ}\text{C}$ (entry 7). In contrast, **6**, bearing the bulkier substituent ($i\text{-Pr}$), afforded the conjugated polyene with a much higher β -addition preference (1:11.4, entry 8). Finally, the reaction of the largest monomer (**7**) at $-40\text{ }^{\circ}\text{C}$ resulted in the highest six-membered ring selectivity (1:13.8, entry 9). As shown in Figure 2.3 (and Fig S2.15, Section 2.6), the ^{13}C NMR spectrum clearly showed the well-resolved signals for both sets of carbonyl and quaternary carbons for easy characterization. Interestingly, the stereochemistry on the olefins in five-membered ring repeat unit was exclusively *cis*, and this would make perfect sense because of the intrinsic nature of Grubbs *Z*-selective catalyst to produce *Z*-olefin (Figure S2.15). Although CP became much slower at $-40\text{ }^{\circ}\text{C}$ (at least 36 h) than at room temperature, the conversion and M_n were similar. More importantly, the preference for β -addition increased significantly with the increasing size of the monomers because the kinetic product was favored at a lower temperature, implying that the activation barrier for β -addition was indeed lower than that of α -addition for **Catalyst 1**. This result shows the first example of β -selective CP to produce conjugated polyenes containing the six-membered rings with Grubbs catalyst based on Ru metal.

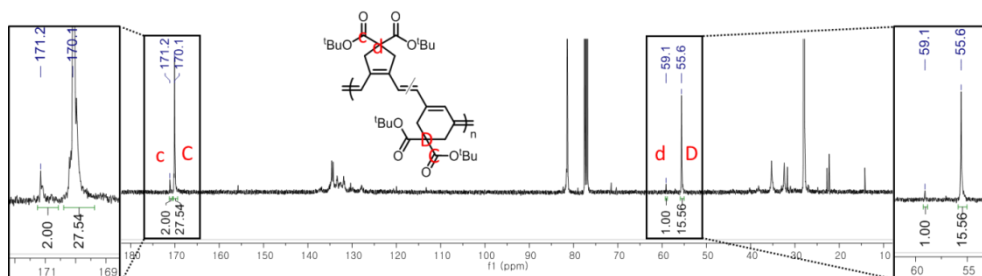
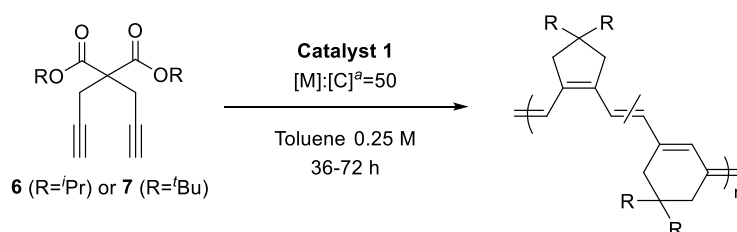


Figure 2.3 ^{13}C NMR spectra of the polymer from entry 9 in Table 2.2

Table 2.3 CP of malonate-type monomers at various temperatures



entry	monomer	temp ($^{\circ}\text{C}$)	conv (%) ^b	yield (%) ^c	M_n (kDa) ^d	\bar{D} ^d	5:6 ^e
1	6	-10	83	78	17.3	1.76	1:5.5
2	6	-40	92	87	16.4	1.69	1:11.4
3	6	-60	70	68	13.4	1.69	1:9.0
4	7	-10	94	90	19.0	1.57	1:7.7
5	7	-15	82	72	20.8	1.51	1:8.3
6	7	-22	79	76	17.3	1.70	1:8.6
7	7	-40	78	50	12.5	1.52	1:13.8
8	7	-60	57	35	11.8	1.57	1:9.9
9	7	-78	nd	nd	5.7	1.44	nd

^aMonomer-to-catalyst ratio. ^bCalculated from ^1H NMR spectra. ^cPrecipitated in hexane at -78 $^{\circ}\text{C}$. ^dDetermined by THF SEC calibrated using polystyrene (PS) standards. ^eCalculated from ^{13}C NMR spectra based on the carbonyl carbon signals.

To further investigate and support the effect of reaction temperature on the regio-selectivity, we conducted CP of **6** and **7** at various temperatures below 0 °C (Table 2.3). The overall β -selectivity appeared higher for P(**7**), containing sterically bulkier substituent which can affect more effective steric hindrance for the main chain of the polymer, compared to P(**6**). For P(**6**) cases, both the reactivity and β -selectivity was the highest at -40 °C (entry 2, 5- β -ring=1:11.4). The selectivity improvement was more obvious in P(**7**) cases; the β -selectivity of the resulting polymer increased by lowering the temperature, from -10 to -40 °C (entries 4-7). However, a too low temperature such as -60 °C was not appropriate for the polymerization efficiency (entries 3, 8, and 9), giving slightly decreased β -selectivity as well. Thus, we chose -40 °C as the optimal reaction temperature in Table 2.2.

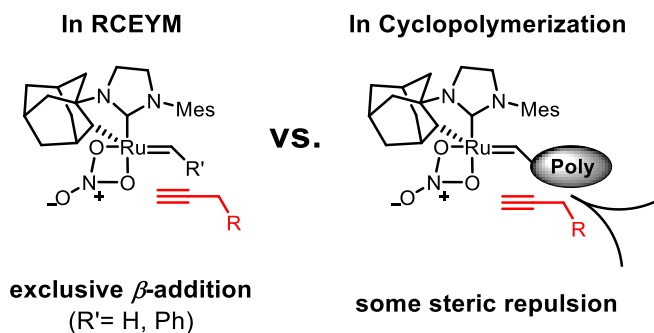


Figure 2.4 Decreased β -addition preference caused by the steric bulkiness of the growing polymer chain

Contrary to the results of RCEYM, which produced only *endo* products via exclusive β -addition, β -selectivity for CP, in general, seemed to be lower than RCEYM due to some degree of competing α -addition, depending on the monomer structures. The different preference for the β -addition selectivity between CP and RCEYM could also be understood from our proposed model modified by the additional steric factors of the growing polymer chain itself (Figure 2.4). In other words, the resting state of the catalytic species in RCEYM was mostly the smallest Ru methylidene and relatively small benzylidene, while the propagation species during CP was the much bulkier alkylidenes containing polymer chains. Therefore, as the polymerization proceeded, this increasing steric bulkiness of the polymer chain created an additional steric repulsion between the substituents of the monomers and the polymer chain itself during the β -addition mode, as depicted in Figure 2.4. As a result, some competing α -addition to produce five-membered rings seemed inevitable, even though the major steric repulsion still came from the alkynes and the adamantyl ligand. P(7) with a low degree of polymerization (DP) of 15 was synthesized to support this assumption, and this conjugated polyene showed an even higher six-membered ring selectivity (1:17.8) compared to P(7) with DP=36 (Table 2.2, entry 10). Now, one can produce conjugated polyenes with up to 95% six-membered ring selectivity using the user-friendly Grubbs catalyst.

Table 2.4 Comparison of physical and electronic properties of P(7) and P(7-I)

polymer	catalyst	solution		film		E_{HOMO} (eV) ^c	T_{d} (°C) ^d	T_{g} (°C) ^e
		λ_{max} (nm) ^a	E_{g} (eV) ^{a,b}	λ_{max} (nm) ^a	E_{g} (eV) ^{a,b}			
P(7)	Catalyst 1	513	1.93	484	1.93	-4.94	245	110
P(7-I)	GIII	588, 547	2.02	515	2.01	-5.14	242	107

^aDetermined by UV-Vis spectroscopy. ^bCalculated from the onset point of the UV-Vis spectra. ^cDetermined by CV. ^dDetermined by TGA. ^eDetermined by DSC.

It would be worthwhile to investigate the properties of the conjugated polyenes containing six-membered rings in detail and compare them to the analogous polyenes with the five-membered ring structure prepared via α -addition because there is only one example for the synthesis of these conjugated polyenes via β -addition.^{10b, 22} To investigate the differences in physical and electronic properties based on the polymer backbone composition, two types of P(7) of the same [M]:[C] were prepared: one produced by Catalyst 1 (Table 2.2, entry 9, P(7), 5-ring:6-ring=1:14), and the other containing a five-membered ring exclusively produced by Grubbs 3rd generation catalyst, GIII (P(7-I)). From their UV-Vis spectra in the solution states, λ_{max} of P(7) appeared at 513 nm without any vibronic peaks,⁴⁰ and this value was lower than that of P(7-I) at 588 nm, which corresponds to the 0-0 vibronic peak (547 nm for 0-1 vibronic peak).^{21c} This implied that the polymer backbone for P(7-I) was more planar presumably due to the presence of *Z*-olefins in P(7) (Figures S2.15 and S2.16). However, due to a much broader absorption spectrum for P(7), its optical bandgap was lower than that of P(7-I) by 0.1 eV (1.93 and 2.02 eV,

respectively) (Table 2.4 and Figure 2.5). In contrast, the UV–Vis analysis of P(7) in the thin film state revealed a significantly blue-shifted spectrum with a lower λ_{max} of 484 nm while maintaining the optical bandgap (presumably because the bulky substituents distorted much of the backbone planarity of the polymer in the film state, shortening the effective conjugation length of the polymer).^{18a, 41} A similar blue-shift with a lower λ_{max} of 515 nm was observed for P(7-I) in the film state (Figure 2.5).

We also measured the highest occupied molecular orbital (HOMO) levels of these two conjugated polymers containing either five- or six-membered ring repeat units by cyclic voltammetry in a dichloromethane solution (Table 2.4). For comparison, the HOMO level of P(7) (mostly six-membered rings) was -4.94 eV, whereas that of P(7-I) (exclusively containing five-membered rings) was -5.14 eV. This implied that P(7) was easier to oxidize and would be more air- and moisture-sensitive than P(7-I). The thermal properties of these polymers were also evaluated by thermogravimetric analysis (TGA) and differential scanning calorimetry (DSC), and they showed similar decomposition temperatures (245 °C for P(7) and 242 °C for P(7-I)) and glass transition temperatures (110 °C for P(7) and 107 °C for P(7-I)) (Table 2.4).

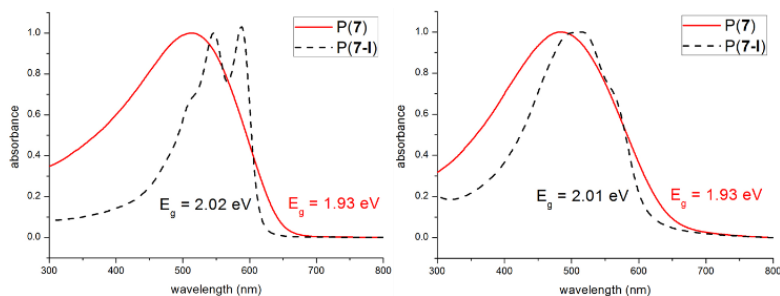


Figure 2.5 UV-Vis spectra of P(7) and P(7-I) in a chloroform solution (left) and the film state (right)

2.4 Conclusion

In summary, we demonstrated unprecedented regio-selectivity among Ru-based catalysts during the RCEYM of terminal enynes and CP of 1,6-heptadiyne derivatives using the commercially available Grubbs *Z*-selective catalyst (**Catalyst 1**). This unique catalyst selectively produced endo products containing six-membered rings by RCEYM and conjugated polyenes containing six-membered rings as a major repeat unit by CP. This new selectivity originated from the preference of **Catalyst 1** for β -addition instead of α -addition, because of the side-bound approach instead of the bottom-bound approach. This study is significant because it is the first example of Ru-catalyzed RCEYM and CP to show high six-membered ring selectivity via β -addition, contrary to the previous results that typical Ru-based catalysts gave only five-membered ring structures during analogous RCEYM and CP. We also investigated the determining factors for high β -selectivity in CP, and found that the increasing steric bulkiness of the substituents on the monomers and lowering the reaction temperature

enhanced the selectivity for β -addition up to 95%. Several physical properties of the resulting polymer containing mostly six-membered ring repeat units were analyzed and compared with those of the analogous conjugated polyenes containing five-membered rings prepared from the same monomer. We believe that these results will contribute not only to an understanding of the reaction pathway of RCEYM and CP, but also to the access of a new potential material prepared by Grubbs *Z*-selective catalyst.

2.5 Experimental Section

Characterization

^1H NMR and ^{13}C NMR was recorded by Varian/Oxford As-500 (500 MHz for ^1H and 125 MHz for ^{13}C) spectrometer and Agilent 400-MR (400 MHz for ^1H and 100 MHz for ^{13}C). Size exclusion chromatography (SEC) analyses were carried out with Waters system (1515 pump, 2414 refractive index detector) and Shodex GPC LF-804 column eluted with THF (GPC grade, Honeywell Burdick & Jackson®) and filtered with a 0.2 μm PTFE filter (Whatman®). The flow rate was 1.0 mL/min, and temperature of the column was maintained at 35 °C. UV/Vis spectra were obtained by Jasco Inc. UV-vis Spectrometer V-650. MALDI-TOF analysis was carried out with Bruker Daltonics autoflex II TOF/TOF. Thermogravimetric analysis (TGA) and differential scanning calorimetry (DSC) was carried out under N_2 gas at a scan rate of 10 °C/min with Q50 and Q10 model devices, respectively, from TA Instruments.

Materials

All reagents which are commercially available from Sigma-Aldrich®, Tokyo Chemical Industry Co. Ltd., Acros Organics, Alfa Aesar®, without additional notes, were used without further purification. **Catalyst 1** was provided from Materia Inc. (C633, CAS# 1352916-84-7), and is also commercially available from Sigma-Aldrich®. Benzene for the RCEYM and toluene for the polymerization were purified by Glass Contour Organic Solvent Purification System, and degassed further by Ar bubbling for 10 minutes before performing reactions.

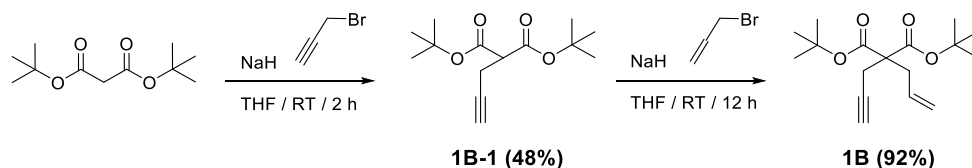
Cyclic Voltammetry (CV)

Cyclic voltammetry (CV) measurement was carried out at the room temperature on a CHI 660 Electrochemical Analyzer (CH Instruments, Inc., Texas, USA) using a degassed acetonitrile solution of tetrabutylammonium hexafluorophosphate (Bu_4NPF_6 , 0.1 M). The polymer solution was prepared by dissolving the polymer in dichloromethane (10 mg/ml). Cyclic voltammogram was recorded using the glassy carbon working electrode and a reference electrode of Ag/Ag^+ (0.1 M AgNO_3 in acetonitrile) with a platinum wire counter electrode at a scan rate of 50 mV/s. The absolute energy level was obtained using ferrocene/ferrocenium as an internal standard. The oxidation potential of ferrocene was regarded as -4.8 eV.

Experimental procedures for the preparation of the substrates

1A,^{35b} 1C,^{35b} 4,^{9b} 5,^{11d} 6,⁴² and 7,^{11d} were prepared by literature methods.

Di-*tert*-butyl 2-allyl-2-(prop-2-yn-1-yl)malonate (**1B**)

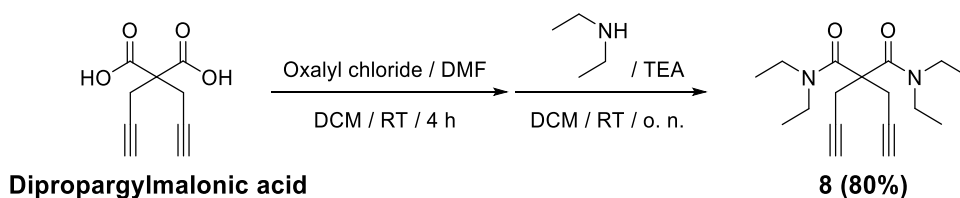


Di-*tert*-butyl malonate (98%, 3.56 mmol, 786 mg) was added to the Ar-purged flask in THF (12 ml). The solution was cooled to 0 °C, and sodium hydride (60% in mineral oil, 3.56 mmol, 142 mg) was added. After stirring for 15 min at room temperature, propargyl bromide in toluene solution (80%, 3.56mmol, 0.40ml) was added to the reaction mixture. After stirring for 2 h at room temperature, the mixture was quenched by the aqueous NH₄Cl solution. The product was extracted with ethyl acetate, and the organic layer was washed with brine. The organic layer was dried with MgSO₄ and concentrated to give a yellow colored liquid. It was purified by flash column chromatography on silica gel (EtOAc:Hexane=1:80→1:50) to afford compound **1B-1** as a colorless liquid (435 mg, 48 %). ¹H NMR (500 MHz, CDCl₃): δ 3.36 (t, J = 7.7 Hz, 1H), 2.68 (dd, J = 7.6, 2.5 Hz, 2H), 2.00 (d, J = 2.6 Hz, 1H), 1.47 (s, 18H). ¹³C NMR (125 MHz, CDCl₃): δ 167.3, 82.1, 80.6, 70.1, 53.1, 27.9, 18.4. HR-MS (ESI) [M+Na]⁺ calcd. for C₁₄H₂₂NaO₄, 277.1410, found, 277.1412.

1B-1 (1.22 mmol, 310 mg) was added to the Ar-purged flask in THF (4 ml). The solution was cooled to 0 °C, and sodium hydride (60% in mineral

oil, 1.22 mmol, 48.8 mg) was added. After stirring for 15 min at room temperature, allyl bromide (99%, 2.44 mmol, 0.21 ml) was added to the reaction mixture. After stirring for 12 h at room temperature, the mixture was quenched by the aqueous NH_4Cl solution. The product was extracted with ethyl acetate, and the organic layer was washed with brine. The organic layer was dried with MgSO_4 and concentrated to give a yellow colored solid. It was purified by flash column chromatography on silica gel ($\text{EtOAc}:\text{Hexane}=1:40$) to afford compound **1B** as a white solid (329 mg, 92 %). ^1H NMR (400 MHz, CDCl_3): δ 5.63 (ddt, $J = 17.4, 10.0, 7.6$ Hz, 1H), 5.25 – 5.06 (m, 2H), 2.71 (dd, $J = 9.8, 5.1$ Hz, 4H), 2.00 (q, $J = 2.5$ Hz, 1H), 1.46 (s, 18H); ^{13}C NMR (100 MHz, CDCl_3): δ 169.1, 132.3, 119.5, 81.9, 79.5, 71.2, 57.4, 36.4, 28.0, 22.6; HR-MS (ESI) $[\text{M}+\text{Na}]^+$ calcd. for $\text{C}_{17}\text{H}_{26}\text{NaO}_4$, 317.1723, found, 317.1720.

$\text{N}^1, \text{N}^1, \text{N}^3, \text{N}^3$ -tetraethyl-2,2-di(prop-2-yn-1-yl)malonamide (**8**)



Dipropargylmalonic acid⁴³ (674.9 mg, 3.746 mmol) was added to the Ar-purged flask in DCM (19 ml). The solution was cooled to 0 °C, then a catalytic amount of DMF (10 drops) and oxalyl chloride (2M soln. in DCM, 11.24 mmol, 5.62 ml) was slowly added. The mixture was stirred for 4 h at room temperature then the solvent was evaporated. The mixture was re-dissolved in DCM (19 ml), and the solution was cooled to 0 °C, then

diethylamine (11.24 mmol, 1.17 ml) and trimethylamine (11.24 mmol, 0.93 ml) were dropwise. After stirring overnight at room temperature, the mixture was quenched by the aqueous NH_4Cl solution. The product was extracted with ethyl acetate, and the organic layer was washed with brine. The organic layer was dried with MgSO_4 and concentrated to give a yellow colored solid. It was purified by flash column chromatography on silica gel ($\text{EtOAc}:\text{Hexane}=1:5$) to afford compound **8** as a white solid (871.0 mg, 80 %). ^1H NMR (400 MHz, CDCl_3): δ 3.31 (br, 8H), 3.08 (br, 4H), 2.02 (s, 2H), 1.15 (t, $J = 7.1$ Hz, 12H); ^{13}C NMR (100 MHz, CDCl_3): δ 168.5, 79.5, 71.9, 55.7, 41.6, 41.4, 24.7, 13.8, 12.8; HR-MS (ESI) $[\text{M}+\text{Na}]^+$ calcd. for $\text{C}_{17}\text{H}_{26}\text{N}_2\text{NaO}_2$, 313.1886, found, 313.1886.

General procedure for the ring-closing enyne metathesis reaction

A 5-mL sized screw-cap vial with a septum was flame dried and charged with enyne **1** and a magnetic bar. The vial was purged with argon four times, and degassed anhydrous benzene was added. After the Ar-purged **Catalyst 1** in another 5-mL vial was dissolved in benzene, the solution was rapidly injected to the enyne solution at room temperature under vigorous stirring. The reaction was quenched by excess ethyl vinyl ether after desired reaction time, and purified by column chromatography on silica gel. The eluent composition for each column chromatography is described below.

2A and **2C** were already reported in previous literature.^{35b}

3A (EtOAc:Hexane= 1:60→1:40)

^1H (500 MHz, CDCl_3): δ 7.35 (d, J = 7.5 Hz, 1H), 7.18 (t, J = 7.8 Hz, 1H), 6.93 (t, J = 7.5 Hz, 1H), 6.87 (d, J = 8.2 Hz, 1H), 6.51 (s, 1H), 6.27 (dd, J = 9.8, 1.0 Hz, 1H), 5.84–5.72 (m, 1H), 4.54–4.42 (m, 1H), 4.21–4.03 (m, 4H), 3.11 (s, 2H), 2.79–2.69 (m, 2H), 1.38–1.29 (m, 6H), 1.19–1.09 (m, 6H); ^{13}C NMR (125 MHz, CDCl_3): δ 171.3, 156.0, 135.5, 132.3, 131.5, 130.4, 128.1, 125.4, 125.1, 120.3, 114.2, 70.9, 61.6, 54.3, 31.9, 31.6, 22.3, 14.1; HR-MS (ESI) $[\text{M}+\text{Na}]^+$ calcd. for $\text{C}_{22}\text{H}_{28}\text{NaO}_5$, 395.1829, found, 395.1830.

2B (EtOAc:Hexane= 1:60→1:40)

^1H (500 MHz, CDCl_3): δ 6.14 (d, J = 9.9 Hz, 1H), 5.81–5.74 (m, 1H), 4.89 (d, J = 15.3 Hz, 2H), 2.75 (s, 2H), 2.57 (dd, J = 3.6, 1.6 Hz, 2H), 1.50–1.36 (s, 18H); ^{13}C NMR (125 MHz, CDCl_3): δ 170.3, 139.9, 128.9, 126.9, 113.0, 81.3, 54.9, 36.1, 31.1, 27.9; HR-MS (ESI) $[\text{M}+\text{Na}]^+$ calcd. for $\text{C}_{17}\text{H}_{26}\text{NaO}_4$, 317.1723, found, 317.1723.

3B (EtOAc:Hexane= 1:60→1:40)

^1H (500 MHz, CDCl_3): δ 7.33 (dt, J = 12.4, 6.2 Hz, 1H), 7.21 – 7.11 (m, 1H), 6.95–6.88 (m, 1H), 6.85 (d, J = 8.2 Hz, 1H), 6.53 (s, 1H), 6.30–6.20 (m, 1H), 5.85–5.74 (m, 1H), 4.57–4.44 (m, 1H), 3.04 (d, J = 1.6 Hz, 2H), 2.62 (dd, J = 3.8, 1.6 Hz, 2H), 1.34 (s, 18H), 1.32–1.27 (m, 6H); ^{13}C NMR (125 MHz, CDCl_3): δ 170.5, 132.7, 131.4, 130.5, 130.4, 127.9, 125.6, 125.0, 120.0, 113.4, 81.3, 70.4, 55.3, 39.3, 31.9, 31.6, 27.9, 22.4; HRMS (ESI) $[\text{M}+\text{Na}]^+$ calcd. for $\text{C}_{26}\text{H}_{36}\text{NaO}_5$, 451.2455, found, 451.2456.

3C (Et₂O:Hexane= 1:40→1:20)

¹H (500 MHz, CDCl₃): δ 7.28 – 7.24 (m, 1H), 7.17 (dd, J = 10.9, 4.7 Hz, 1H), 6.95 – 6.83 (m, 2H), 6.48 (s, 1H), 6.28 (d, J = 9.8 Hz, 1H), 5.87 – 5.78 (m, 1H), 4.56 – 4.45 (m, 1H), 4.22 (dd, J = 8.4, 6.1 Hz, 1H), 4.13 (dt, J = 14.3, 6.6 Hz, 2H), 3.03 – 2.95 (m, 1H), 2.70 – 2.50 (m, 2H), 2.42 (dd, J = 7.8, 2.7 Hz, 2H), 1.38 – 1.29 (m, 9H); ¹³C NMR (125 MHz, CDCl₃): δ 175.50, 155.88, 134.51, 131.93, 130.43, 127.96, 127.53, 126.64, 123.80, 120.20, 114.06, 70.96, 60.56, 39.87, 29.86, 29.33, 28.44, 22.42, 22.30, 14.34; HRMS (ESI) [M+Na]⁺ calcd. for C₁₉H₂₄NaO₃, 323.1618, found, 323.1620.

General procedure for the cyclopolymerization

A 5-mL sized screw-cap vial with a septum was flame dried and charged with monomer and a magnetic bar. The vial was purged with argon four times, and degassed anhydrous toluene was added. After the Ar-purged **Catalyst 1** in another 5-mL vial was dissolved in toluene, the solution was rapidly injected to the monomer solution at an experimental temperature (RT – –40 °C) under vigorous stirring. The reaction was quenched by excess ethyl vinyl ether after desired reaction time, and partially precipitated in hexane at –78 °C, remaining small amount of crude mixture (~ 10%). Obtained solid was filtered and dried in vacuo. Monomer conversion was calculated from the ¹H NMR spectrum of the remained crude mixture.

^1H and ^{13}C NMR characterization of polymers

P(4) ^1H (400 MHz, CDCl_3): δ 6.96–5.95 (br m, 2H), 4.21 (br m, 4H), 3.57–2.95 (br m, 4H), 1.25–1.24 (br m, 6H); ^{13}C (100 MHz, CDCl_3): δ 171.9, 170.9, 135.1, 134.4, 134.0, 133.1, 132.2, 132.1, 131.9, 61.7, 58.0, 54.6, 40.2, 35.0, 32.3, 22.2, 14.1.

P(5) ^1H (400 MHz, CDCl_3): δ 6.88–5.93 (br m, 2H), 4.18 (br m, 2H), 3.16–2.68 (br m, 4H), 1.28 (br m, 3H); ^{13}C (100 MHz, CDCl_3): δ 175.7, 174.9, 136.5, 135.6, 134.2, 132.6, 128.1, 127.6, 122.9, 121.1, 120.1, 70.8, 60.8, 41.5, 41.0, 40.2, 36.1, 31.9, 29.5, 27.0, 14.4.

P(6) ^1H (400 MHz, CDCl_3): δ 6.92–5.81 (br m, 2H), 5.03 (br m, 2H), 3.54–2.91 (br m, 4H), 1.33–1.09 (br m, 12H); ^{13}C (100 MHz, CDCl_3): δ 171.4, 170.3, 134.4, 134.1, 133.1, 131.9, 130.2, 68.9, 57.9, 54.5, 54.4, 35.1, 32.2, 29.7, 21.6.

P(7) ^1H (400 MHz, CDCl_3): δ 6.91–5.79 (br m, 2H), 3.47–2.75 (br m, 4H), 1.42–1.26 (br m, 18H); ^{13}C (100 MHz, CDCl_3): δ 171.2, 170.1, 135.2, 134.7, 134.3, 133.3, 131.9, 81.4, 59.1, 55.6, 53.5, 35.3, 32.4, 29.8, 27.9.

P(8) ^1H (400 MHz, CDCl_3): δ 6.85–5.76 (br m, 2H), 3.31–2.35 (br m, 12H), 1.15–1.09 (br m, 12H); ^{13}C (100 MHz, CDCl_3): δ 171.9, 170.7, 135.2, 134.4, 130.9, 130.2, 53.5, 53.2, 41.6, 40.7, 37.8, 33.8, 29.8, 22.2, 13.9, 12.9.

2.6 Supporting Information

Supporting data for the alkyne polymerization of 1C

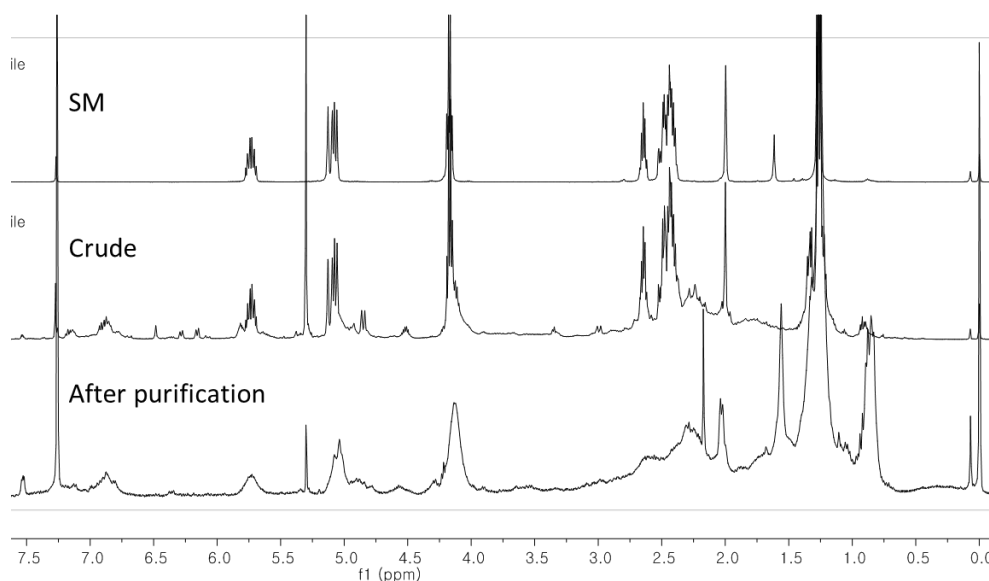


Figure S2.1 Comparison of ^1H NMR spectra of SM, crude mixture and purified oligomer from entry 6, Table 2.1

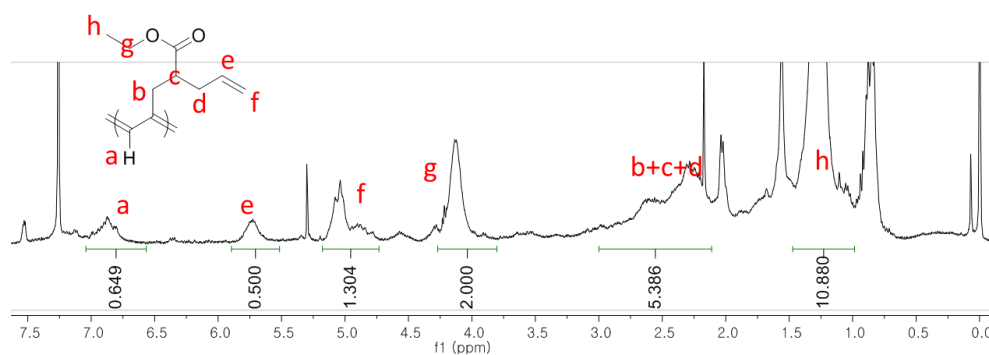


Figure S2.2 ^1H NMR spectra of purified oligomer from entry 6, Table 2.1

Broad oligomeric signals, presumably derived from the alkyne polymerization, were observed in ^1H NMR spectrum of the reaction crude mixture. Silica column chromatography to remove the metal gave a brown powder with oligomeric signals, which matched with the polymer structure. Several groups with a lot of fragmentation were observed in the spectra. The interval between each group was ~ 166 , which was the mass of **1C**, and that of each fragmentation was ~ 17 , which suggests that there were various kinds and the combination of alkali metal adducts (Na^+ -bound or K^+ -bound).

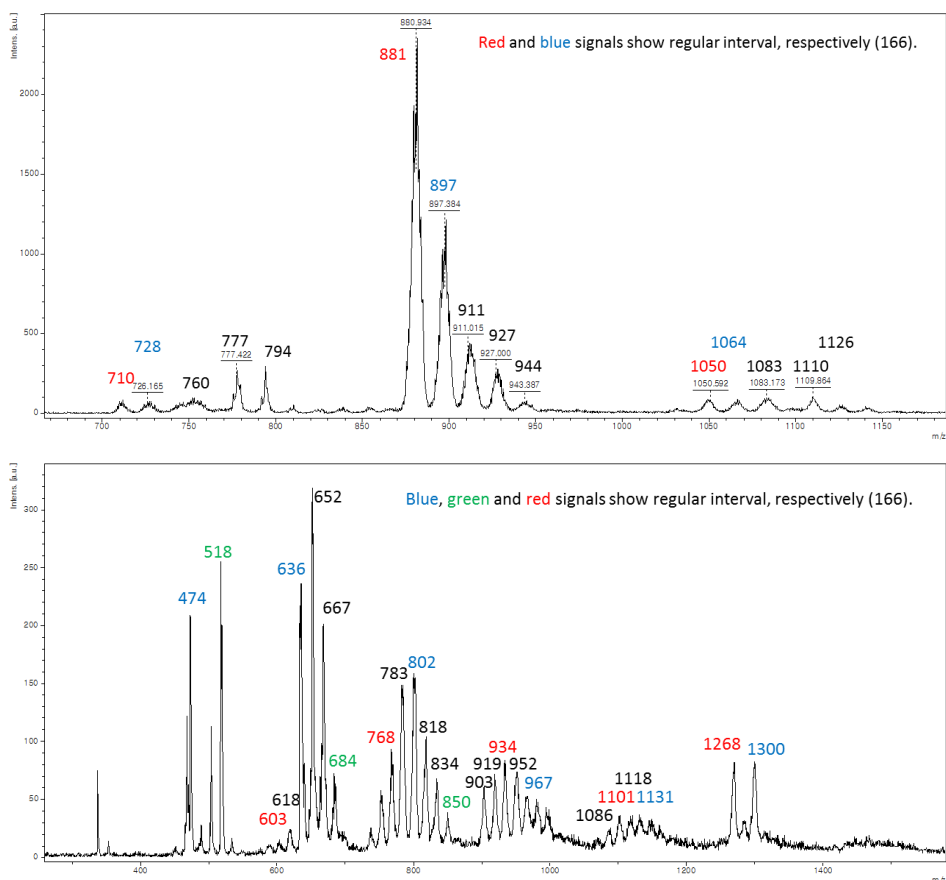


Figure S2.3 MALDI-TOF spectra of purified oligomer from entry 6, Table 2.1

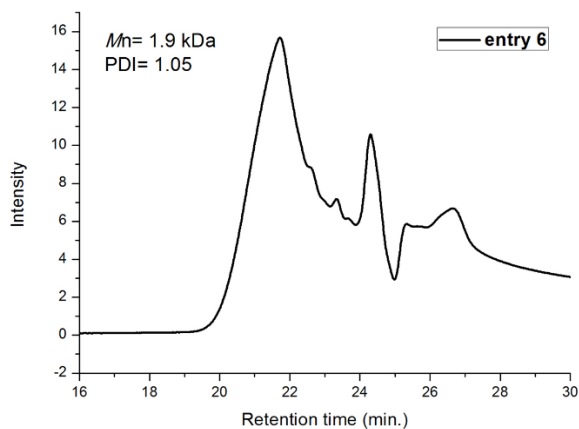


Figure S2.4 SEC trace of purified oligomer from entry 6, Table 2.1

^{13}C NMR spectra of the polymers in Table 2.2

Those spectra were used for the determination of the ratio between five- and six-ring on the polymer backbone.

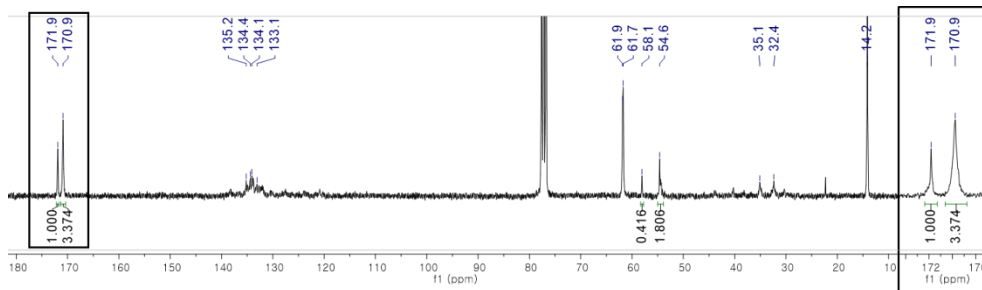


Figure S2.5 ^{13}C NMR spectra of polymer from entry 1, Table 2.2

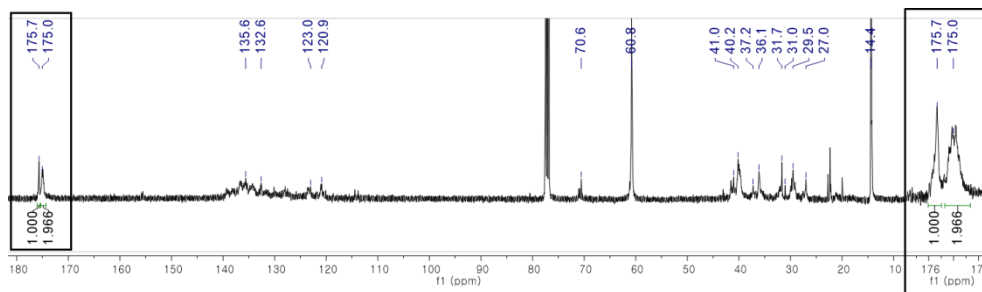


Figure S2.6 ^{13}C NMR spectra of polymer from entry 2, Table 2.2

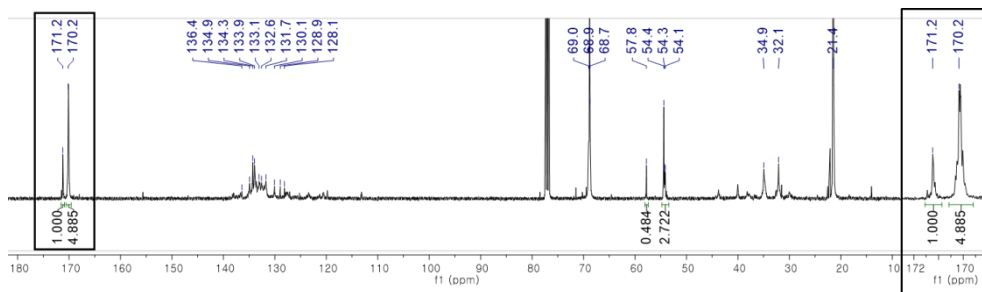


Figure S2.7 ^{13}C NMR spectra of polymer from entry 3, Table 2.2

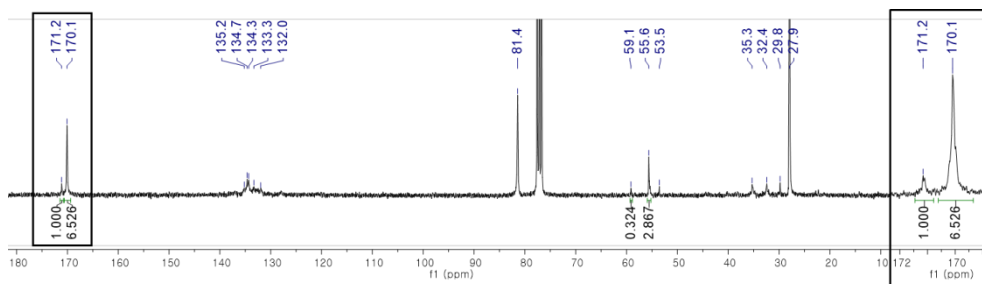


Figure S2.8 ^{13}C NMR spectra of polymer from entry 4, Table 2.2

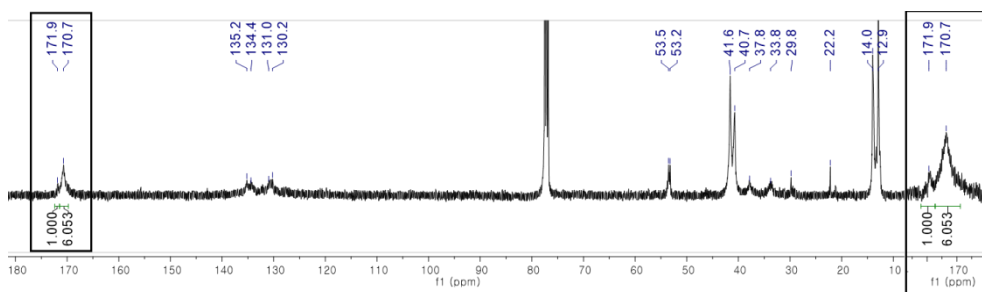


Figure S2.9 ^{13}C NMR spectra of polymer from entry 5, Table 2.2

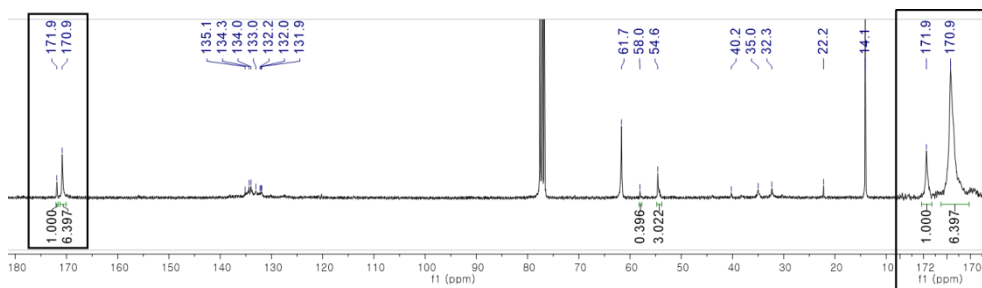


Figure S2.10 ^{13}C NMR spectra of polymer from entry 6, Table 2.2

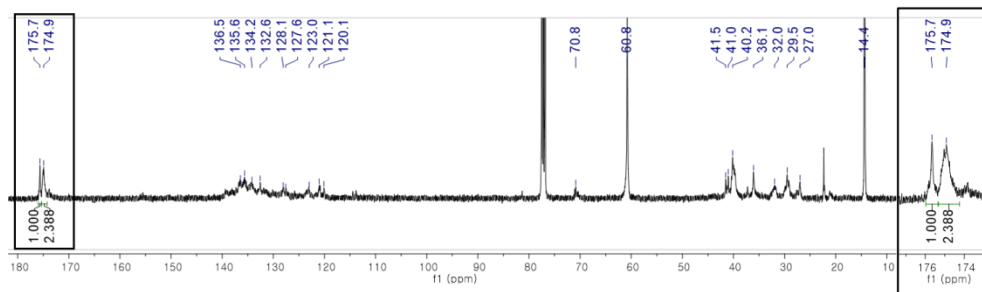


Figure S2.11 ^{13}C NMR spectra of polymer from entry 7, Table 2.2

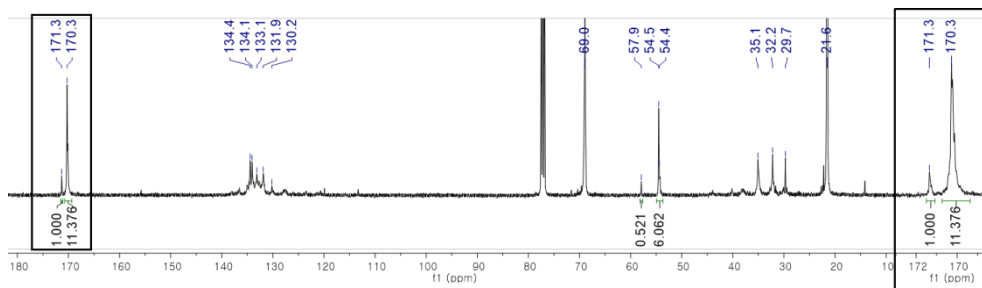


Figure S2.12 ^{13}C NMR spectra of polymer from entry 8, Table 2.2

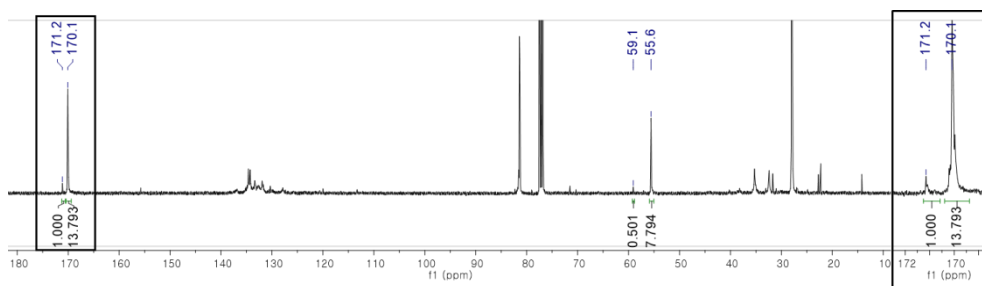


Figure S2.13 ^{13}C NMR spectra of polymer from entry 9, Table 2.2

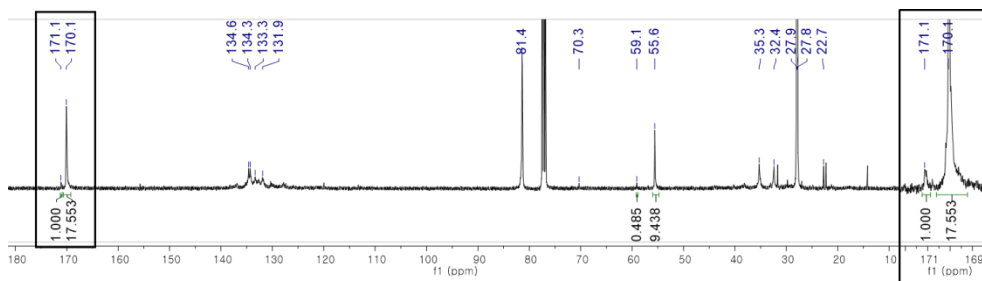


Figure S2.14 ^{13}C NMR spectra of polymer from entry 10, Table 2.2

^{13}C NMR spectra of P(7-I) and P(7)

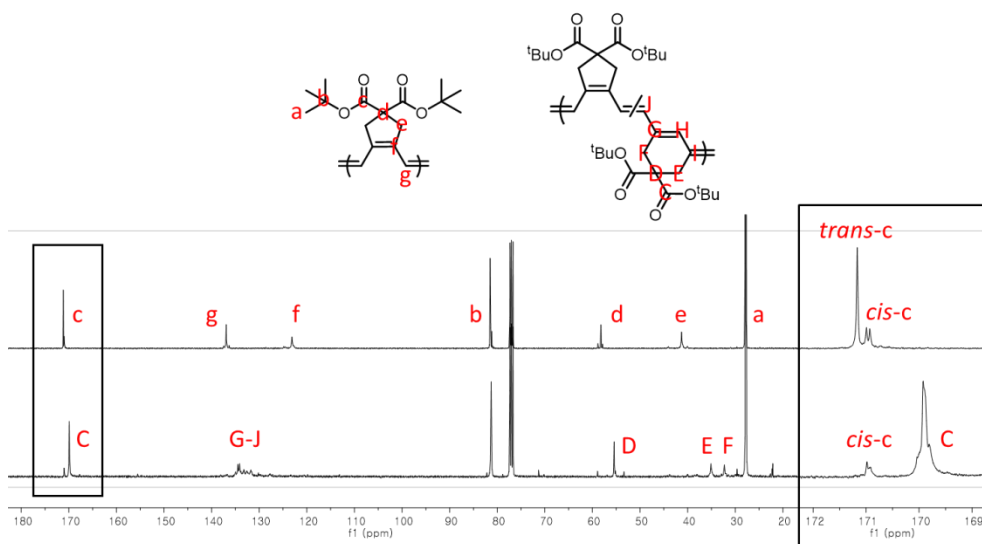
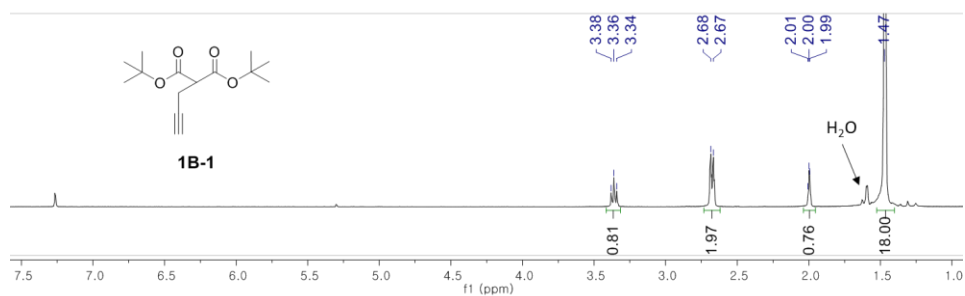


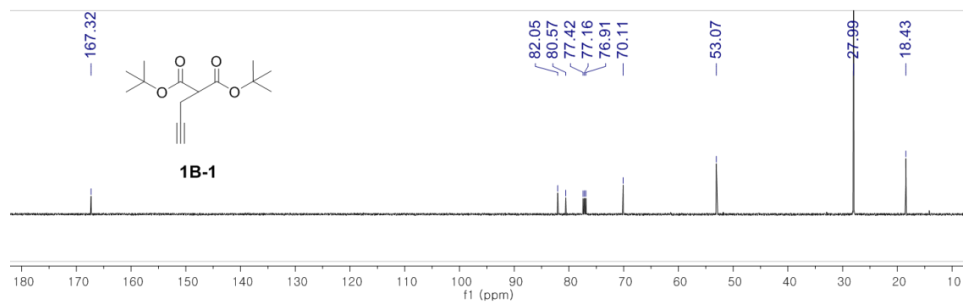
Figure S2.15 ^{13}C NMR spectra of P(7-I) (up) and P(7) (down) in Table 2.4

^1H and ^{13}C NMR spectra of the substrates and the products

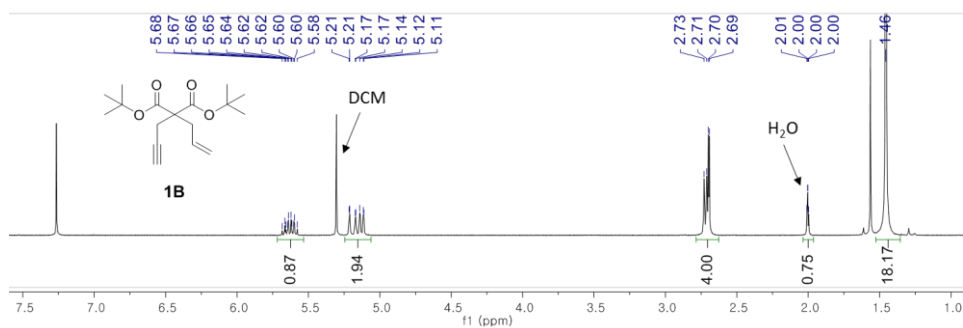
1B-1 (^1H , 500 MHz, CDCl_3)



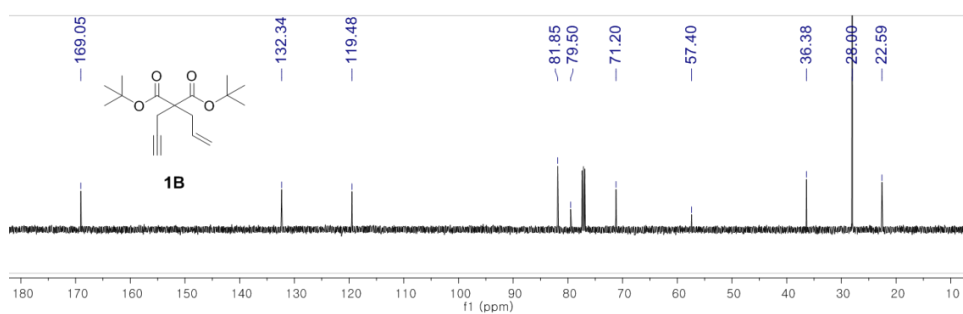
1B-1 (^{13}C , 125 MHz, CDCl_3)



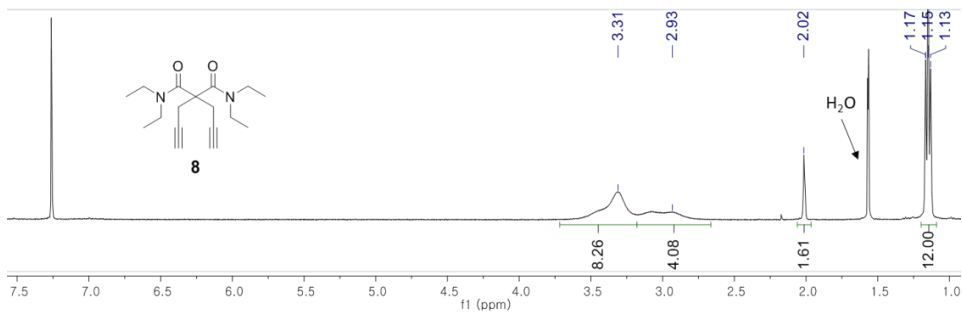
1B (^1H , 400 MHz, CDCl_3)



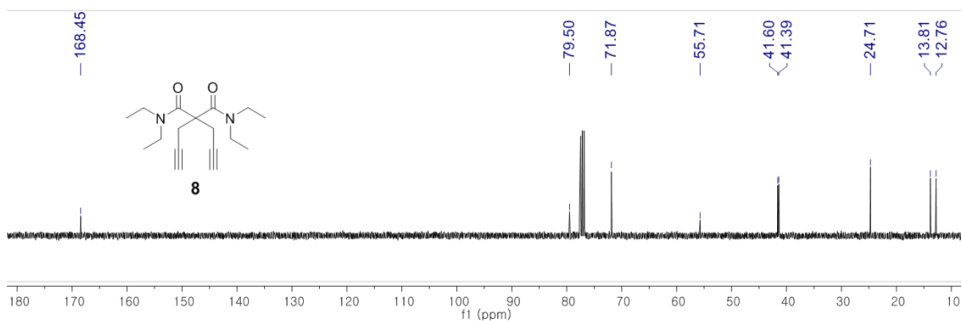
1B (^{13}C , 100MHz, CDCl_3)



8 (^1H , 400 MHz, CDCl_3)



8 (^{13}C , 100MHz, CDCl_3)



Chemical structure of 3A: CCOC(=O)C1=CC=C(C=C1)/C=C/c2ccccc2OC(C)C

¹H NMR spectrum (CDCl₃):

Chemical Shift (ppm)	Integration
7.36, 7.34, 7.18, 7.17	0.97, 1.05, 0.99, 1.03
6.95, 6.93, 6.88, 6.86	0.91
6.28, 6.25	0.94
5.81, 5.80, 5.79	0.95
4.50, 4.49, 4.47, 4.14, 4.13, 4.11	0.96, 4.00
3.11	1.89
2.73	1.98
1.52 (H ₂ O)	-
1.32, 1.30, 1.15, 1.13	7.47, 6.12

3A

Chemical structure of **3A** is shown above the spectrum. The structure is a 1,4-diene derivative with an ethyl ester group, a vinyl group, and a 4-isopropoxyphenyl group.

Chemical shifts (ppm) labeled on the spectrum:

- 171.27
- 156.03
- 135.45
- 132.25
- 131.53
- 130.39
- 128.07
- 125.41
- 125.12
- 120.30
- 114.17
- 70.93
- 61.55
- 54.25
- 31.94
- 31.60
- 22.34
- 14.07

Chemical structure of **2B** is shown as an inset. The ^1H NMR spectrum (CDCl₃) displays the following peaks (ppm) and integration values:

Chemical Shift (ppm)	Integration
6.13, 6.13, 5.79, 5.79, 5.77, 5.76	0.84, 0.88
4.90, 4.87	2.00
2.75, 2.57, 2.57, 2.56	2.02, 2.05
1.43, 1.43	18.62

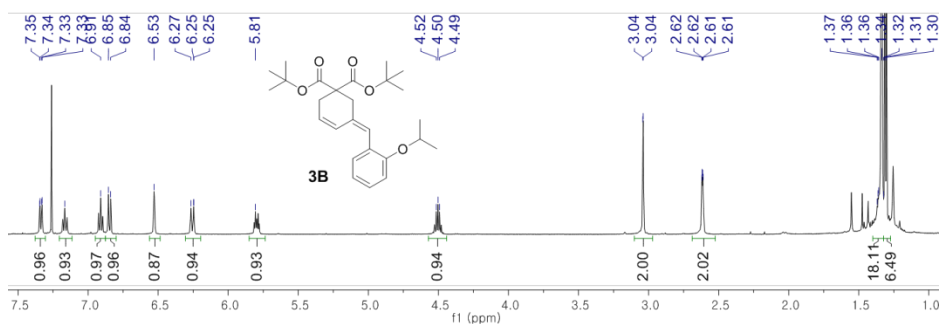
A water peak (H₂O) is indicated at approximately 3.3 ppm.

2B

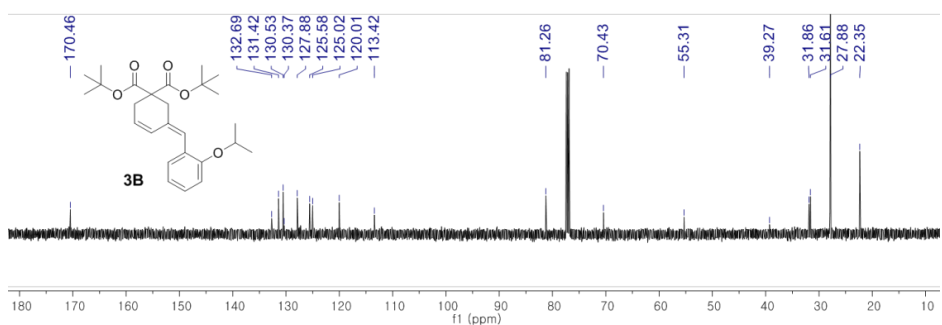
170.32, 139.85, 128.89, 126.96, 113.03, 81.32, 54.97, 36.13, 31.09, 27.94

f1 (ppm)

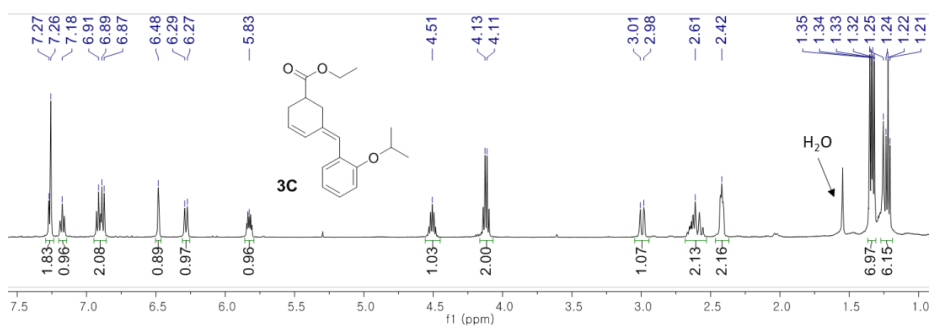
3B (^1H , 500 MHz, CDCl_3)



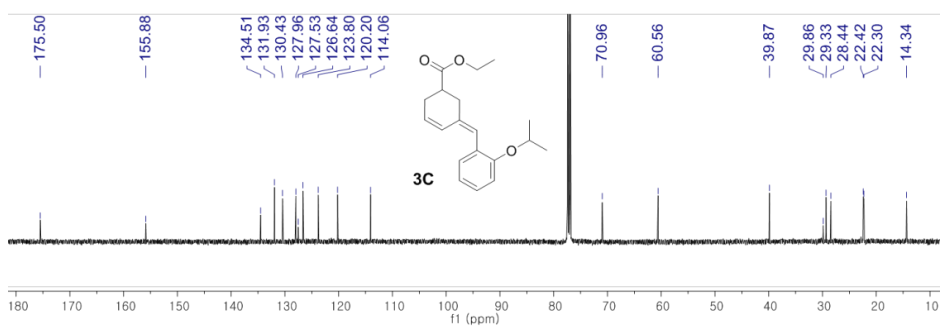
3B (^{13}C , 125 MHz, CDCl_3)



3C (^1H , 500 MHz, CDCl_3)



3C (^{13}C , 125 MHz, CDCl_3)



NOESY NMR of P(7) and conformational analysis

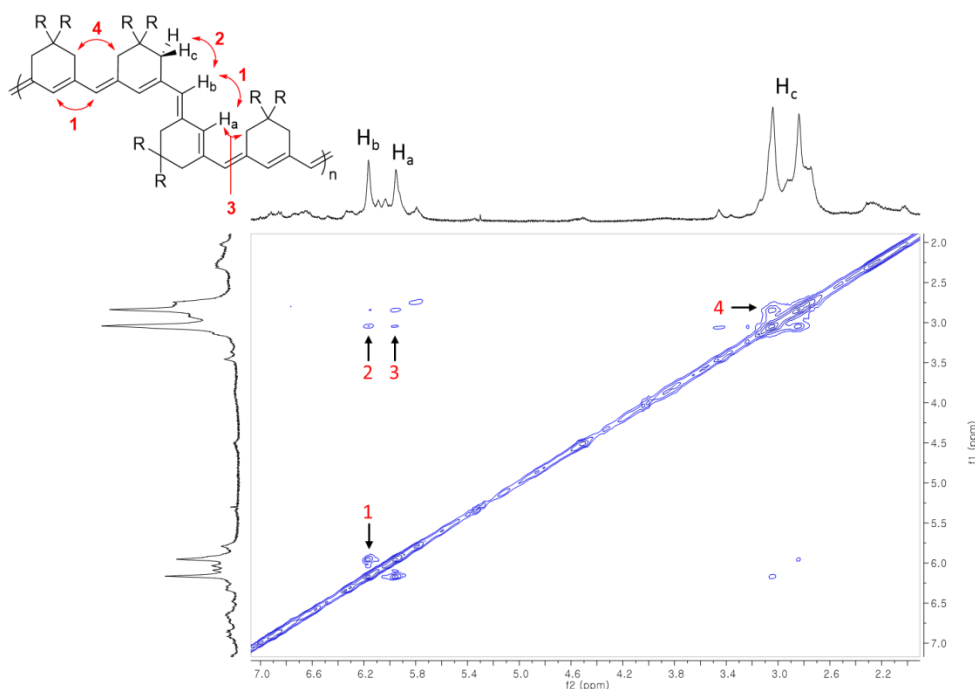


Figure S2.16 NOESY NMR of P(7) and conformational analysis

There can be both *cis* and *trans* conformation of the olefins in the polymer backbone. In case of P(7-I), there is a small portion of *cis* conformers (about 15%) right after the polymerization (as depicted in Fig S2.15), and one can observe the *cis*-to-*trans* isomerization by aging experiments. The vibronic peak in longer wavelength in UV-Vis absorption spectrum increased with increasing *trans* conformers.^{21c}

In contrast, the UV-Vis absorption spectrum of P(7) neither contained any discrete vibronic peak nor showed any changes by aging or blue LED irradiation. One informative aspect in ¹³C NMR was that all of the 5-membered ring repeat units existed in *cis* conformation (as depicted in Fig S15). This statement was added to the manuscript. Therefore, the λ_{max} of

P(7) would be somewhat red-shifted than P(7-I) which contains majorly *trans* olefins.

However, we couldn't find out any clues about the conformation of 6-membered ring repeat units by ^1H NMR spectrum, which led us to try 2D NMR (NOESY) analysis of P(7). When focusing on the 6-membered ring repeat unit only, we found that both *s-trans* and *s-cis* conformation could exist to support the observed NOE 1, 2, 3 and 4. NOE 2 and 3 could appear in *s-cis* conformation, while NOE 4 in *s-trans* conformation.

2.7 References

1. (a) Kang, E.-H.; Lee, I. S.; Choi, T.-L., *J. Am. Chem. Soc.* **2011**, *133*, 11904; (b) Kang, E.-H.; Lee, I.-H.; Choi, T.-L., *ACS Macro Lett.* **2012**, *1*, 1098; (c) Kim, J.; Kang, E.-H.; Choi, T.-L., *ACS Macro Lett.* **2012**, *1*, 1090; (d) Kang, E.-H.; Choi, T.-L., *ACS Macro Lett.* **2013**, *2*, 780; (e) Kang, E.-H.; Yu, S. Y.; Lee, I. S.; Park, S. E.; Choi, T.-L., *J. Am. Chem. Soc.* **2014**, *136*, 10508; (f) Yang, S.; Shin, S.; Choi, I.; Lee, J.; Choi, T.-L., *J. Am. Chem. Soc.* **2017**, *139*, 3082.
2. (a) Lee, I. S.; Kang, E.-H.; Park, H.; Choi, T.-L., *Chem. Sci.* **2012**, *3*, 761; (b) Park, H.; Lee, H. K.; Choi, T. L., *Polym. Chem.* **2013**, *4*, 4676; (c) Song, J. A.; Park, S. E.; Kim, T. S.; Choi, T. L., *ACS Macro Lett.* **2014**, *3*, 795; (d) Park, H.; Lee, H.-K.; Kang, E.-H.; Choi, T.-L., *J. Polym. Sci. A* **2015**, *53*, 274.
3. (a) Schattenmann, F. J.; Schrock, R. R., *Macromolecules* **1996**, *29*, 8990; (b) Schattenmann, F. J.; Schrock, R. R.; Davis, W. M., *J. Am. Chem. Soc.* **1996**, *118*, 3295.
4. Keitz, B. K.; Endo, K.; Patel, P. R.; Herbert, M. B.; Grubbs, R. H., *J. Am. Chem. Soc.* **2012**, *134*, 693.
5. (a) Endo, K.; Grubbs, R. H., *J. Am. Chem. Soc.* **2011**, *133*, 8525; (b) Keitz, B. K.; Endo, K.; Herbert, M. B.; Grubbs, R. H., *J. Am. Chem. Soc.* **2011**, *133*, 9686; (c) Rosebrugh, L. E.; Herbert, M. B.; Marx, V. M.; Keitz, B. K.; Grubbs, R. H., *J. Am. Chem. Soc.* **2013**, *135*, 1276; (d) Bronner, S. M.; Herbert, M. B.; Patel, P. R.; Marx, V. M.; Grubbs, R. H., *Chem. Sci.* **2014**, *5*, 4091; (e) Herbert, M. B.; Suslick, B. A.; Liu, P.; Zou, L.; Dornan, P. K.; Houk, K. N.; Grubbs, R. H., *Organometallics* **2015**, *34*, 2858.
6. (a) Cannon, J. S.; Grubbs, R. H., *Angew. Chem., Int. Ed.* **2013**, *52*, 9001; (b) Herbert, M. B.; Marx, V. M.; Pederson, R. L.; Grubbs, R. H., *Angew. Chem., Int. Ed.* **2013**, *52*, 310; (c) Mangold, S. L.; O'Leary, D. J.; Grubbs, R. H., *J. Am.*

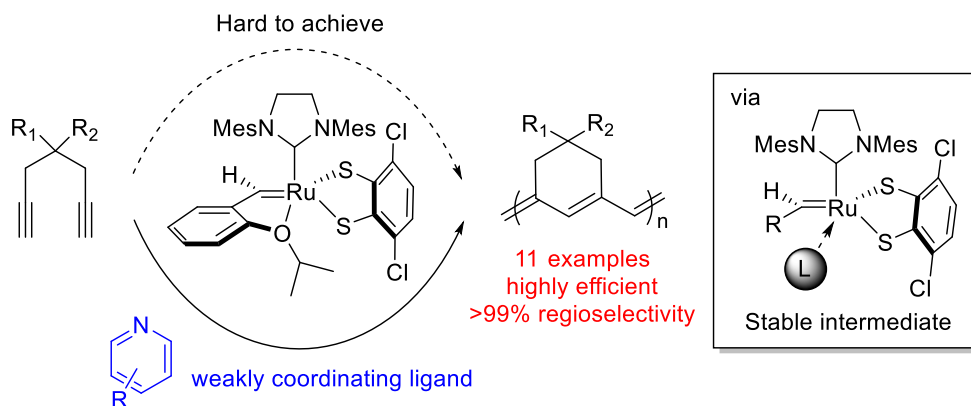
- Chem. Soc.* **2014**, *136*, 12469; (d) Quigley, B.; Grubbs, R. H., *Chem. Sci.* **2014**, *5*, 501.
7. Marx, V. M.; Herbert, M. B.; Keitz, B. K.; Grubbs, R. H., *J. Am. Chem. Soc.* **2013**, *135*, 94.
8. (a) Hartung, J.; Grubbs, R. H., *J. Am. Chem. Soc.* **2013**, *135*, 10183; (b) Hartung, J.; Dornan, P. K.; Grubbs, R. H., *J. Am. Chem. Soc.* **2014**, *136*, 13029; (c) Hartung, J.; Grubbs, R. H., *Angew. Chem., Int. Ed.* **2014**, *53*, 3885.
9. Miyazaki, H.; Herbert, M. B.; Liu, P.; Dong, X.; Xu, X.; Keitz, B. K.; Ung, T.; Mkrtumyan, G.; Houk, K. N.; Grubbs, R. H., *J. Am. Chem. Soc.* **2013**, *135*, 5848.
10. (a) Keitz, B. K.; Fedorov, A.; Grubbs, R. H., *J. Am. Chem. Soc.* **2012**, *134*, 2040; (b) Rosebrugh, L. E.; Marx, V. M.; Keitz, B. K.; Grubbs, R. H., *J. Am. Chem. Soc.* **2013**, *135*, 10032.
11. (a) Liu, P.; Xu, X.; Dong, X.; Keitz, B. K.; Herbert, M. B.; Grubbs, R. H.; Houk, K. N., *J. Am. Chem. Soc.* **2012**, *134*, 1464; (b) Dang, Y.; Wang, Z. X.; Wang, X., *Organometallics* **2012**, *31*, 7222; (c) Dang, Y.; Wang, Z. X.; Wang, X., *Organometallics* **2012**, *31*, 8654.
12. (a) Romero, P. E.; Piers, W. E., *J. Am. Chem. Soc.* **2005**, *127*, 5032; (b) Wenzel, A. G.; Grubbs, R. H., *J. Am. Chem. Soc.* **2006**, *128*, 16048.
13. Diver, S. T.; Giessert, A. J., *Chem. Rev.* **2004**, *104*, 1317.
14. (a) Kinoshita, A.; Mori, M., *Synlett* **1994**, 1020; (b) Stragies, R.; Schuster, M.; Blechert, S., *Angew. Chem., Int. Ed.* **1997**, *36*, 2518; (c) Kitamura, T.; Sato, Y.; Mori, M., *Chem. Commun.* **2001**, 1258; (d) Dieltiens, N.; Moonen, K.; Stevens, C. V., *Chem. Eur. J.* **2007**, *13*, 203.
15. Mori, M.; Sakakibara, N.; Kinoshita, A., *J. Org. Chem.* **1998**, *63*, 6082.
16. (a) Singh, R.; Schrock, R. R.; Muller, P.; Hoveyda, A. H., *J. Am. Chem. Soc.* **2007**, *129*, 12654; (b) Lee, Y. J.; Schrock, R. R.; Hoveyda, A. H., *J. Am.*

- Chem. Soc.* **2009**, *131*, 10652; (c) Zhao, Y.; Hoveyda, A. H.; Schrock, R. R., *Org. Lett.* **2011**, *13*, 784.
17. Park, H.; Kang, E.-H.; Müller, L.; Choi, T.-L., *J. Am. Chem. Soc.* **2016**, *138*, 2244.
18. (a) Liu, J. Z.; Lam, J. W. Y.; Tang, B. Z., *Chem. Rev.* **2009**, *109*, 5799; (b) Kumar, P. S.; Wurst, K.; Buchmeiser, M. R., *J. Am. Chem. Soc.* **2009**, *131*, 387.
19. (a) Sohn, J. H.; Kim, K. H.; Lee, H. Y.; No, Z. S.; Ihee, H., *J. Am. Chem. Soc.* **2008**, *130*, 16506; (b) Kim, K. H.; Ok, T.; Lee, K.; Lee, H. S.; Chang, K. T.; Ihee, H.; Sohn, J. H., *J. Am. Chem. Soc.* **2010**, *132*, 12027; (c) Lee, O. S.; Kim, K. H.; Kim, J.; Kwon, K.; Ok, T.; Ihee, H.; Lee, H. Y.; Sohn, J. H., *J. Org. Chem.* **2013**, *78*, 8242; (d) Gutekunst, W. R.; Hawker, C. J., *J. Am. Chem. Soc.* **2015**, *137*, 8038.
20. Fox, H. H.; Schrock, R. R., *Organometallics* **1992**, *11*, 2763.
21. Fox, H. H.; Wolf, M. O.; O'Dell, R.; Lin, B. L.; Schrock, R. R.; Wrighton, M. S., *J. Am. Chem. Soc.* **1994**, *116*, 2827.
22. Anders, U.; Nuyken, O.; Buchmeiser, M. R., *Des. Monomers Polym.* **2003**, *6*, 135.
23. Yamamoto, T.; Omote, M.; Miyazaki, Y.; Kashiwazaki, A.; Lee, B. L.; Kanbara, T.; Osakada, K.; Inoue, T.; Kubota, K., *Macromolecules* **1997**, *30*, 7158.
24. Ryoo, M. S.; Lee, W. C.; Choi, S. K., *Macromolecules* **1990**, *23*, 3029.
25. Mayershofer, M. G.; Nuyken, O.; Buchmeiser, M. R., *Macromolecules* **2006**, *39*, 3484.
26. Czekelius, C.; Hafer, J.; Tonzetich, Z. J.; Schrock, R. R.; Christensen, R. L.; Müller, P., *J. Am. Chem. Soc.* **2006**, *128*, 16664.
27. Atkinson, R. S.; Grimshire, M. J., *J. Chem. Soc., Perkin Trans. 1* **1986**, 1215.

Chapter 3. Toward Perfect Regiocontrol for β -
Selective Cyclopolymerization of 1,6-Heptadiyne
Derivatives Using a Ru Dithiolate Catalyst

3.1 Abstract

In chapter 2, we discovered that a chelated Ru catalyst could promote regioselective β -addition to produce analogous polyenes containing six-membered rings with moderate to good β -selectivity. Since then, we have focused our research on pursuing more active and β -selective regiocontrol to produce conjugated polymers with excellent β -selectivity, with a much broader range of monomers. In this chapter, we demonstrate highly β -selective CP by combining a new dithiolate-chelated Ru-based catalyst with weakly coordinating pyridine additives, which significantly enhance the conversion and β -selectivity. An in-depth mechanistic investigation by ^1H NMR revealed a prominent role for the additives, which improve the stability of the propagating carbene.

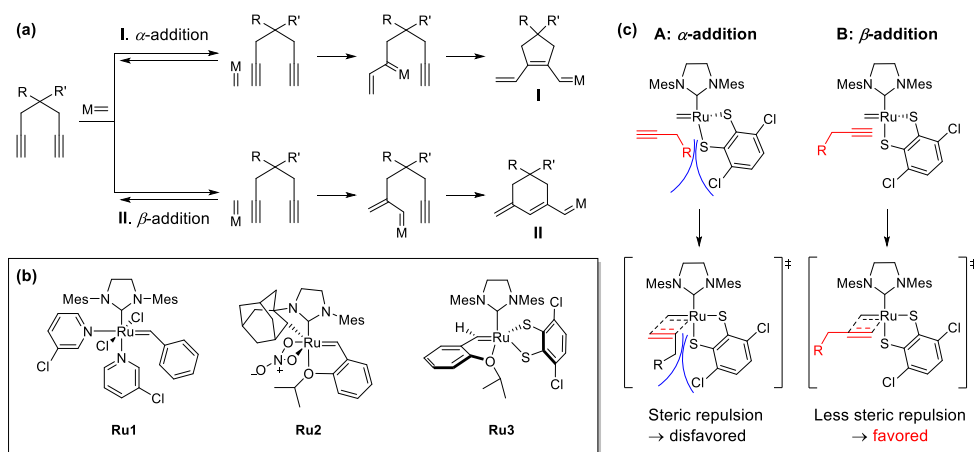


3.2 Introduction

Cyclopolymerization (CP) of terminal diynes via an olefin metathesis is one of the most efficient and powerful tools for the synthesis of conjugated polymers.¹ One of the most important issues for CP is controlling regioselectivity, which is determined by the orientation of the approaching metal carbenes toward the terminal alkynes.² For example, 1,6-heptadiyne derivatives undergo CP to produce five-membered rings by α -addition, where the metal approaches the side chains (Scheme 3.1a, Pathway I). The orientation of the metal away from the side chain for β -addition allows for CP to give six-membered rings (Pathway II). After the pioneering work of the Schrock and Buchmeiser groups, conjugated polyenes containing either six-³ or five-membered rings⁴ were successfully prepared by modifying Mo catalysts. Another breakthrough came when the Buchmeiser group reported the first CP employing user-friendly Ru-based catalysts to give five-membered-ring polyenes via complete α -addition.⁵ Our group also reported living and controlled CP using a fast-initiating, third-generation Grubbs catalyst (Scheme 3.1b, Ru1).⁶

Ru-catalyzed β -selective CP was able to achieve by our group, employing a new class of Ru-based catalysts containing a chelating adamantyl group on the *N*-heterocyclic carbene (NHC) ligand (Ru2),⁷ known as Grubbs *Z*-selective catalysts. The unconventional selectivity of this unique catalyst led us to demonstrate a ring-closing enyne metathesis via exclusive β -selectivity and CP to produce conjugated polyenes with good to high β -selectivity (67–95%).⁸ After extensive optimization of the monomer

structures and reaction conditions, a dialkyne monomer derived from di-*tert*-butyl malonate underwent CP with up to 93% of six-membered rings or β -selectivity. We proposed that this new regioselectivity originated from a side-bound pathway of alkynes toward the Ru center,⁹ which was contrary to the well-known, bottom-bound pathway for conventional Grubbs catalysts.¹⁰



Scheme 3.1 (a) Two possible pathways for CP of 1,6-heptadiynes, (b) various Ru-based catalysts, and (c) proposed model for the preference of β -addition in Ru3-catalyzed CP

Although this was a meaningful achievement as the first example for Ru catalysts to undergo β -selective CP, there still remained some drawbacks: only malonate monomers bearing sterically bulky groups showed good β -selectivity at a low temperature (e.g., $-40\text{ }^{\circ}\text{C}$), and long reaction time (over 36 h) was therefore required. We thus explored the possibility of developing significantly improved β -selective CP and anticipated Ru catalysts containing catechothiolate ligands developed by the Hoveyda group (**Ru3**)¹¹

would operate by a similar mechanism¹¹⁻¹² and show β -selective CP, as depicted in Scheme 3.1c.

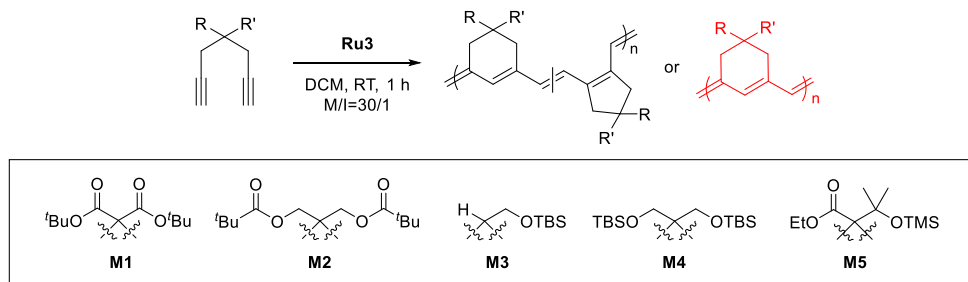
Here, we report superior β -selective CP by **Ru3** at room temperature and disclose the origin of the different regio-preference of **Ru1**–**Ru3** by computational studies. After our full account of the complete screening of additives and monomers, detailed kinetic studies reveal mechanistic insights leading to plausible models for improved β -selective CP.

3.3 Results and discussion

Initially, we employed the substrate **M1** containing *tert*-butyl malonate in a monomer to catalyst (M/I) ratio of 30:1 at room temperature (entry 1, Table 3.1). To our delight, the resulting conjugated polymer **P1** contained a very high proportion of six-membered rings in the polymer (1:16.6, 94% six-membered ring) even at room temperature. This finding is a significant improvement of the β -selectivity compared to **Ru2**, which showed a lower six-membered ring composition (1:6.5) at room temperature. Higher selectivity of 1:13.8 was only possible by lowering the temperature to $-40\text{ }^{\circ}\text{C}$ with prolonged reaction time over 24 hours.⁸ A different *tert*-butyl ester-containing substrate **M2** also exhibited high β -selectivity using **Ru3**, while **Ru2** resulted in poor selectivity (1:11.8 vs. 1:1.5, entry 2). To test for a broader substrate scope, we introduced weaker chelating ether groups (**M3**–**M5**). The mono-substituted diyne **M3** also produced the conjugated polyene bearing six-membered ring exclusively when polymerized at room temperature (entry 3). This selectivity is remarkable because the analogous

CP using Ru2 showed no selectivity at all (Table S3.1 in section 3.6, <1:99 vs. 1:1, entry 3). With an increased steric influence in the bis-silylether monomer **M4**, the CP proceeded more efficiently and retained the excellent β -selectivity unlike what was seen when Ru2 was used (Table S3.1, <1:99 vs. 1:1.7, entry 4). Finally, a monomer containing both ester and bulky ether moieties underwent complete conversion and exclusive β -addition at room temperature (Table S3.1, <1:99 vs. 1:1.4, entry 5). The last three results represent the first examples of producing conjugated polyenes with complete six-membered ring repeat units using a user-friendly Ru catalyst system and they highlight the dramatic improvement of regiocontrol and monomer scope that the new strategy enables.

Table 3.1 β -Selective CP of various 1,6-heptadiynes using Ru3



entry	monomer	conv (%) ^a	yield (%) ^b	M_n (kDa) ^c	\bar{D} ^e	5:6 ^d
1 ^c	M1	95	93	16.1	1.71	1:16.1
2	M2	84	53	15.3	1.61	1:11.8
3	M3	51	47	6.7	1.51	<1:99
4	M4	>99	89	19.6	1.79	<1:99
5	M5	>99	70	25.8	1.92	<1:99

^aDetermined from ¹H NMR. ^bPrecipitated in MeOH at -78 °C. ^cDetermined from THF-SEC.

^d5-Membered:6-membered rings, determined from ¹³C NMR. ^ePrecipitated in hexane at -78 °C.

The different regioselectivity of the three catalysts (Ru1–Ru3) was easily distinguishable in ^1H NMR spectra of the crude reaction mixtures prepared using Ru1, Ru2, and Ru3 (Figure 3.1). The olefin signals on the conjugated polymer backbone showed different chemical shifts, depending on the ring size of the repeat units; around 6.7 ppm from five-membered rings, whereas 6.2 and 5.8 ppm from six-membered rings. While CP using Ru1 generated the conjugated polymers containing five-membered rings as the only repeat unit via exclusive α -addition, Ru2 generated a mixture of five- and six-membered rings on the polymer backbone, which is well-reflected in complex proton signals at 6.7–5.8 ppm. To our surprise, CP using Ru3 gave much more clear spectra in most of the monomers, mainly showing six-membered-ring signals via a high level of β -addition (Figure 3.1).

The backbone selectivity of these conjugated polyenes was also analyzed using ^{13}C NMR (Figure 3.2); P5 synthesized using Ru1 showed distinctive signals corresponding to the carbonyl and quaternary carbon in the five-membered rings at 176.3 and 60.9 ppm, whereas the analogous carbons on the six-membered rings prepared using Ru3 appeared at 174.2 and 60.4 ppm, respectively. Interestingly, the same polymer P5 prepared using Ru2 showed a mixture of two signals corresponding to the two possible regiochemistries in both the ^1H and ^{13}C NMR spectra (Figures 3.1 and 3.2), and the ratio between six- and five-membered rings was determined to be 1.4:1 by NMR integration.

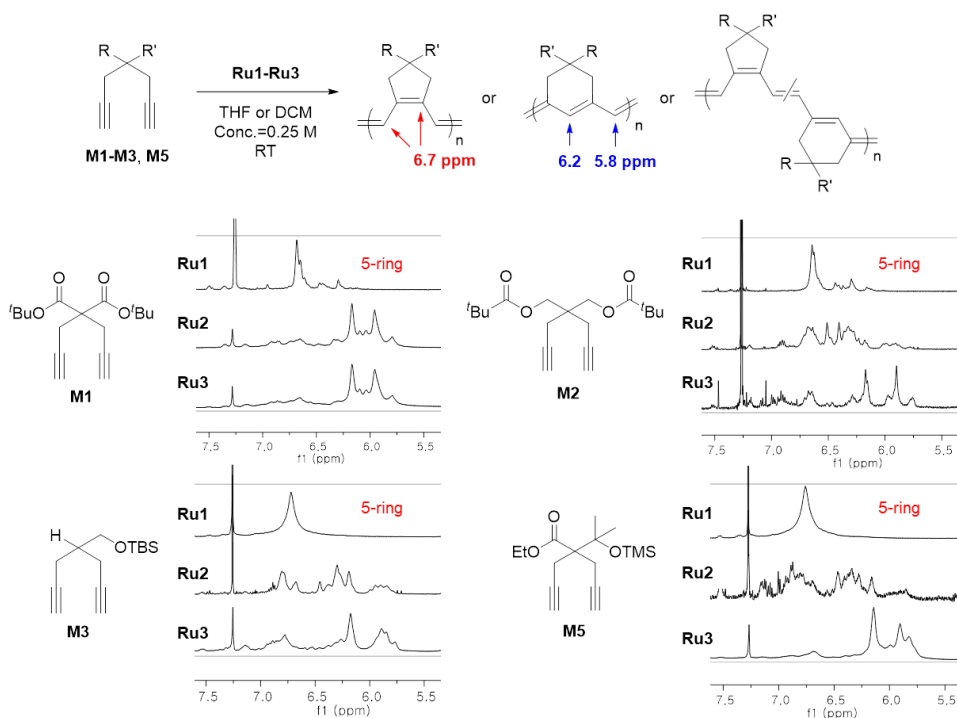


Figure 3.1 Conjugated backbone signals in ^1H NMR spectra of the crude reaction mixtures from various monomers and Ru catalysts

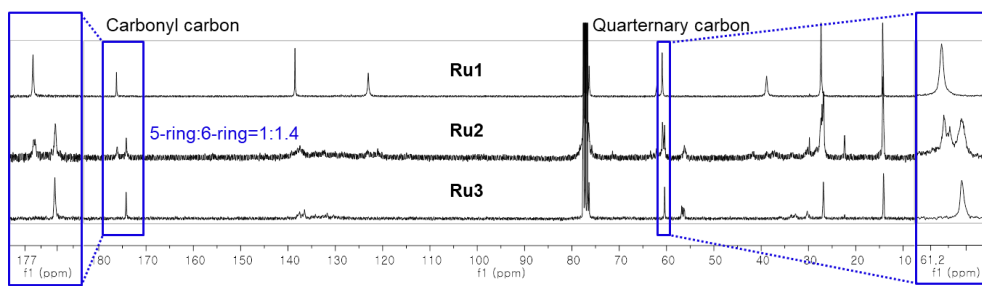


Figure 3.2 Comparison of ^{13}C NMR spectra of P5 synthesized using Ru1-Ru3

We embarked on a combined experimental and computational study to establish a conceptual foundation for our optimization efforts. By investigating the calculated reaction energy profiles of the insertion step mediated by Ru1-Ru3 via density functional theory (DFT) studies, we

found that the geometrical difference of the three catalysts might change the electronic properties of Ru carbene, thereby induced the switch of the intrinsic electronic demand; the carbene in trigonal bipyramidal geometry (Ru3) will be much less electrophilic than the carbene in octahedral geometry (Ru1), due to stronger π -backdonation (Figure 3.3).¹³ Therefore, the electronic preference for α -addition is reduced, and steric factors may become more important in the Ru3 system, favoring β -addition even more so than Ru2. As a result, we suggested the origin of the α - and β -selectivity of CP based on electronic and steric factors of various Ru catalysts, which is in accordance with the experimental results.¹³

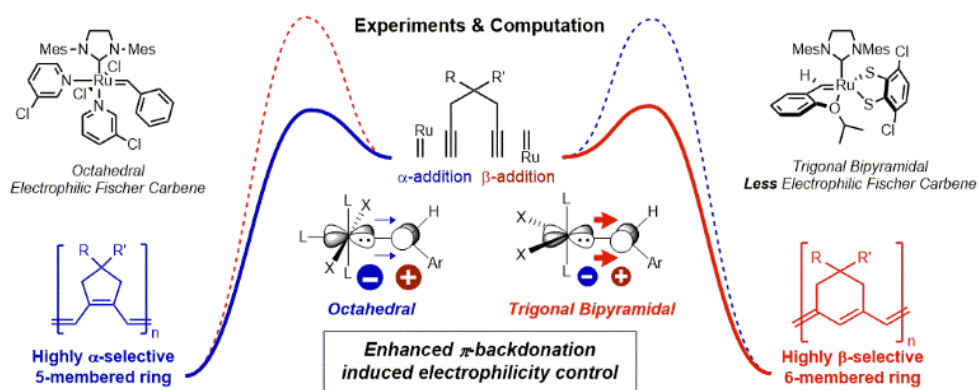
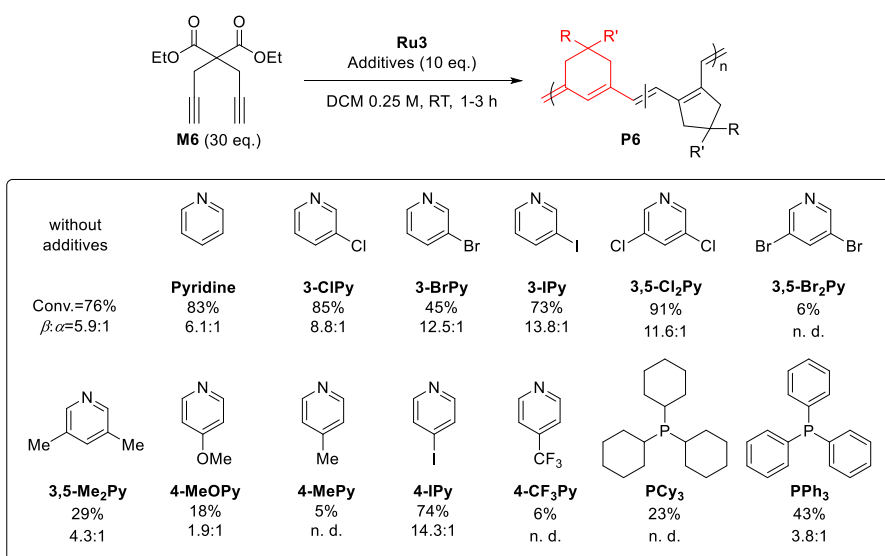


Figure 3.3 Understanding the origin of the regioselectivity in CPs

Although the β -selectivity of CP was improved by using Ru3, the polymerization efficiency of several monomers remained too low (entry 3 in Table 3.1). With this preliminary data, we decided to investigate the breadth of the monomer scope and the versatility of CP in detail by understanding the factors that contribute to the activity and β -selectivity of CP.

Scheme 3.2 CP of **M6** using **Ru3** with various pyridine additives^a



^aConversion and regioselectivity were determined by ¹H NMR spectra.

As an initial attempt, we tested diethyl dipropargylmalonate (DEDPM, **M6**), one of the most commonly studied monomers for CP, with a monomer to initiator (**Ru3**) ratio (M/I) of 30:1 at room temperature. While the monomer conversion in tetrahydrofuran (THF) was low as 34%, it dramatically increased to 76% by changing the solvent to non-coordinating dichloromethane (DCM). This was rather surprising because DCM is a poor reaction solvent for conventional CP.¹⁴ Notably, the six-membered-ring selectivity as a result of β -addition was quite high, 5.9:1, as determined by ¹H NMR (Figure S3.7), compared to the previous moderate selectivity of 3.4:1 obtained by **Ru2** at room temperature.⁸ In order to further increase the β -selectivity, CP was conducted at a low temperature by adopting the strategy used in our previous study using **Ru2**.⁸ However, the result was not satisfactory, providing only 10% conversion of the monomer at 0 °C. Instead,

we screened some pyridine derivatives as an additive (Scheme 3.2) because our previous results for CP using **Ru1** indicated that weakly coordinating ligands such as 3,5-dichloropyridine (3,5-Cl₂Py) enhanced polymerization efficiency and controllability.^{6c} Unfortunately, addition of 10 equiv of pyridine to the initiator **Ru3** resulted in an insignificant improvement in monomer conversion and selectivity (83% and 6.1:1), while various 3-halogen-substituted pyridines, such as 3-ClPy, 3-BrPy, and 3-IPy, led to significantly higher β -selectivity (8.8–12.8:1) with low to good conversions. To our delight, 3,5-Cl₂Py significantly enhanced both polymerization efficiency and regioselectivity (91% conversion, 11.6:1), while analogous 3,5-dibromopyridine and 3,5-lutidine gave even lower conversion and selectivity than in the case without additives. A series of 4-substituted pyridines were also examined, but other than 4-iodopyridine, which gave a good result (74% conversion, 14.3:1), both electron-donating (Me or OMe) and withdrawing (CF₃) groups led to poor results. Phosphine additives, such as PCy₃ and PPh₃ were tested, but both conversion and regioselectivity were lower than even non-additive case. Among the various pyridine derivatives tested, 3,5-Cl₂Py was selected as the optimal additive that gave the best conversion and selectivity.

With this optimized condition, we investigated the CP of various ester-containing monomers (**M1,2,6–8**) that showed good efficiency and selectivity with the previous **Ru2** catalyst.⁸ As depicted in Scheme 3.2, **M6** was successfully polymerized to give the corresponding polymer **P6**, and its regioselectivity calculated from ¹H NMR spectra matched well with that from the ¹³C NMR spectra (Table 3.2, entries 1 and 2). Dispersities (*D*s) of

the resulting polymers appeared relatively broad, which might be attributed to the slow initiation. Compared to **M6**, **M7** containing a bulkier isopropyl group afforded **P7** with an M_n up to 14 kDa with greater incorporation of six-membered-rings, either without or with the additive (6.8:1 and 14.7:1, respectively, entries 3 and 4). We then tested **M1** derived from di-*tert*-butyl malonate, which showed the highest polymerization efficiency and selectivity in the previous study using **Ru2**,⁸ and the selectivity dramatically improved, generating the corresponding **P1** with an M_n up to 19 kDa and higher β -selectivity of 16.6:1 and 26.8:1 (entries 5 and 6). Additionally, amide-containing **M8** and another ester-containing **M2** were tested for CP to give **P8** and **P2** with good to excellent conversion and high selectivity (8.2:1 in entry 7 and 11.8:1 in entry 9), while the 3,5-Cl₂Py additive seemed to negatively affect the β -selectivity (entries 8 and 10).

Table 3.2 CP of 1,6–heptadiynes containing various substituents using Ru3

<div style="display: flex; justify-content: space-around; align-items: flex-end;"> <div> <p>DEDPM (M6)</p> </div> <div> <p>D'PrDPM (M7)</p> </div> <div> <p>D'BuDPM (M1)</p> </div> <div> <p>BisAmide (M8)</p> </div> <div> <p>BisOPiv (M2)</p> </div> </div>							
<div style="display: flex; justify-content: space-around; align-items: flex-end;"> <div> <p>MonoOTBS (M3)</p> </div> <div> <p>BisOTBS (M4)</p> </div> <div> <p>BisOTIPS (M9)</p> </div> <div> <p>BisOBn (M10)</p> </div> <div> <p>BisOEt (M11)</p> </div> <div> <p>Et-TMS (M5)</p> </div> </div>							

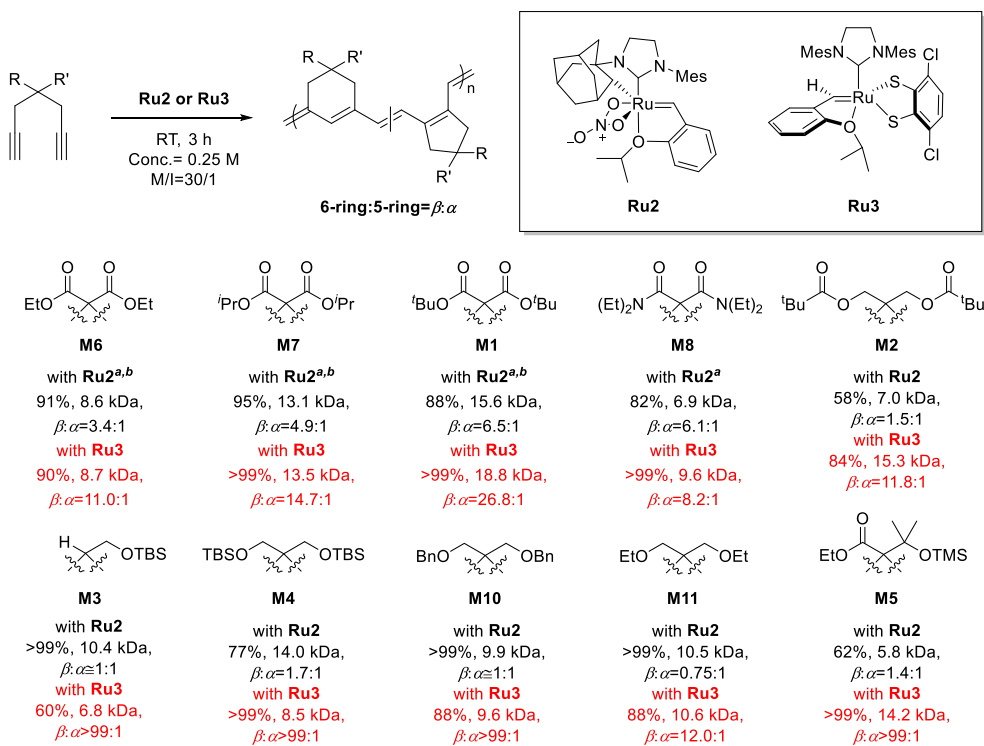
entry	monomer	M/I/Add	conv (%) ^a	yield (%) ^b	<i>M_n</i> (kDa) ^c	<i>Đ</i> ^c	6:5 ^d
1	M6	30/1/–	76	56	4.7	1.50	5.8:1
2	M6	30/1/10	91	89	8.7	1.75	11.0:1
3	M7	30/1/–	93	81	12.9	1.77	6.8:1
4	M7	30/1/10	>99	>99	13.5	1.58	14.7:1
5	M1	30/1/–	95	93	16.1	1.71	16.6:1
6	M1	30/1/10	>99	77	18.8	1.46	26.8:1
7	M8	30/1/–	>99	76	9.6	1.52	8.2:1
8	M8	30/1/10	>99	98	12.5	1.41	6.2:1
9 ^e	M2	30/1/–	84	53	15.3	1.61	11.8:1
10 ^e	M2	30/1/10	>99	75	17.6	1.34	8.6:1
11 ^e	M3	30/1/–	51	47	6.7	1.51	6–only
12 ^e	M3	30/1/10	60	33	6.8	1.50	6–only
13 ^e	M4	30/1/–	>99	89	19.6	1.79	6–only
14 ^e	M4	30/1/10	>99	64	8.5	1.41	6–only
15 ^e	M9	30/1/–	27	nd	nd	nd	nd
16 ^e	M9	30/1/10	95	60	15.0	1.30	6–only
17 ^e	M10	30/1/–	32	nd	nd	nd	nd
18 ^e	M10	30/1/10	88	64	9.6	1.66	6–only
19 ^e	M11	30/1/–	76	70	8.6	1.60	8.0:1
20 ^e	M11	30/1/10	>99	68	7.9	1.81	12.0:1
21 ^e	M5	30/1/–	>99	70	25.8	1.92	6–only
22 ^e	M5	30/1/10	>99	80	14.2	1.45	6–only

^aDetermined from ¹H NMR. ^bPrecipitated in hexane at -78 °C. ^cDetermined from THF-SEC. ^d6-Membered:5-membered rings, determined from ¹³C NMR. ^ePrecipitated in methanol at -78 °C.

To expand the monomer range in CP, we then examined CP of various ether-containing 1,6-heptadiyne derivatives (**M3**–**5**,**9**–**11**). First, **M3** containing a mono-substituted TBS-protected ether group at the C4 position was polymerized under standard conditions to give a low conversion of 51%, but to our surprise, **P3** contained only six-membered rings via exclusive β -addition, as determined by ¹³C NMR analysis. (Table 3.2, entry 11). Again, we tested the polymerization with the 3,5-Cl₂Py additive and **P3** again gave exclusive six-membered-ring selectivity, with a higher conversion of 60% (entry 12). CP of **M4** with bulkier bis-substituted TBS afforded complete conversion and exclusive β -selectivity under both without or with the additive (entries 13 and 14). Monomers containing bulky substituents, such as **M9** and **M10**, showed lower reactivity and unsatisfactory conversions at room temperature (27% and 32%, respectively, entries 15 and 17), but, with the help of the additive, both polymerized well to give **P9** and **P10** with excellent β -selectivity (94% and 88%, respectively, entries 16 and 18). **M11**, having an ethyl ether side chain, exhibited in good polymerization efficiency (76%), but decreased β -selectivity compared to **M10** was observed, owing to smaller side chains (8.0:1, entry 19). Fortunately, both conversion and selectivity improved to 99% and 12:1, respectively, with the help of the additive (entry 20). Based on the critical influence of steric factors on β -selectivity, we tried CP of **M5** that contains both ester and bulky ether moieties,¹⁵ which produced **P5** with excellent

conversion, β – regioselectivity ($>99:1$) and high M_n (up to 25 kDa), and under both polymerization conditions (entries 21 and 22). In short, we successfully promoted CP of various monomers via selective β – addition, thereby significantly expanding the monomer scope range compared to previous reports.⁸

Scheme 3.3 Comparison of the polymerization efficiency and selectivity using Ru2 and Ru3



^aSee reference 8. ^bM/I = 50/1.

Overall, the reactivity of **Ru2** and **Ru3** toward various monomers appeared to be similar, but the β -selectivity at room temperature to give six-membered-ring repeat units on the polymer backbone was far higher in the **Ru3** case (summarized in Scheme 3.3). For **M1,6–8** derived from malonates, moderate to good β -selectivity (3.4:1–6.5:1) was observed with **Ru2**, but β -selectivity significantly increased to 8.2:1–26.8:1 with **Ru3** (Scheme 3.3). Surprisingly, for other monomers, **Ru2** afforded the corresponding polymers with poor regioselectivity (nearly 1:1 mixtures of five- and six-membered rings), whereas **Ru3** promoted excellent β -selective CP to produce polymers containing exclusively six-membered-rings (**M3**, **M4**, **M10**, and **M5**), or as a major portion (**M2** and **M11**, ~12:1) (Scheme 3.3).

We characterized the optical, electronic, and physical properties of the new conjugated polyenes prepared via β -addition, which are summarized in Table S3.3 (Section 3.6). From the UV-Vis absorption spectra, λ_{max} of the conjugated polyenes with six-membered rings appears between 519–539 nm, which is significantly lower than that of five-membered-ring polymers (around 590 nm), and no vibronic peak derived from 0–0, 0–1 transition is observed. On the other hand, their optical band gaps obtained from the onset point from the UV-Vis spectra were consistently lower by approximately 0.1 eV (1.9 vs. 2.0 eV). For thermal properties, we found that the decomposition temperature (T_d) appears to increase with increasing size of the substituents, from 219 to 370 °C, while their glass transition temperatures (T_g) are not much different (71 to 133 °C).

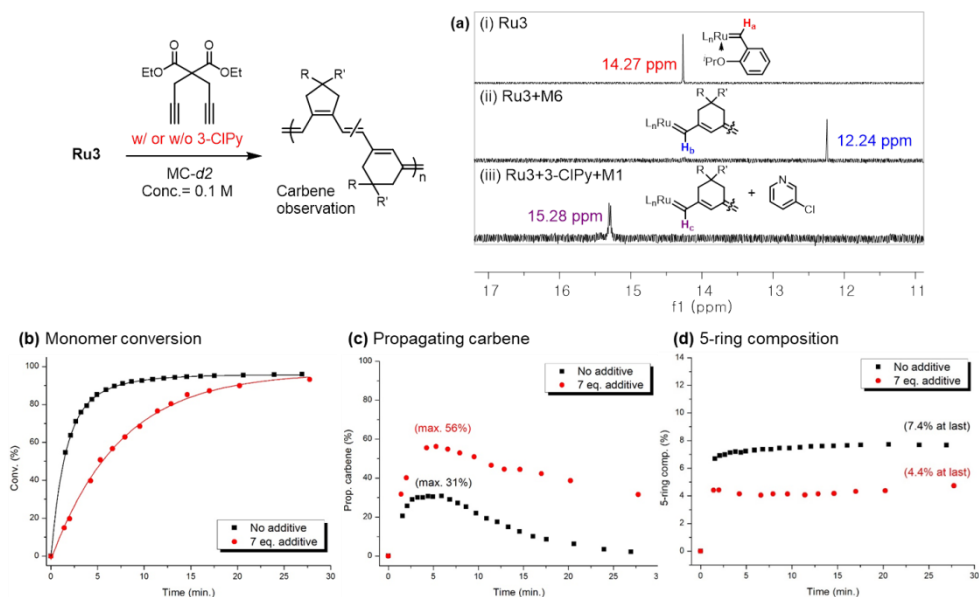


Figure 3.4 (a) ^1H NMR spectra of the initial carbene of Ru3 (i), and propagating carbene of Ru3 without and with additive (ii, iii). Plots of (b) monomer conversion, (c) propagating carbene, and (d) five-membered ring composition vs. time for the CP of M6 with $[\text{M}]:[\text{I}]=20:1$

To gain better insight into why the additive to Ru3 enhances activity, a series of *in situ* kinetic experiments was conducted by monitoring the polymerization of a model compound M6 by ^1H NMR ($[\text{M}]:[\text{I}]=20:1$ in 0.1 M $\text{DCM}-d_2$, Figure 3.4). The initial benzylidene in Ru3 at 14.27 ppm shifted to 12.24 ppm, corresponding to a new propagating carbene. Meanwhile, adding the additive 3-ClPy (note: for NMR experiment, liquid 3-ClPy was used instead of solid 3,5-Cl₂Py because it was easier to add to the NMR tube), resulted in another chemical shift for the propagating carbene to 15.28 ppm (Figure 3.4a). By monitoring the conversion, CP without pyridine additives proceeded about four times faster than with 7

equiv of additives (Figures 3.4b and S3.7, $k_p=0.126$ vs. 0.458). However, the population of propagating carbene increased up to 56% with the additive compared to a maximum of 31% in the case of no additive (Figure 3.4c). Furthermore, the decrease in the propagating carbene or catalyst decomposition was significantly slower with the additive. This result indicates that the additive indeed coordinates to the Ru metal thereby enhancing the stability of the propagating carbenes.^{6c} Therefore, although polymerization is slower owing to competitive coordination of the additive, a higher conversion is obtained because of a longer lifetime of the propagating carbenes (Figure 3.4c). More significantly, the β -selectivity could be monitored by integrating the allylic signal from the five-membered ring repeating unit, and as a result, lower α -selectivity (4.4% vs. 7.4%) or higher β -selectivity (21.7:1 vs. 12.5:1) was observed with the additive in the NMR tube reaction (Figure 3.4d).

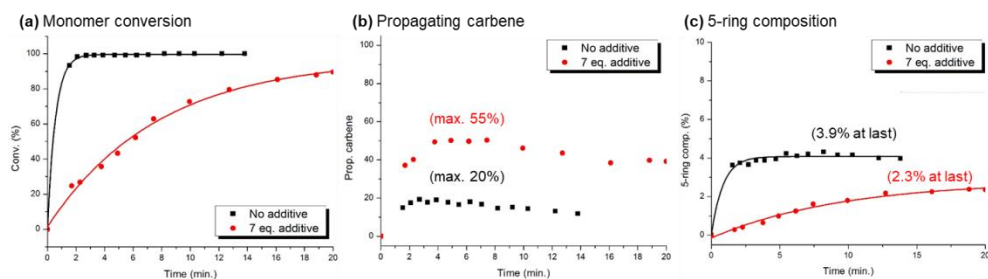


Figure 3.5 Plots of (a) monomer conversion, (b) propagating carbene, and (c) five-membered ring composition vs. time for the CP of **M7** with $[M]:[I]=20:1$

The similar effects of the pyridine additive were observed in kinetic experiments by ^1H NMR, during CP of **M7** ($[\text{M}]:[\text{I}]=20:1$ in 0.1 M DCM- d_2 , Figure 3.5). Addition of 7 equiv of 3-chloropyridine to **Ru3**, led to slower polymerization, higher generation of the propagating carbenes, and higher β -selectivity of the polymer backbone.

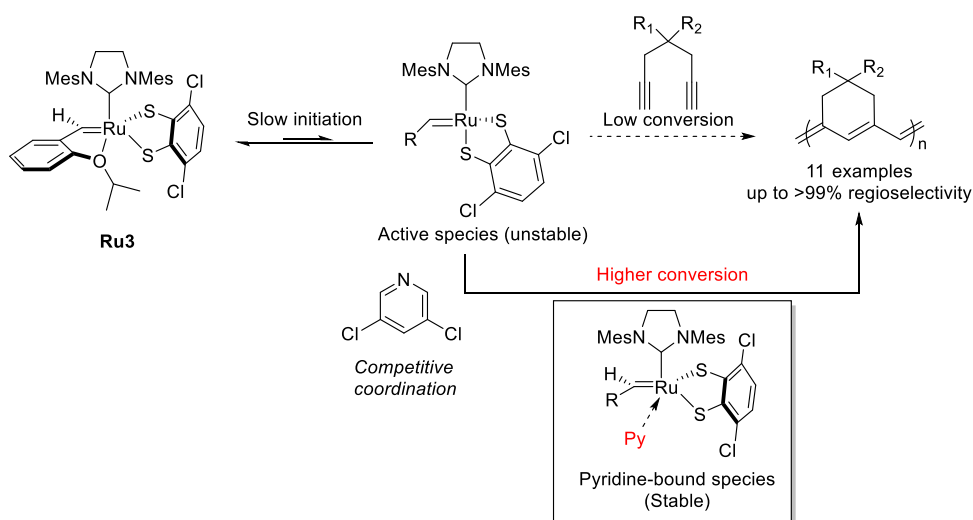


Figure 3.6 Proposed scheme showing the effects of pyridine additive

Although it is not clear how the additive enhances β -selectivity, we suggest a plausible model for the additive's effect on CP when using **Ru3** (Figure 3.6).¹⁶ Initiation of **Ru3** generates an unstable 14 e^- active species, which readily decomposes to give low conversion in CP. However, the right pyridine additives can enhance the stability of the propagating species by weak coordination to the metal, which lowers the termination rate. These features allow for more efficient polymerization, which somehow produces higher β -selectivity as well.

3.4 Conclusion

In summary, we successfully synthesized various conjugated polyenes containing six-membered ring repeat units via highly selective β -addition in the CP of 1,6-heptadiynes using a new Ru-based catalyst (**Ru3**). Based on our findings on the geometry and electronic character of **Ru3**, and with the help of pyridine additives, we developed efficient and regioselective CP, which afforded far greater β -selectivity than the previously reported CP using another chelated catalyst (**Ru2**). In particular, while **Ru2** promoted satisfactory β -selective CP only with malonate-type monomers, and very poor selectivity for various other monomers, **Ru3** exhibited high to exclusive β -selectivity for all monomers, demonstrating its superior monomer scope. The optoelectronic and thermal properties of the resulting conjugated polymers were compared with those of previously reported polyenes containing five-membered rings. Finally, through in-depth mechanistic investigation using ^1H NMR spectroscopy, we found that pyridine additives play an important role in enhancing not only the stability of the propagating carbenes, but also the β -addition regioselectivity. These extensive studies on CP using a Ru catalyst bearing catechothiolate ligands and the effect of exogenous pyridine additives should expand the understanding and applicability of Ru-catalyzed olefin metathesis polymerization.

3.5 Experimental Section

Materials

All reagents which are commercially available from Sigma–Aldrich®, Tokyo Chemical Industry Co. Ltd., Acros Organics, Alfa Aesar®, without additional notes, were used without further purification. Dichloromethane for the polymerization was purified by Glass Contour Organic Solvent Purification System, and degassed further by Ar bubbling for 10 minutes before performing reactions. Thin-layer chromatography (TLC) was carried out on MERCK TLC silica gel 60 F254, and flash column chromatography was performed using MERCK silica gel 60 (0.040~0.063 mm).

Characterization

¹H–NMR and ¹³C–NMR were recorded by Varian/Oxford As–500 (500 MHz for ¹H and 125 MHz for ¹³C) and Agilent 400–MR (400 MHz for ¹H and 100 MHz for ¹³C) spectrometers. ¹³C NMR for the polymers were mainly recorded by Bruker (600 MHz for ¹H and 150 MHz for ¹³C) spectrometers in the National Instrumentation Center for Environmental Management (NICEM) at SNU. High-resolution mass spectroscopy (HRMS) analyses were performed by the ultrahigh resolution ESI Q–TOF mass spectrometer (Bruker, Germany) in the Sogang Centre for Research Facilities. Size exclusion chromatography (SEC) analyses were carried out with Waters system (1515 pump, 2414 refractive index detector) and Shodex GPC LF–804 column eluted with THF (GPC grade, Honeywell Burdick & Jackson®) and filtered with a 0.2 μm PTFE filter (Whatman®).

The flow rate was 1.0 mL/min, and the temperature of the column was maintained at 35 °C. UV–Vis spectra were obtained by Jasco Inc. UV/vis Spectrometer V-650. Thermogravimetric analysis (TGA) and differential scanning calorimetry (DSC) were carried out under N₂ gas at a scan rate of 10 °C/min with Q50 and Q10 model devices, respectively, from TA Instruments. Cyclic voltammetry (CV) measurements were carried out on a CHI 660 Electrochemical Analyzer (CH Instruments, Inc., Texas, USA).

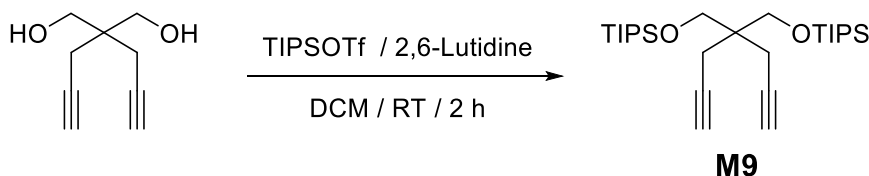
Cyclic Voltammetry (CV)

Cyclic voltammetry (CV) measurement was carried out at the room temperature on a CHI 660 Electrochemical Analyzer (CH Instruments, Inc., Texas, USA) using a degassed acetonitrile solution of tetrabutylammonium hexafluorophosphate (Bu₄NPF₆, 0.1 M). The polymer solution was prepared by dissolving the polymer in dichloromethane (10 mg/ml). Cyclic voltammogram was recorded using the glassy carbon working electrode and a reference electrode of Ag/Ag⁺ (0.1 M AgNO₃ in acetonitrile) with a platinum wire counter electrode at a scan rate of 50 mV/s. The absolute energy level was obtained using ferrocene/ferrocenium as an internal standard. The oxidation potential of ferrocene was regarded as -4.8 eV.

Experimental procedures for the preparation of the monomers

Ru1,¹⁴ Ru3,¹¹ M1,⁸ M2,¹⁷ M3,⁸ M4,¹⁷ M5–M8,⁸ M10,¹⁷ and M11¹⁸ were prepared by literature methods.

M9 (3,3,9,9-tetraisopropyl-2,10-dimethyl-6,6-di(prop-2-yn-1-yl)-4,8-dioxa-3,9-disilaundecane)



To a solution of 4,4-Bis(hydroxymethyl)-1,6-heptadiyne¹⁹ (460 mg, 3.0 mmol) in dichloromethane (9 mL), 2,6-lutidine (1.4 mL, 12 mmol) was added and the mixture was cooled down to 0 °C, followed by the addition of triisopropylsilyl trifluoromethanesulfonate (1.1 mL, 6 mmol). After stirring overnight at room temperature, the mixture was quenched by the aqueous NH₄Cl solution. The product was extracted with ethyl acetate, and the organic layer was washed with brine. The organic layer was dried with MgSO₄ and concentrated to give a yellow colored solid. It was purified by flash column chromatography on silica gel (Hexane 100%) to afford compound **M9** as a colorless liquid (1.2 g, 84%). ¹H NMR (500 MHz, CDCl₃): δ 3.71 (s, 4H), 2.37 (d, J = 2.7 Hz, 4H), 1.95 (t, J = 2.6 Hz, 2H), 1.07 (s, 42H); ¹³C NMR (125 MHz, CDCl₃): δ 81.6, 70.5, 64.1, 44.2, 21.4, 18.2, 12.2; HR-MS (ESI) m/z for C₂₇H₅₂NaO₂Si₂ [M+Na]⁺, calcd. 487.3398, found: 487.3399.

General procedure for the cyclopolymerization

A 5-mL sized screw-cap vial with a septum was flame dried and charged with monomer and a magnetic bar. The vial was purged with argon four times, and degassed anhydrous dichloromethane was added. After the Ar-purged catalyst (**Ru1–Ru3**) in another 5-mL vial was dissolved in dichloromethane, the solution was rapidly injected to the monomer solution at an experimental temperature (RT) under vigorous stirring. The reaction was quenched by excess ethyl vinyl ether after desired reaction time, and partially precipitated in hexane at $-78\text{ }^{\circ}\text{C}$, remaining small amount of crude mixture ($\sim 10\%$). Obtained solid was filtered and dried in vacuo. Monomer conversion was calculated from the ^1H NMR spectrum of the remaining crude mixture.

^1H and ^{13}C NMR characterization of polymers

P(6)

^1H (500 MHz, CDCl_3): δ 7.04 – 5.73 (br m, 2H), 4.40 – 3.88 (br s, 4H), 3.62 – 2.69 (br m, 4H), 1.50 – 1.01 (br s, 6H).; ^{13}C (125 MHz, CDCl_3): δ 171.9, 170.0, 134.5, 134.1, 133.1, 131.8, 61.7, 58.1, 54.7, 35.1, 32.4, 14.2.

P(7)

^1H (500 MHz, CDCl_3): δ 6.94 – 5.69 (br m, 2H), 5.22 – 4.82 (br s, 2H), 3.62 – 2.60 (br m, 4H), 1.50 – 0.97 (br s, 12H); ^{13}C (125 MHz, CDCl_3): δ 171.4, 170.3, 136.5, 134.4, 134.1, 133.1, 131.9, 69.0, 57.9, 54.5, 35.0, 32.2, 21.6.

P(1)

^1H (500 MHz, CDCl_3): δ 6.93 – 5.71 (br m, 2H), 3.56 – 2.46 (br m, 4H), 1.74 – 1.07 (br m, 18H); ^{13}C (125 MHz, CDCl_3): δ 171.1, 170.1, 134.6, 134.3, 133.3, 131.9, 81.4, 59.1, 55.7, 35.3, 32.4, 27.7.

P(8)

^1H (500 MHz, CDCl_3): δ 6.85 – 5.63 (br m, 2H), 3.71 – 2.52 (br m, 12H), 1.30 – 0.66 (br s, 12H); ^{13}C (125 MHz, CDCl_3): δ 171.8, 170.7, 135.1, 134.1, 130.9, 130.2, 57.3, 53.2, 41.5, 40.6, 37.8, 33.5, 13.9, 12.8.

P(9)

^1H (500 MHz, CDCl_3): δ 6.98 – 5.57 (br m, 2H), 4.44 – 3.45 (br m, 4H), 2.98 – 1.91 (br m, 4H), 1.57 – 0.66 (br m, 18H); ^{13}C (125 MHz, CDCl_3): δ 178.0, 177.9, 133.9, 132.8, 67.2, 66.3, 39.1, 37.9, 34.3, 31.6, 27.3.

P(3)

^1H NMR (500 MHz, CDCl_3): δ 7.06 – 5.47 (br m, 2H), 4.01 – 3.21 (br s, 2H), 3.21 – 1.47 (br m, 4H), 1.12 – 0.57 (br s, 9H), 0.37 – -0.40 (br s, 6H); ^{13}C NMR (125 MHz, CDCl_3): δ 137.0, 134.6, 130.9, 67.3, 37.2, 32.6, 29.8, 26.1, 18.5, -5.2.

P(4)

^1H NMR (500 MHz, CDCl_3): δ 6.96 – 5.58 (br m, 2H), 3.79 – 3.07 (br s, 4H), 2.71 – 1.92 (br d, 4H), 1.07 – 0.63 (br s, 18H), 0.24 – -0.26 (br m, 12H); ^{13}C NMR (125 MHz, CDCl_3): δ 135.6, 135.4, 133.8, 132.4, 65.3, 40.6, 33.5, 30.6, 26.2, 18.4, -5.3.

P(9)

^1H NMR (500 MHz, CDCl_3): δ 6.91 – 5.56 (br m, 2H), 3.89 – 3.18 (br s, 4H), 2.78 – 2.09 (br d, 4H), 1.38 – 0.71 (br s, 42H); ^{13}C NMR (125 MHz, CDCl_3): δ 135.9, 135.2, 133.3, 132.3, 66.4, 66.0, 41.3, 33.6, 31.0, 18.3, 12.2.

P(10)

^1H NMR (500 MHz, CDCl_3): δ 7.46 – 6.99 (br m, 10H), 4.63 – 4.19 (br s, 4H), 3.61 – 3.10 (br s, 4H), 2.86 – 2.21 (br m, 4H); ^{13}C NMR (125 MHz, CDCl_3): δ 139.2, 135.6, 135.1, 133.4, 132.3, 128.3, 127.3, 73.3, 73.3, 39.6, 34.4, 31.4.

P(11)

^1H NMR (500 MHz, CDCl_3): δ 6.92 – 5.62 (br m, 2H), 3.40 (br d, 8H), 2.80 – 2.07 (br m, 4H), 1.39 – 0.92 (br s, 6H); ^{13}C NMR (125 MHz, CDCl_3): δ 135.9, 135.4, 133.0, 132.0, 74.2, 73.7, 73.6, 67.0, 66.8, 39.4, 34.1, 31.2, 15.3.

P(5)

^1H NMR (500 MHz, CDCl_3): δ 7.00 – 5.58 (br m, 2H), 4.35 – 3.79 (br s, 2H), 3.79 – 2.14 (br m, 4H), 1.65 – 0.82 (br d, 9H), 0.56 – -0.22 (br s, 9H); ^{13}C NMR (125 MHz, CDCl_3): δ 174.2, 137.5, 136.5, 134.2, 131.7, 130.3, 76.4, 60.4, 56.8, 56.6, 56.3, 56.2, 35.9, 33.7, 32.7, 30.2, 26.8, 14.2, 2.7.

Procedure for *in situ* NMR experiments

Ru3 (0.003 mmol, 1 eq) and hexamethyldisilane (internal standard, 5 μ l) were dissolved in DCM-*d*2 (400 μ L). Initial benzylidene was measured by the integral ratio of Ru3 to hexamethyldisilane in ^1H NMR spectrum. (After the addition of 7 equiv of the pyridine additive,) Monomer (0.06 mmol, 20 eq) solution in DCM-*d*2 (200 μ l) was added to the Ru3 solution and mixed by shaking NMR tube for 5 sec. The reaction was monitored by ^1H NMR over time. The k_i or k_p values were obtained from the slope of linear $-\ln [\text{Ru3}]/[\text{Ru3}]_0$ or $-\ln [\text{M}]/[\text{M}]_0$ vs. time graphs, respectively.

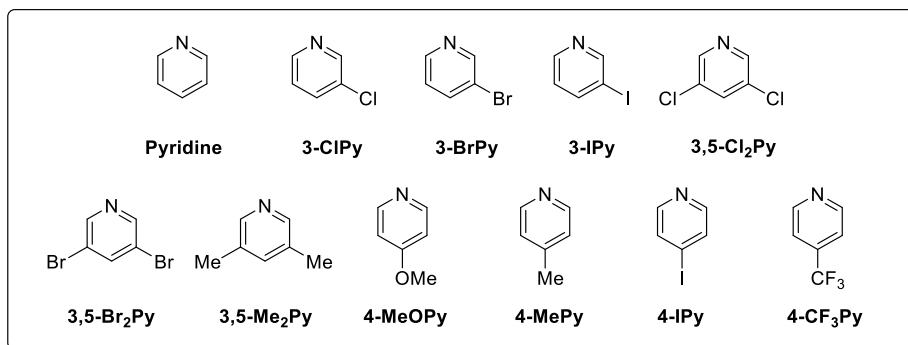
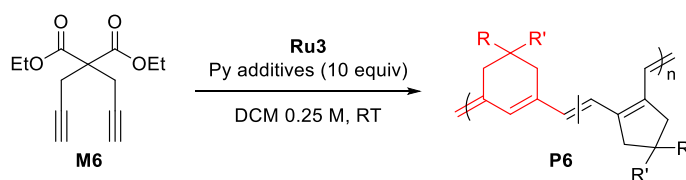
3.6 Supporting Information

Table S3.1 CP of various 1,6-heptadiynes using Ru1 and Ru2^a

<div style="display: flex; justify-content: space-around; align-items: center;"> <div> M1 </div> <div> M2 </div> <div> M3 </div> <div> M4 </div> <div> M5 </div> </div>							
entry	cat	monomer	conv (%) ^b	yield (%) ^c	<i>M_n</i> (kDa) ^d	<i>Đ</i> ^d	5:6 ^e
1	Ru1	M1	>99	69	8.9	1.12	>99:1
2	Ru1	M2	>99	73	15.2	1.34	>99:1
3	Ru1	M3	>99	98	10.1	1.26	>99:1
4	Ru1	M4	>99	97	12.6	1.11	>99:1
5	Ru1	M5	>99	82	12.7	1.12	>99:1
6 ^{f,g}	Ru2	M1	88	43	15.6	1.54	1:6.5
7	Ru2	M2	58	50	7.0	1.53	1:1.5
8	Ru2	M3	>99	75	10.4	1.97	≈ 1:1
9	Ru2	M4	96	79	13.1	1.65	1:1.7
10	Ru2	M5	62	49	6.3	1.41	1:1.4

^aReaction conditions: for the reaction using Ru1, 0.5 M in THF, 30 min.; for the reaction using Ru2, 0.25 M in THF, 3 h. ^bDetermined from ¹H NMR. ^cPrecipitated in MeOH at – 78 °C. ^dDetermined from THF-SEC. ^e5-Membered:6-membered rings, determined from ¹³C NMR. ^fPrecipitated in hexane at – 78 °C. ^gM/I=50.

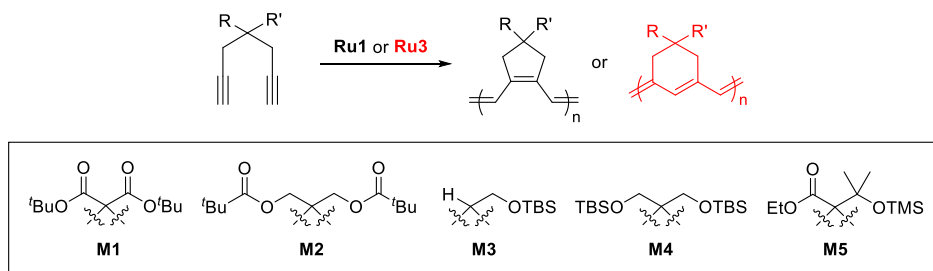
Table S3.2 CP of M6 using Ru3 with various pyridine additives



	additive	M/I/Add	conv (%) ^a	yield (%) ^b	<i>M_n</i> (kDa) ^c	<i>Đ</i> ^c	6:5 (¹ H) ^a
1	none	30/1/-	76	58	6.8	1.58	5.9:1
2	Pyridine	30/1/10	83	46	6.6	1.48	6.1:1
3	3-ClPy	30/1/10	85	76	7.1	1.63	8.8:1
4	3-BrPy	30/1/10	45	37	6.0	1.43	12.5:1
5	3-IPy	30/1/10	73	15	5.3	1.43	13.8:1
6	3,5-Cl ₂ Py	30/1/10	91	65	8.1	1.62	11.6:1
7	3,5-Br ₂ Py	30/1/10	6.1	—	—	—	—
8	3,5-Me ₂ Py	30/1/10	29	29	6.4	1.46	4.3:1
9	4-MeOPy	30/1/10	18	11	3.5	1.31	1.9:1
10	4-MePy	30/1/10	4.5	—	—	—	—
11	4-IPy	30/1/10	74	22	5.4	1.48	14.3:1
12	4-CF ₃ Py	30/1/10	6.2	—	—	—	—

^aDetermined from ¹H NMR. ^bPrecipitated in hexane at -78 °C. ^cDetermined by THF SEC calibrated using polystyrene standards.

Table S3.3 Comparison of the properties (five- vs. six-membered rings)



monomer	cat	solution		film		E_{HOMO} (eV)	PL (nm)	stokes shift (nm)	T_{d} (°C)	T_{g} (°C)
		λ_{max} (nm)	E_{g} (eV)	λ_{max} (nm)	E_{g} (eV)					
M1	Ru1	588, 547	2.02	515	2.01	-4.98	643	96	242	107
	Ru3	519	1.92	477	1.93	-4.73	nd	nd	219	127
M2	Ru1	580, 541	2.03	576, 535	2.01	-4.98	640	99	360	133
	Ru3	527	1.91	494	1.91	-4.83	643	116	326	106
M3	Ru1	586, 546	2.00	548	1.94	-4.77	645	99	320	nd
	Ru3	508	1.94	503	1.87	-4.62	644	124	313	71
M4	Ru1	594, 552	1.97	572, 529	2.02	-5.12	641	89	357	92
	Ru3	539	1.85	517	1.86	-5.12	nd	nd	370	93
M5	Ru1	598, 556	1.97	598, 551	1.94	-4.74	643	87	334	83
	Ru3	537	1.83	496	1.86	-4.52	641	104	361	100

UV-Vis and PL spectra of the polymers

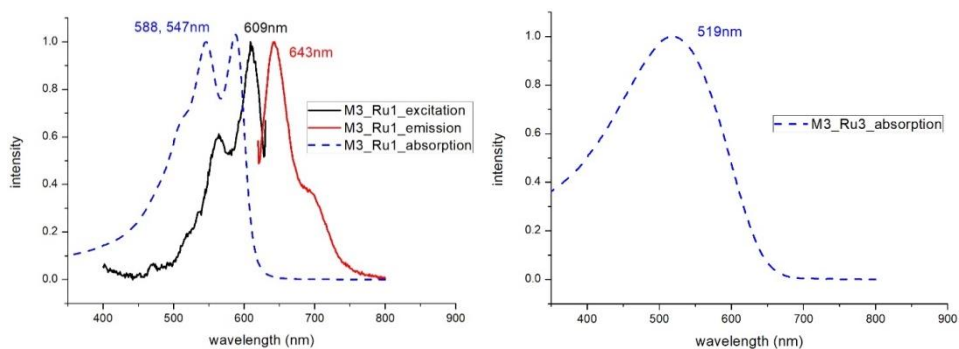


Figure S3.1 UV-Vis and PL spectra of P1 (tBuMal)

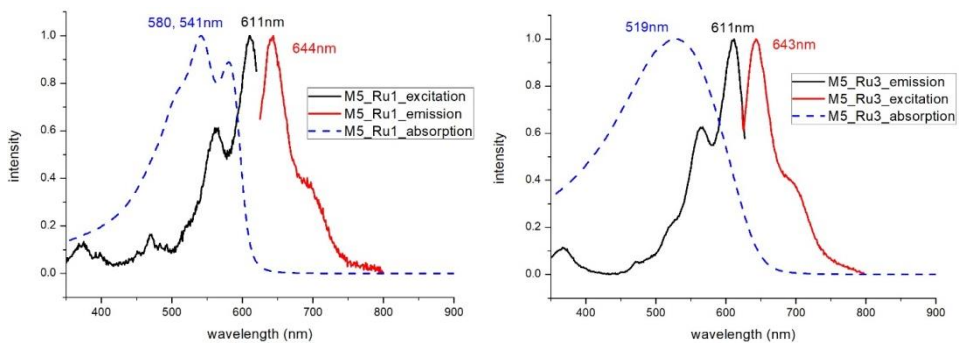


Figure S3.2 UV-Vis and PL spectra of P2 (BisOPiv)

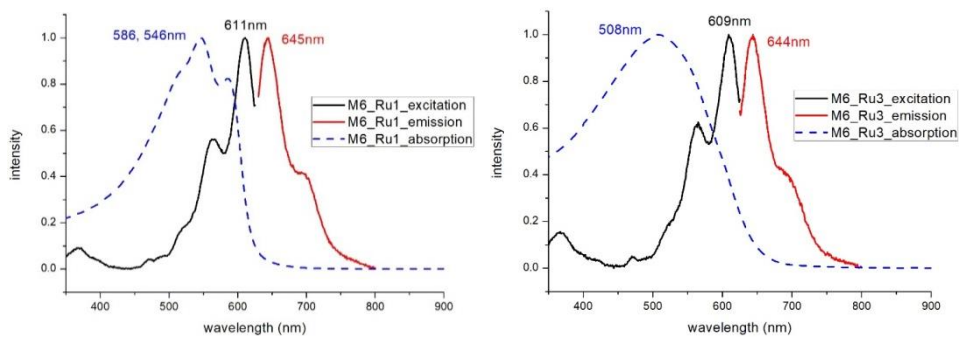


Figure S3.3 UV-Vis and PL spectra of P3 (MonoOTBS)

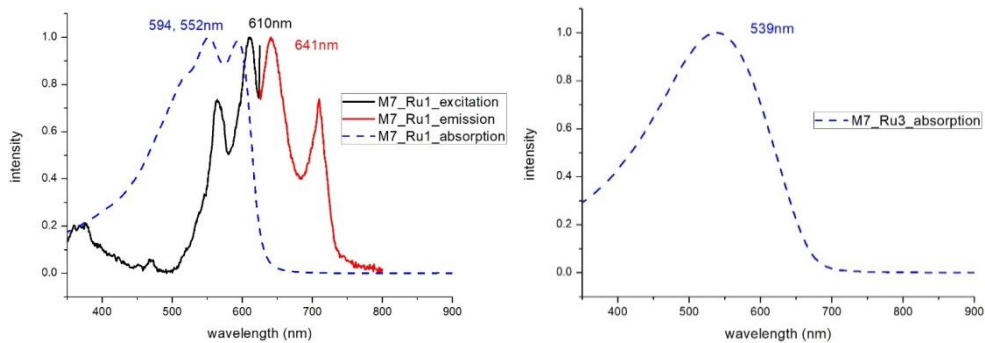


Figure S3.4 UV-Vis and PL spectra of P4 (BisOTBS)

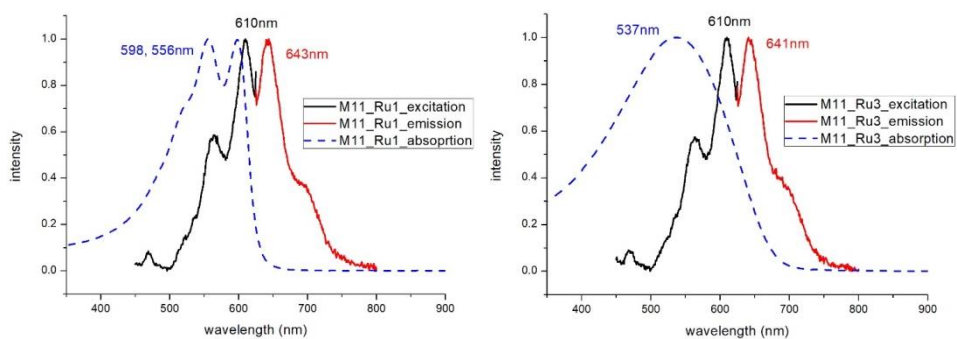


Figure S3.5 UV-Vis and PL spectra of P5 (Et-TMS)

In situ NMR experiments

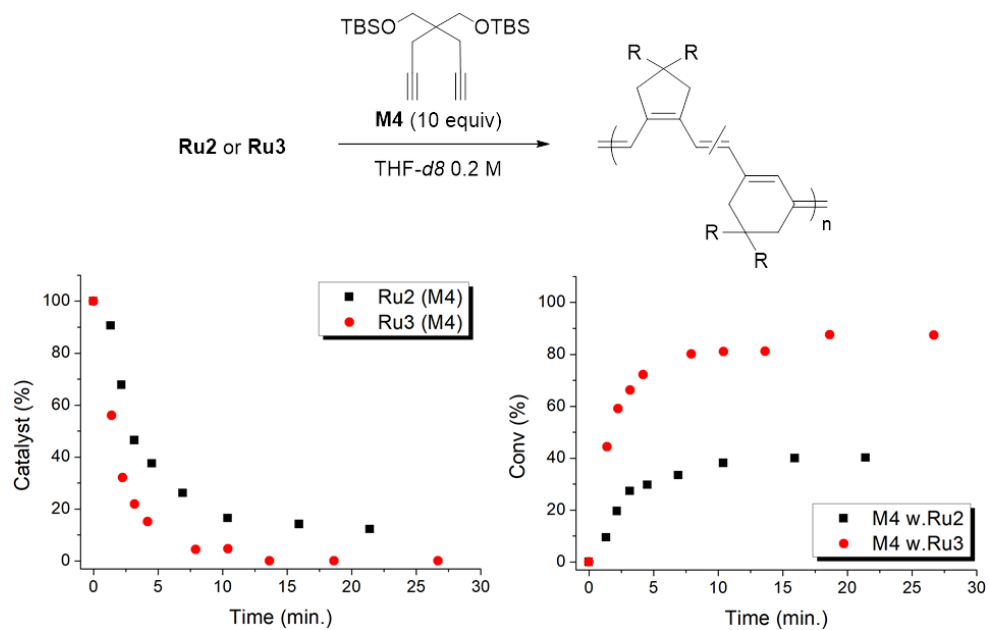
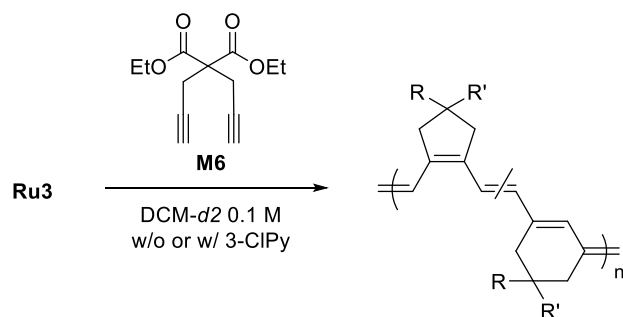


Figure S3.6 Faster initiation and higher polymerization efficiency of Ru3 than Ru2, during CP of M4



M/I/Add	k_i	k_p	k_i/k_p
20/1/-	0.4847	0.4584	1.0574
20/1/7	0.4432	0.1263	3.5091

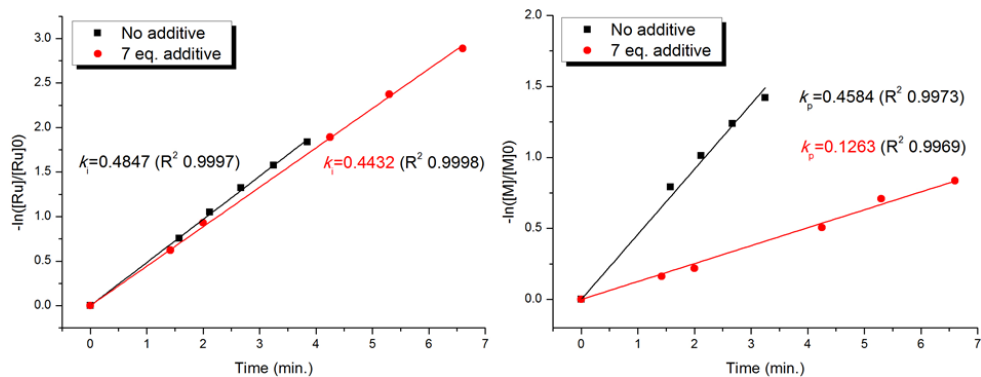


Figure S3.7 Comparison of k_i (left) and k_p (right) values in CP of M6 using Ru3, with or without 3-chloropyridine additives

Calculation of the regioselectivity for P6 using ^1H NMR

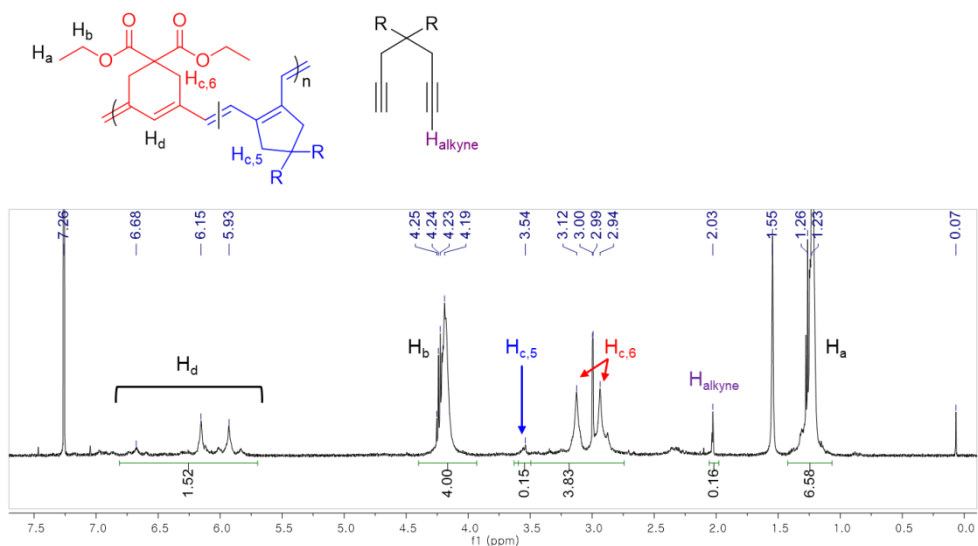


Figure S3.8 ^1H NMR spectrum of the crude mixture of entry 2 in Table 3.2

$$\text{Monomer conversion} = 1 - \frac{\text{H}_{alkyne}}{2.0}$$

$$\text{The composition of five-membered ring} = \frac{2 * \text{H}_{c,5} / \text{H}_{originated from propargylic}}{\text{Monomer conversion}}$$

e.g. (entry 2 in Table 3.2)

$$\text{Composition of five-membered ring} = \frac{2 * 0.15 / 3.83}{0.91} = 0.086$$

(\therefore 6-ring:5-ring=11.6:1)

3.7 References

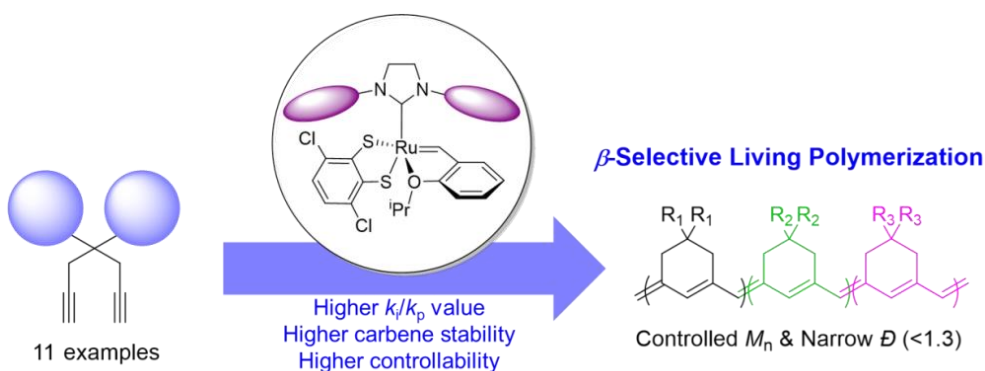
1. Choi, S. K.; Gal, Y. S.; Jin, S. H.; Kim, H. K., *Chem. Rev.* **2000**, *100*, 1645.
2. Fox, H. H.; Wolf, M. O.; O'Dell, R.; Lin, B. L.; Schrock, R. R.; Wrighton, M. S., *J. Am. Chem. Soc.* **1994**, *116*, 2827.
3. (a) Schattenmann, F. J.; Schrock, R. R., *Macromolecules* **1996**, *29*, 8990; (b) Schattenmann, F. J.; Schrock, R. R.; Davis, W. M., *J. Am. Chem. Soc.* **1996**, *118*, 3295.
4. (a) Anders, U.; Nuyken, O.; Buchmeiser, M. R.; Wurst, K., *Angew. Chem., Int. Ed.* **2002**, *41*, 4044; (b) Anders, U.; Wagner, M.; Nuyken, O.; Buchmeiser, M. R., *Macromolecules* **2003**, *36*, 2668; (c) Buchmeiser, M. R.; Sen, S.; Unold, J.; Frey, W., *Angew. Chem., Int. Ed.* **2014**, *53*, 9384; (d) Herz, K.; Unold, J.; Hänle, J.; Schowner, R.; Frey, W.; Buchmeiser, M. R.; Sen, S., *Macromolecules* **2015**, *48*, 4768.
5. (a) Krause, J. O.; Zarka, M. T.; Anders, U.; Weberskirch, R.; Nuyken, O.; Buchmeiser, M. R., *Angew. Chem., Int. Ed.* **2003**, *42*, 5965; (b) Krause, J. O.; Nuyken, O.; Buchmeiser, M. R., *Chem. Eur. J.* **2004**, *10*, 2029; (c) Halbach, T. S.; Krause, J. O.; Nuyken, O.; Buchmeiser, M. R., *Macromol. Rapid Commun.* **2005**, *26*, 784; (d) Mayershofer, M. G.; Nuyken, O.; Buchmeiser, M. R., *Macromolecules* **2006**, *39*, 3484; (e) Kumar, P. S.; Wurst, K.; Buchmeiser, M. R., *J. Am. Chem. Soc.* **2009**, *131*, 387; (f) Vygodskii, Y. S.; Shaplov, A. S.; Lozinskaya, E. I.; Vlasov, P. S.; Malyshkina, I. A.; Gavrilova, N. D.; Kumar, P. S.; Buchmeiser, M. R., *Macromolecules* **2008**, *41*, 1919; (g) Autenrieth, B.; Anderson, E. B.; Wang, D.; Buchmeiser, M. R., *Macromol. Chem. Phys.* **2013**, *214*, 33.
6. (a) Kang, E.-H.; Lee, I. S.; Choi, T.-L., *J. Am. Chem. Soc.* **2011**, *133*, 11904; (b) Lee, I. S.; Kang, E.-H.; Park, H.; Choi, T.-L., *Chem. Sci.* **2012**, *3*, 761; (c) Kang, E.-H.; Yu, S. Y.; Lee, I. S.; Park, S. E.; Choi, T.-L., *J. Am. Chem. Soc.* **2014**, *136*, 10508; (d) Song, J. A.; Park, S. E.; Kim, T. S.; Choi, T. L., *ACS Macro*

- Lett.* **2014**, *3*, 795; (e) Song, J. A.; Choi, T.-L., *Macromolecules* **2017**, *50*, 2724.
7. Keitz, B. K.; Endo, K.; Patel, P. R.; Herbert, M. B.; Grubbs, R. H., *J. Am. Chem. Soc.* **2012**, *134*, 693.
 8. Jung, K.; Kang, E.-H.; Sohn, J.-H.; Choi, T.-L., *J. Am. Chem. Soc.* **2016**, *138*, 11227.
 9. (a) Liu, P.; Xu, X.; Dong, X.; Keitz, B. K.; Herbert, M. B.; Grubbs, R. H.; Houk, K. N., *J. Am. Chem. Soc.* **2012**, *134*, 1464; (b) Dang, Y.; Wang, Z. X.; Wang, X., *Organometallics* **2012**, *31*, 7222; (c) Dang, Y.; Wang, Z. X.; Wang, X., *Organometallics* **2012**, *31*, 8654.
 10. (a) Romero, P. E.; Piers, W. E., *J. Am. Chem. Soc.* **2005**, *127*, 5032; (b) Wenzel, A. G.; Grubbs, R. H., *J. Am. Chem. Soc.* **2006**, *128*, 16048.
 11. Koh, M. J.; Khan, R. K.; Torker, S.; Yu, M.; Mikus, M. S.; Hoveyda, A. H., *Nature* **2015**, *517*, 181.
 12. (a) Khan, R. K.; Torker, S.; Hoveyda, A. H., *J. Am. Chem. Soc.* **2013**, *135*, 10258; (b) Koh, M. J.; Khan, R. K.; Torker, S.; Hoveyda, A. H., *Angew. Chem., Int. Ed.* **2014**, *53*, 1968; (c) Mikus, M. S.; Torker, S.; Hoveyda, A. H., *Angew. Chem., Int. Ed.* **2016**, *55*, 4997.
 13. Jung, H.; Jung, K.; Hong, M.; Kwon, S.; Kim, K.; Hong, S. H.; Choi, T. L.; Baik, M. H., *J. Am. Chem. Soc.* **2018**, *140*, 834.
 14. Kang, E.-H.; Lee, I. S.; Choi, T.-L., *J. Am. Chem. Soc.* **2011**, *133*, 11904.
 15. Park, H.; Lee, H. K.; Choi, T. L., *Polym. Chem.* **2013**, *4*, 4676.
 16. Walsh, D. J.; Lau, S. H.; Hyatt, M. G.; Guironnet, D., *J. Am. Chem. Soc.* **2017**, *139*, 13644.
 17. Madine, J. W.; Wang, X.; Widenhoefer, R. A., *Org. Lett.* **2001**, *3*, 385.
 18. Wang, X.; Chakrapani, H.; Madine, J. W.; Keyerleber, M. A.; Widenhoefer, R. A., *J. Org. Chem.* **2002**, *67*, 2778.
 19. Anders, U.; Nuyken, O.; Buchmeiser, M. R.; Wurst, K., *Macromolecules* **2002**, *35*, 9029.

Chapter 4. Living β -Selective Cyclopolymerization
of 1,6-Heptadiyne Derivatives Using Ru Dithiolate
Catalysts

4.1 Abstract

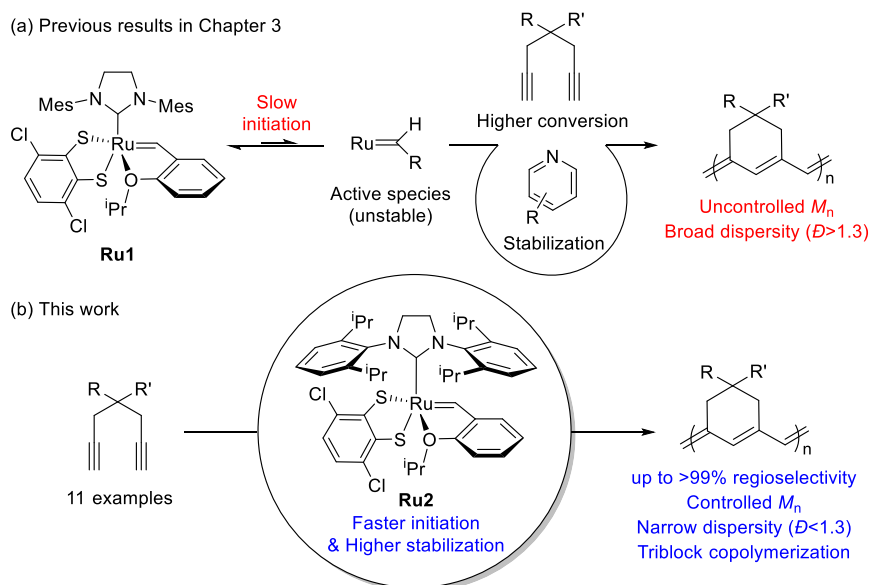
In this chapter, we report a living β -selective CP by rational engineering of the steric factor on monomer or catalyst structures. As a result, the molecular weight of the conjugated polymers from various monomers could be controlled with narrow dispersities, according to the catalyst loading. A mechanistic investigation by *in situ* kinetic studies using ^1H NMR spectroscopy revealed that with appropriate pyridine additives, imposing a steric demand on either the monomer or the catalyst significantly improved the stability of the propagating carbene, as well as the relative rates of initiation over propagation, thereby achieving living polymerization. Furthermore, we successfully prepared diblock and even triblock copolymers with a broad monomer scope.



4.2 Introduction

In chapter 3, we found that a Ru-based olefin metathesis catalyst **Ru1** containing a dithiolate ligand¹ exerted far higher β -selectivity in CP of 1,6-heptadiyne monomers (85–99% β -selectivity),² and we examined the origin of the exceptional regioselectivity using DFT calculations, concluding that **Ru1** which adopts trigonal bipyramidal geometry would prefer β -addition due to electronic effects.³ However, this catalyst showed very slow initiation rate (k_i) and relatively fast propagation rate (k_p) leading to low k_i/k_p values and poor MW control, the non-living manner. Furthermore, the relatively low stability of the propagating carbene seemed to result in fast termination and broad dispersity (\mathcal{D}) (Scheme 4.1a).²

Scheme 4.1 (a) Proposed scheme showing the effects of the pyridine additive and the limitations of this method, and (b) Living β -selective CP using fast-initiating **Ru2**



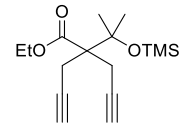
General requirements for living polymerization, which means a polymerization without chain transfer and termination, are (i) fast initiation (high k_i/k_p), (ii) a linear relationship between the degree of polymerization and number-average molecular weight (M_n), and (iii) narrow \mathcal{D} lower than 1.5. Among many polymerization methods, β -selective living CP is a challenging area, as there is only one example using Schrock's Mo catalyst and just one monomer.⁴ In this chapter, we introduce two strategies to achieve β -selective living CP with user-friendly Ru catalysts: lowering k_p by introducing pyridine additives and sterically bulky substituents on monomers, and dramatically increasing k_i by employing a catalyst with a bulkier ligand. These strategies, combined with a synergetic effect of stabilized propagating species by steric demand, led to successful a controlled polymerization. Furthermore, we successfully demonstrated the first example of fully β -selective diblock and triblock copolymerizations (Scheme 4.1b). Finally, a mechanistic investigation using *in situ* kinetic experiments clarified the role of pyridine additives and allowed quantification of their effects by direct comparison of k_i/k_p values.

4.3 Results and Discussion

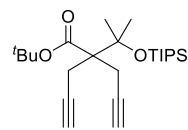
To achieve a living polymerization, high stability of the propagating species and a high k_i/k_p value are crucial. In previous studies, we discovered that pyridine additives might coordinate to **Ru1** competitively with the monomer to slow down the polymerization and stabilize the propagating species.² However, living polymerization was not achieved, presumably due to low k_i and decomposition of **Ru1**. Since CP of monomer **M1** containing a *gem*-dimethyl group showed improved \bar{D} with the addition of 3,5-Cl₂Py (reduced from 1.92 to 1.45),² we expected that living polymerization might be achieved by introducing an even bulkier side chain, which would increase the stabilization on the propagating species and the k_i/k_p value. Therefore, we synthesized **M2**, replacing the ethyl ester and TMS side chains of **M1** with the sterically bulky *tert*-butyl ester and TIPS substituents (Table 4.1), and obtained conjugated polyene **P2** containing six-membered rings via exclusive β -addition. Without additives, CP of **M2** using **Ru1** at RT in DCM showed poor reactivity with less than 10% conversion (entry 1). Though carrying out the reaction in THF at 70 °C increased the conversion to 94%, a broad \bar{D} of 1.69 still implied uncontrolled CP (entry 2).

Table 4.1 Living polymerization of M2 using Ru1 with 3,5-dichloropyridine

cf) **M1**

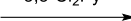


<Previous results using **Ru1**>
w/o additive, $M_n = 25.8$ kDa, $\bar{D} = 1.92$
w/ 3,5-Cl₂Py, $M_n = 14.2$ kDa, $\bar{D} = 1.45$

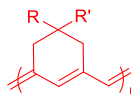


M2

Ru1
3,5-Cl₂Py
DCM 0.25 M



P2
6-ring only



entry	M/I/Add	temp (°C)	time (h)	conv (%) ^a	yield (%) ^b	M_n (kDa) ^c	\bar{D} ^c
1	30/1/-	25	1	<10	nd	nd	nd
2 ^d	30/1/-	70	3	94	69	18.2	1.69
3	15/1/10	25	1	>99	50	7.3	1.18
4	30/1/10	25	3	>99	81	13.0	1.19
5	45/1/15	25	3	>99	89	22.0	1.23
6	60/1/20	25	3	>99	78	30.4	1.20
7	75/1/25	20	8	98	79	38.2	1.39

^aDetermined by ¹H NMR. ^bPrecipitated in methanol at -78 °C. ^cDetermined by THF SEC calibrated using polystyrene standards. ^dConducted in THF.

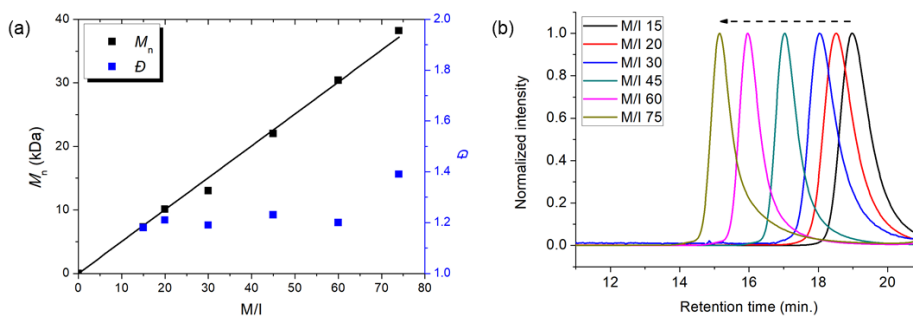
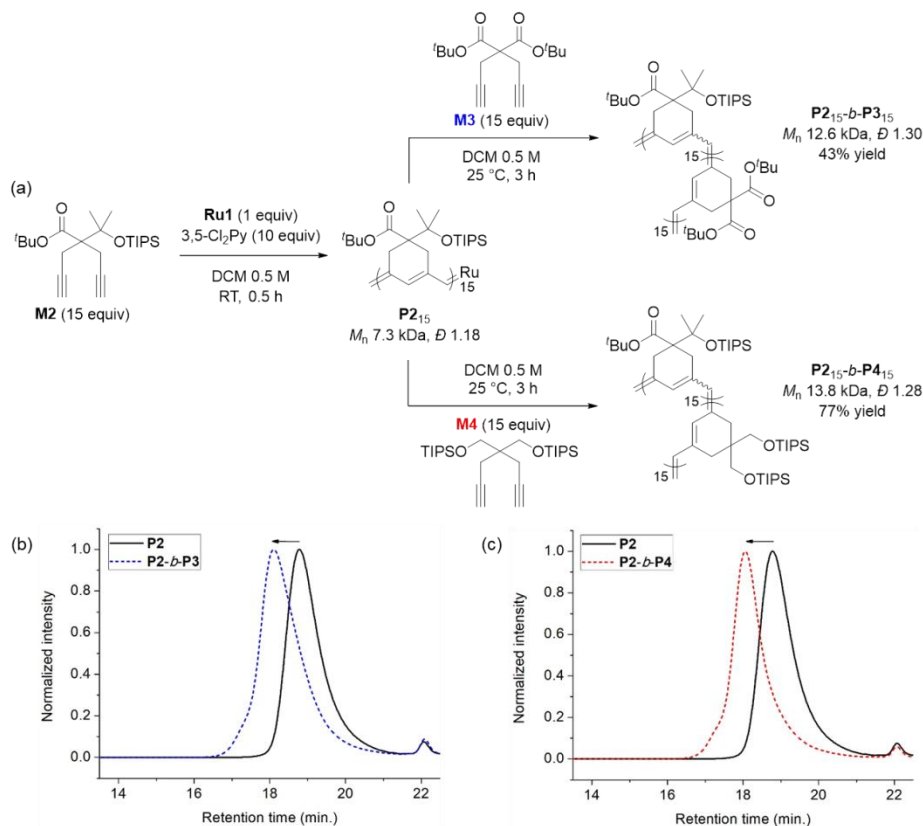


Figure 4.1 (a) plots of M_n vs. M/I and corresponding \bar{D} values for P2 and (b) SEC traces of P2 from entries 3 – 7 in Table 4.1

Gratifyingly, with the addition of 3,5-Cl₂Py, **P2** was synthesized at RT with a higher conversion, and excellent molecular weight control was achieved, with a linear increase in M_n from 7.3 to 38.2 kDa with M/I between 15 and 75 (entries 3–7, Figure 4.1a). Furthermore, the dispersities were less than 1.23, implying a successfully controlled polymerization, except for the highest-MW polymer (M/I of 75, entry 7, Figure 4.1b).

Having achieved β -selective living polymerization, we attempted diblock copolymerization at RT using **M2** as the first monomer (Scheme 4.2), because β -selective block copolymerization has never been reported, to the best of our knowledge. After complete consumption of 15 equiv of **M2**, we added another 15 equiv of **M3**, containing the di-*tert*-butyl malonate moiety, as the second monomer to prepare the fully conjugated polymer **P2-*b*-P3** by β -addition (Scheme 4.2a). Block copolymerization was confirmed by SEC analyses, showing the complete shift of the traces from the **P2** homopolymer (7.3 kDa) to the block copolymer (12.6 kDa), with a narrow dispersity (1.30, Scheme 4.2b). An analogous diblock copolymerization was successful when 15 equiv of **M4** was introduced as the second monomer, to afford **P2-*b*-P4**, with a M_n of 13.8 kDa and \mathcal{D} of 1.28, which was verified by SEC analyses (Scheme 4.2c). Remarkably, these two diblock copolymers showed perfect β -selectivity, confirmed by ¹³C NMR measurements. Although living homopolymerizations of **M3** and **M4** were not possible, we were able to prepare well-defined diblock copolymers from the **P2** macromonomer as the initiation and stability of the living chain end were established in the first block.



Scheme 4.2 (a) Diblock copolymerization of with **M2** as the first monomer, and **M3**(above) and **M4**(below) as the second monomers. SEC traces of homopolymer **P2** and diblock copolymers: (b) **P2-*b*-P3**, and (c) **P2-*b*-P4**.

To understand the origin of the successful living polymerization, we conducted a mechanistic investigation using *in situ* NMR analysis by monitoring initiation and propagation of **Ru1** during CP of **M2** (*M/I*=20 in 0.1 M DCM-*d*2). With the pyridine additives, the signal intensity of the new propagating carbene gradually increased by up to 74% during the first 40 minutes, whereas that from a smaller monomer, diethyl malonate-derived **M5**, increased by only 56% in 5 minutes and then decreased continuously to 32% at 25 min. (Figure S4.2). This result supports our

hypothesis that a bulkier monomer enhances the stability of the propagating species. Furthermore, from this *in situ* NMR monitoring, k_i and k_p for CP of M2 were obtained with and without the 3-ClPy additive (Figure 4.2a, b). With 7 equiv of 3-ClPy, k_p was approximately three times lower than without the pyridine additive (0.15 vs. 0.05), due to the competitive coordination to form a dormant $18 e^-$ species, while k_i did not significantly change. Therefore, the overall k_i/k_p value increased by 2.3 times with the use of 3-ClPy (3.07 vs. 1.31). SEC analyses of the resulting P2s demonstrated that an M_n of 10.1 kDa (close to the theoretical value, 8.1 kDa) with a narrow D (1.21) was obtained using 3-ClPy, whereas an unusually high M_n of 38.0 kDa and a broad D (2.05) were found without addition of 3-ClPy (Figure 4.2c). In short, sterically bulky monomers and pyridine additives increase the stability of the propagating species (from Ru1) as well as the k_i/k_p value, thereby promoting living polymerization.

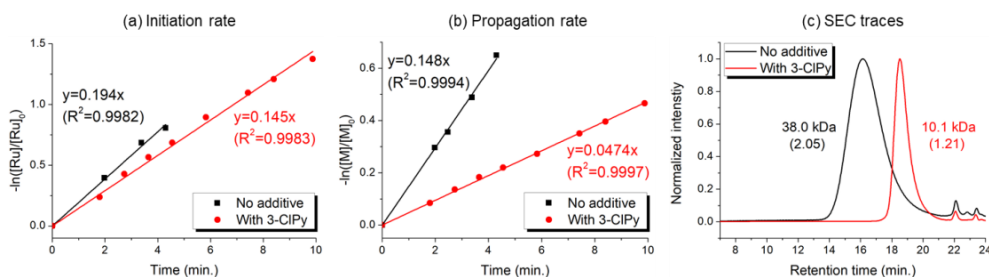


Figure 4.2 Plots of (a) $-\ln([Ru]/[Ru]_0)$ and (b) $-\ln([M]/[M]_0)$ vs. time for the CP of M2 for M/I=20, with and without 3-ClPy, and (c) SEC traces of the resulting polymers

However, living polymerization of monomers with smaller substituents was not possible using this approach. We then envisioned that a faster initiating β -selective catalyst would be necessary to increase the scope of suitable monomers for living polymerization. The Wagener group improved the initiation efficiencies of Grubbs and Hoveyda–Grubbs catalysts by replacing mesityl groups in the *N*-heterocyclic carbene (NHC) ligand with much bulkier *N*-2,6-diisopropylphenyl (DIPP) groups, facilitating dissociation of the Ru–O bond.⁵ This inspired us to use new dithiolate catalyst **Ru2**⁶ containing the bulky DIPP NHC ligand (Figure 4.3a) to promote living CP with an even higher β -selectivity, as a result of steric repulsion between the DIPP group and monomer substituents in the metallacyclobutene intermediates (Figure 4.3b).

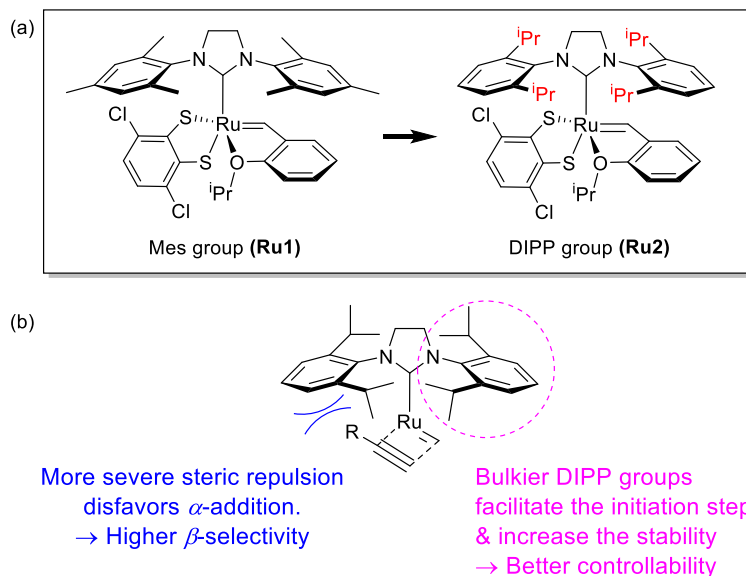


Figure 4.3 (a) Modifying ligands for living polymerization, and (b) Model for improved β -selectivity and controllability of CP using **Ru2**

To explore the effect of the DIPP group on the initiation, we measured the initiation rate of **Ru1** ($k_{i,Ru1}$) to compare it with that of **Ru2** ($k_{i,Ru2}$).⁶ Following the reported protocol, the consumption of **Ru1** was monitored by ¹H NMR spectroscopy upon addition of butyl vinyl ether at both 0 °C and –20 °C, and $k_{i,Ru1}$ were determined to be 2.84×10^{-4} and 1.53×10^{-5} s⁻¹, respectively. The values are about 11.8 and 400 times slower than $k_{i,Ru2}$ measured under identical conditions (Figure 4.4). Therefore, **Ru2** should be an effective catalyst for living β -selective CP.

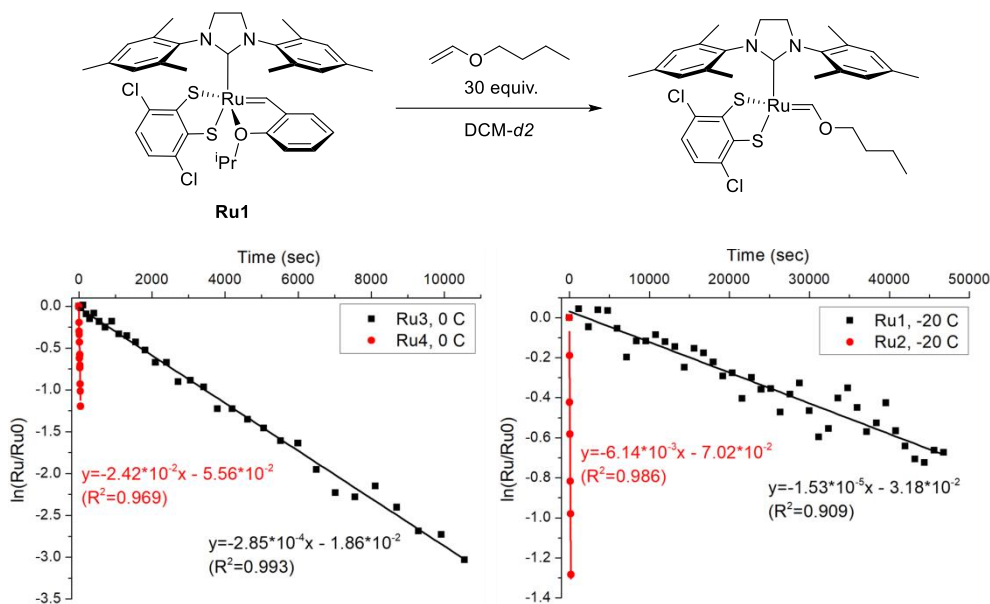
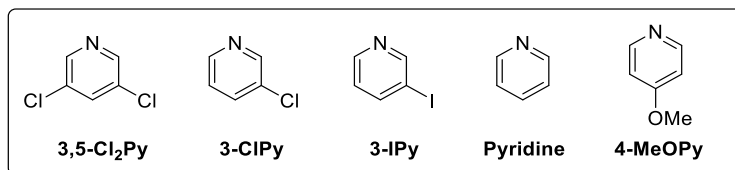
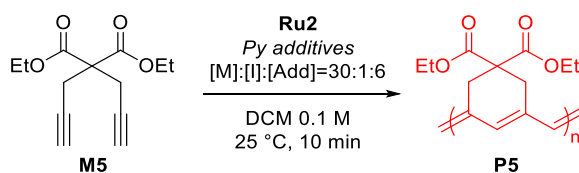


Figure 4.4 The plot of $\ln([Ru]/[Ru]_0)$ vs. time for measuring the initiation rates of **Ru1** at 0 °C (left) and –20 °C (right) using ¹H NMR.

To test β -selective CP using **Ru2**, we chose diethyl dipropargyl malonate (**M5**) as a model monomer because its β -selectivity can be easily measured using ^1H NMR (Table 4.2). The reaction with an M/I of 30, without an additive, was completed in just one minute with a high β -selectivity of 95% (Table 4.2, entry 1). This indicated that **Ru2** was more active and highly β -selective compared with **Ru1**, which, when used under the same reaction conditions, resulted in a 76% conversion and 85% β -selectivity after 1 hour.² However, with **Ru2**, the propagation was too fast for controlled polymerization; thus, M_n and \mathcal{D} values were higher than expected. To lower the k_p , 6 equiv. (with respect to the catalyst) of 3,5- Cl_2Py , which was the optimal additive for **Ru1**, was used, but \mathcal{D} was still broad (1.41), implying that 3,5- Cl_2Py was not effective for **Ru2** (entry 2). To our delight, the use of sterically less bulky mono-halogenated pyridine derivatives such as 3- ClPy and 3- IPy led to much narrower dispersities (\mathcal{D} of 1.19, entries 3 and 4). These results led us to speculate that the binding affinity of the additives affected the controllability of CP, so we tried more basic ligands such as pyridine and 4-MeOPy. As a result, we observed controlled polymerizations with even narrower dispersities (\mathcal{D} of 1.11 and 1.10, respectively, entries 5 and 6), and the highest β -selectivity of 97% in the pyridine case.

Table 4.2 Optimization of pyridine additives for CP of M5 using Ru2



entry	additive	conv (%) ^a	yield (%) ^b	M_n (kDa) ^c	\bar{D}^c	β -selectivity (%) ^a
1	–	>99	99	13.6	1.86	95
2	3,5-Cl ₂ Py	>99	99	14.2	1.41	95
3	3-ClPy	>99	92	10.8	1.19	96
4	3-IPy	>99	72	9.6	1.19	94
5	Pyridine	>99	77	9.6	1.11	97
6	4-MeOPy	>99	78	9.1	1.10	95

^aDetermined by ¹H NMR. ^bPrecipitated in hexane at –78 °C. ^cDetermined by THF SEC calibrated using polystyrene standards.

To investigate how various pyridine additives with different electronic properties affected the efficiency and selectivity of CP, we conducted *in situ* kinetic studies using ¹H NMR and monitored the changes in the propagating carbenes with four pyridine additives (M/I=20 in 0.1 M DCM-*d*2, Figure 4.5). First, upon addition of 3,5-Cl₂Py to the Ru2, the carbene signal for Ru2 at 14.47 ppm decreased to 71% without generating a new carbene signal. After the addition of the monomer M5, to our surprise, Ru2 fully initiated with complete conversion of M5 in 80 seconds. This indicates superior reactivity of Ru2 to CP since for Ru1, only half of the catalyst initiated after 80 seconds, and it took 10 minutes for the complete conversion of M5 (Figure S4.3). However, virtually no propagating carbene

or Fischer carbene signal was detected after quenching with ether vinyl ether (EVE), suggesting complete decomposition of the catalyst. Therefore, we concluded that coordination of the bulkier and less basic 3,5-Cl₂Py to **Ru2** was not efficient for stabilizing the active species, and led to broad dispersity (Figure 4.6b, \mathcal{D} of 1.86). When the stronger ligand 3-ClPy was added, the amount of **Ru2** dropped to 88% while a new carbene signal equivalent to 12% of the initial **Ru2** signal appeared at 16.92 ppm. This new carbene is thought to be pyridine-bound **Ru2**, given the downfield shift, and the sum of two carbene signals was 100%, suggesting no decomposition of the catalyst. Upon the addition of **M5**, the signals of **M5** and both carbenes disappeared in 90 seconds, and a new propagating carbene signal appeared at 15.54 ppm, with 86% intensity relative to the initial **Ru2** signal. When we added the more strongly binding pyridine and 4-methoxypyridine to **Ru2**, new carbene signals at 16.8 ppm were observed with higher relative intensities of 30 and 46%, respectively. These two effective ligands slowed down the propagation and stabilized the resulting propagating carbenes (15.71 ppm), with 85 and 84% intensities, respectively, which persisted throughout the reactions. Given that the propagating carbene signal in the reaction with **Ru1** and **M5** only reached 56% of the initial **Ru1** signal intensity, the higher values (up to 86%) observed with **Ru2** strongly support that the bulky DIPP ligand efficiently stabilizes the propagating species, thereby improving the controllability, with \mathcal{D} as low as 1.11.

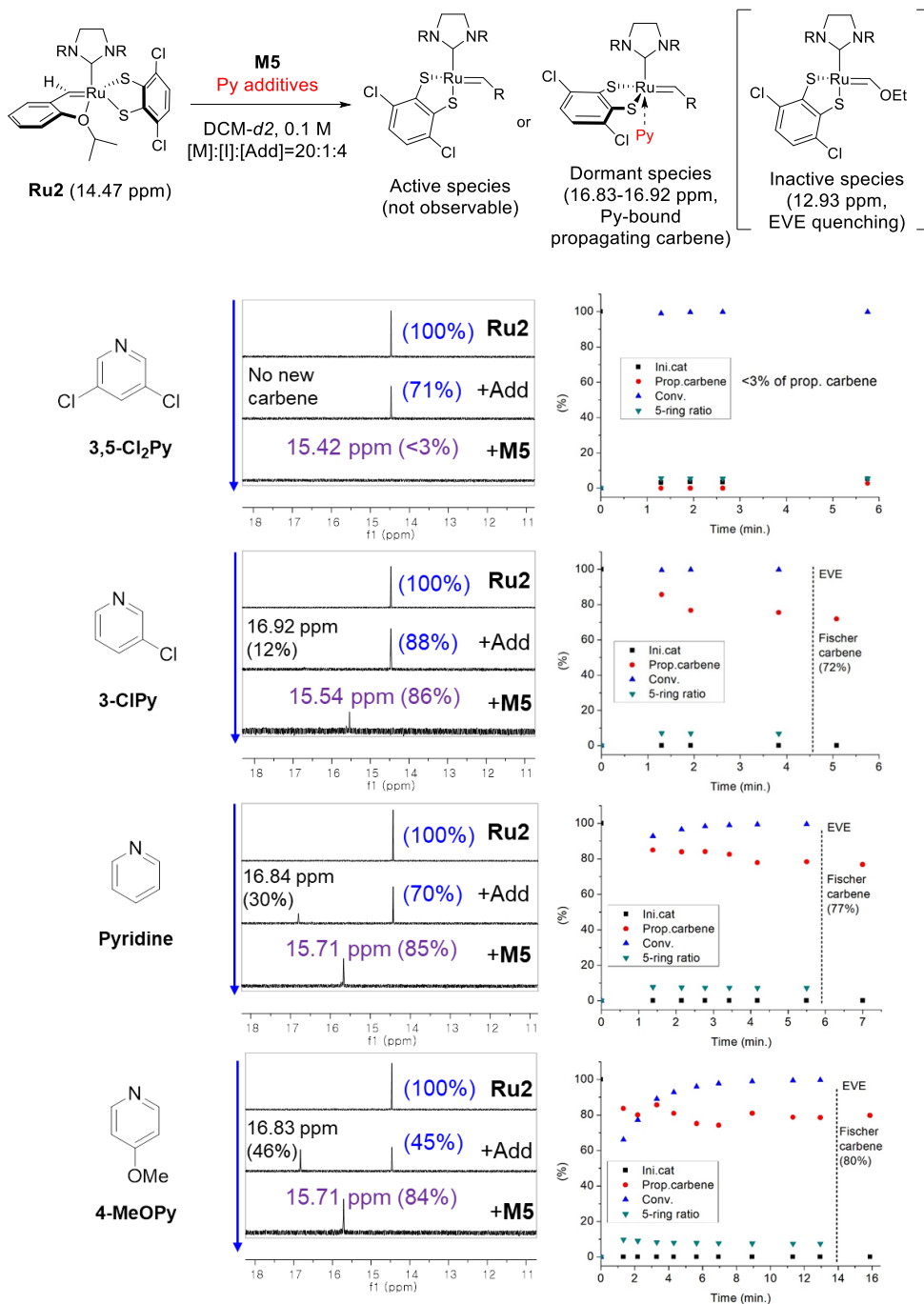


Figure 4.5 Scheme for the ^1H NMR kinetic experiments (top) and ^1H NMR spectra showing the changes in carbene signals during CP of M5 using Ru2 with various pyridine additives, and their corresponding plots in real time

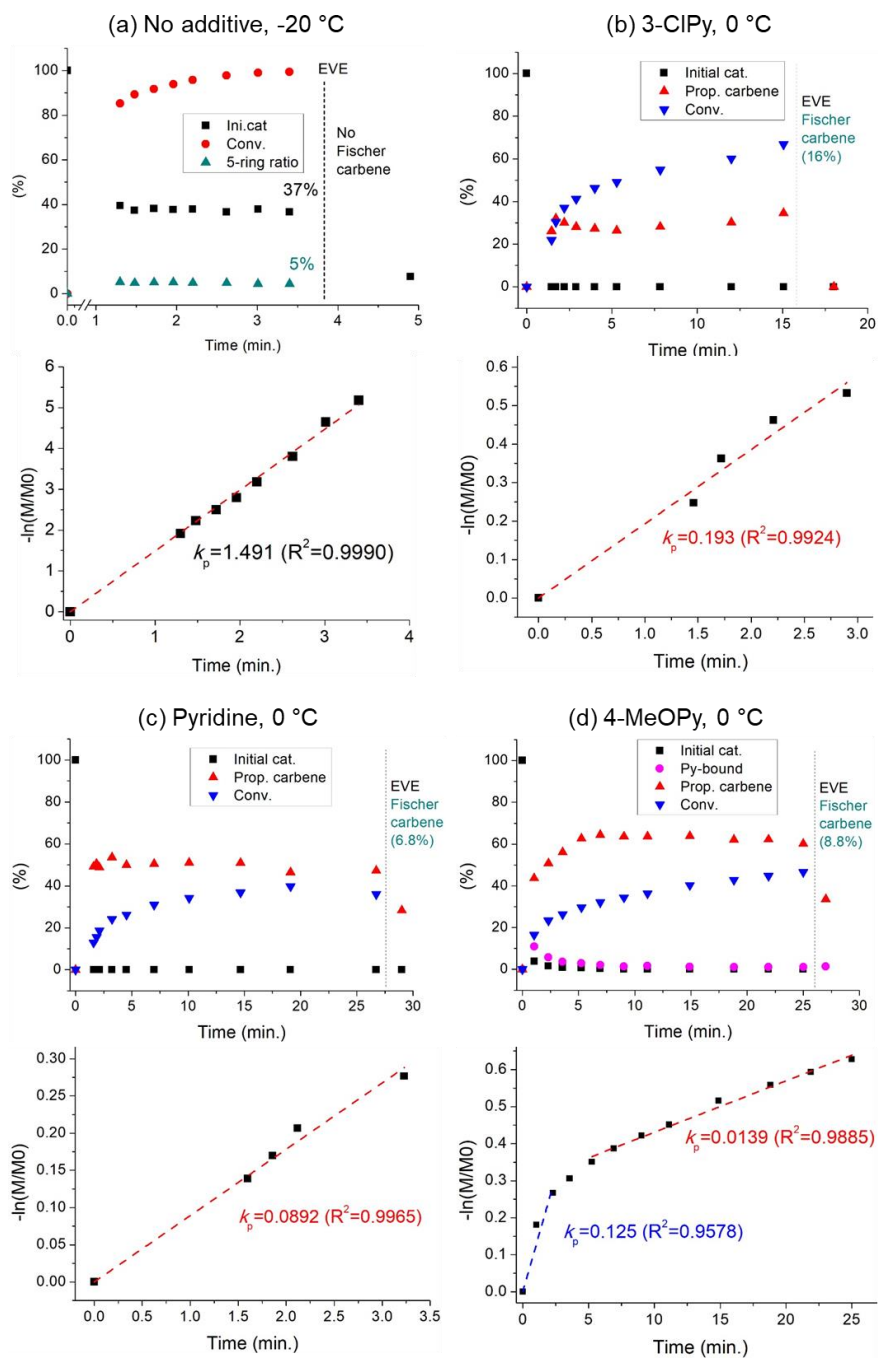


Figure 4.6 Results from *in situ* kinetic experiments at low temperature and their corresponding plots of $-\ln(M/M_0)$ vs. time for (a) no additive at -20 °C, (b) 3-chloropyridine, (c) pyridine, and (d) 4-methoxypyridine as an additive at 0 °C

Further *in situ* kinetic experiments for CP of **M5** using **Ru2** were conducted at a lower temperature to obtain the accurate k_p values, either without additives or with three kinds of pyridine additives (3-ClPy, Pyridine, and 4-MeOPy), which resulted in similar stabilization effect on the propagating carbene from the kinetic studies at RT. As described in Figure 4.6b–d, under the three pyridine additives, the signal from **Ru2** completely disappeared after addition of **M5**. The propagating carbene (red dot) was generated in a higher portion, and the monomer conversion (blue dot) increased slower with the order of 3-ClPy, Pyridine, and 4-MeOPy. The corresponding k_p values were calculated using the slope from their $-\ln(M/M_0)$ vs. time plots of as 0.193, 0.0892, and 0.0139, respectively. Combining with the k_i values in Figure 4.4, the k_i/k_p values were obtained as 1.25×10^{-2} , 2.71×10^{-2} , and 17.4×10^{-2} , respectively (see Table S4.1 for the calculated k_i/k_p values). In particular, a pyridine-bound carbene signal (pink dot, Figure 4.6d) in 4-MeOPy bearing the strongest binding affinity remained for 5 min after the monomer addition, so we regarded it as an induction period, and the k_p value was obtained after this period. Without additives, the reaction was very fast even at $-20\text{ }^\circ\text{C}$, giving far higher k_p (1.49) and lower k_i/k_p value (4.12×10^{-3}) compared to the cases with pyridine additives (Figure 4.6a). To sum up, we found out that pyridine additives are essential for the controlled polymerization, which requires high k_i/k_p value (Table S4.1).

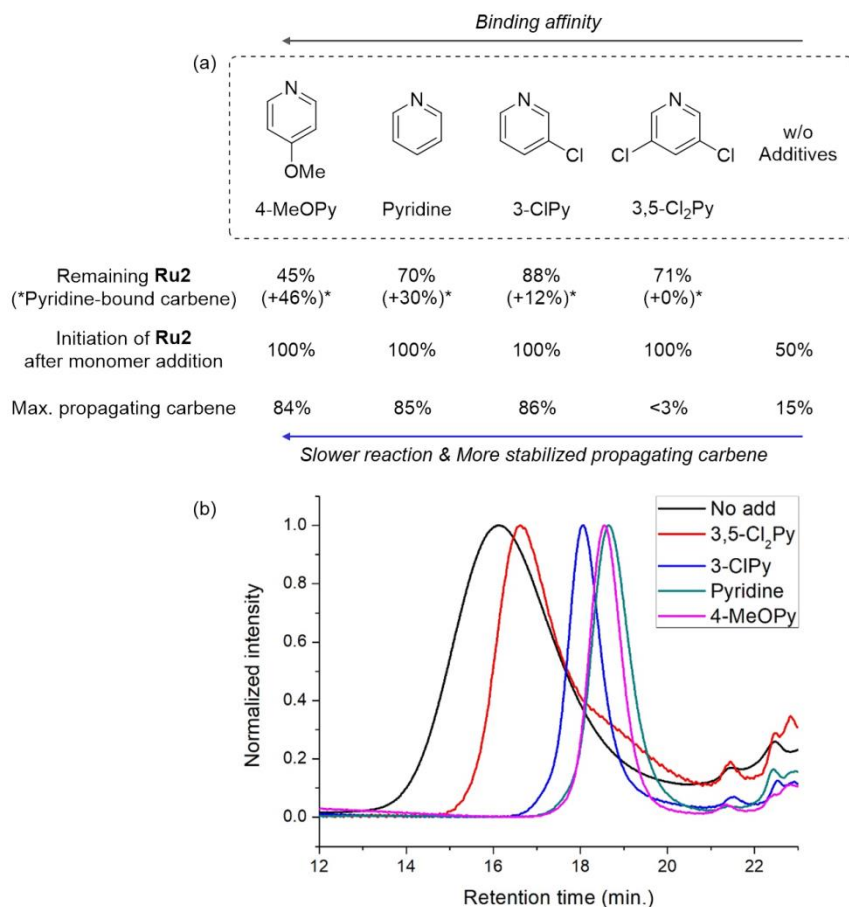


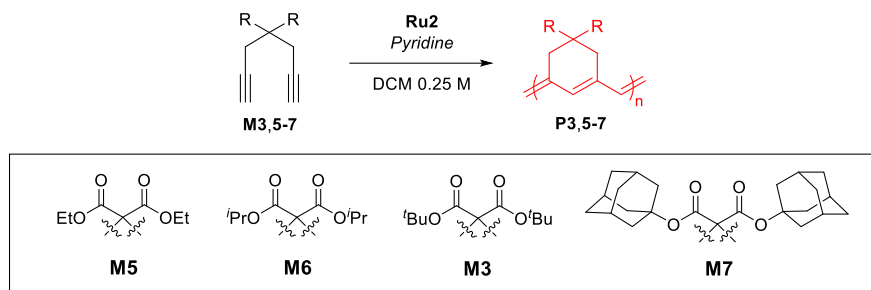
Figure 4.7 (a) Summary of the results from the kinetic experiments at RT, showing the relationship with the binding affinity of the additives and (b) THF-SEC traces of the corresponding polymers

A summary of the kinetic experiments is shown in Figure 4.7a, demonstrating that the stronger electron-donating pyridine additives tend to stabilize the propagating carbenes more by forming 18 e⁻ dormant states. This is well-reflected in the corresponding SEC traces showing a narrow Gaussian distribution for pyridine and 4-MeOPy, and broad dispersities with long tailings due to chain termination for the cases with no additive or

weakly coordinating 3,5-Cl₂Py (Figure 4.7b). We selected pyridine as the optimal additive because it gave the highest β -selectivity as well as a low \bar{D} (Table 4.2).

Using pyridine as an additive, we investigated controlled β -selective CP of various malonate-type monomers (Table 4.4). We observed the complete conversion of **M5**, with controlled M_n and narrow dispersity (1.15) for M/Is of up to 50, and ¹³C NMR analysis confirmed the high β -selectivity (94%), showing the six-membered-ring on the polymer backbone (entry 1). For the higher M/I of 75, we obtained **P5** with an expected M_n of 21 kDa, but a broadening appeared in the SEC trace with \bar{D} of 1.50, even after several optimizations (entry 2). Additionally, a higher-molecular-weight shoulder corresponding to doubling of the molecular weight appeared in the SEC trace of the resulting polymer, presumably due to the bimolecular decomposition of Ru2 after prolonged reaction time.⁷ We were able to solve this problem by reducing the reaction time or concentration (Figure S4.5). Using monomer **M6**, containing an isopropyl group, CP proceeded with high reactivity for M/Is of 15 to 75 and a corresponding linear increase in M_n from 5.7 to 24.4 kDa, while retaining high β -selectivity (94%) and narrow \bar{D} values (<1.15), except for the highest DP polymer (M/I of 75) where a severe broadening in the SEC trace was observed (entries 3–6, Figure 4.8a).

Table 4.3 CP of various malonate type 1,6-heptadiyne monomers using Ru2 and pyridine



entry	monomer	M/I/Add	temp (°C)	time	conv (%) ^a	yield (%) ^b	M_n (kDa) ^c	\bar{D}^c	β -selectivity (%) ^d
1	M5	50/1/10	25	15 min	>99	86	15.5	1.15	94
2		75/1/10	20	30 min	92	87	20.7	1.50	
3	M6	15/1/5	25	3 min	>99	86	5.7	1.10	
4		30/1/10	25	10 min	>99	64	10.2	1.10	
5		50/1/10	20	30 min	>99	85	19.1	1.15	94
6		75/1/10	15	4 h	85	75	24.4	1.94	
7	M3	15/1/5	25	10 min	>99	56	6.6	1.07	
8		30/1/10	25	30 min	>99	70	11.4	1.06	
9		50/1/15	25	2 h	>99	81	15.3	1.14	97
10		75/1/20	25	3 h	>99	82	24.2	1.15	
11		100/1/25	25	4 h	>99	97	41.0	1.30	
12	M7	15/1/5	25	10 min	>99	62	5.6	1.08	
13		30/1/10	25	20 min	>99	72	11.0	1.12	
14		50/1/15	25	2 h	>99	86	21.0	1.19	>99
15		75/1/10	15	4 h	>99	76	26.6	1.23	

^aDetermined by ¹H NMR. ^bPrecipitated in hexane at -78°C. ^cDetermined by THF SEC calibrated using polystyrene standards. ^dDetermined by ¹³C NMR.

Taking a lesson from our previous work that introducing a sterically bulkier substituent improved both the stability of the propagating species and β -selectivity, we chose monomer **M3** with a much bulkier *tert*-butyl group, which was polymerized to yield **P3** with a higher β -selectivity of 97%.

More importantly, we observed improved polymerization efficiency and controllability, generating **P3** with a linear increase in M_n up to 41 kDa and narrow dispersities (\mathcal{D} of 1.06–1.30 for M/Is 15–100, entries 7–11, Figures 4.8b, d). Maximizing the steric bulkiness by introducing an adamantyl group in **M7**, we successfully conducted CP with complete conversion, producing **P7** with a linear increase in M_n (6–27 kDa) and narrow \mathcal{D} (1.12–1.23) for M/Is of 15 to 75 (entries 12–15, Figure 4.8c). Notably, **P7** contained only six-membered-ring repeat units via exclusive β -addition, as determined by ^{13}C NMR analysis.

Figure 4.8 Plots of M_n vs. M/I and corresponding \mathcal{D} values of (a) **P6**, (b) **P3**, (c) **P7**, and (d) SEC traces of **P3** from entries 7–11 in Table 4.3

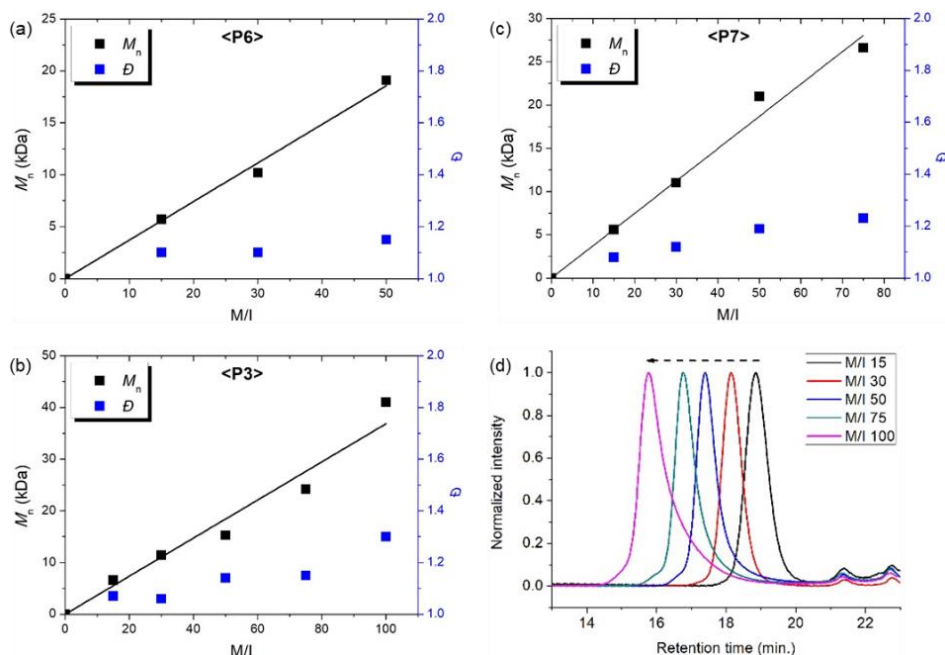


Table 4.4 CP of various 1,6-heptadiynes using Ru2 and pyridine

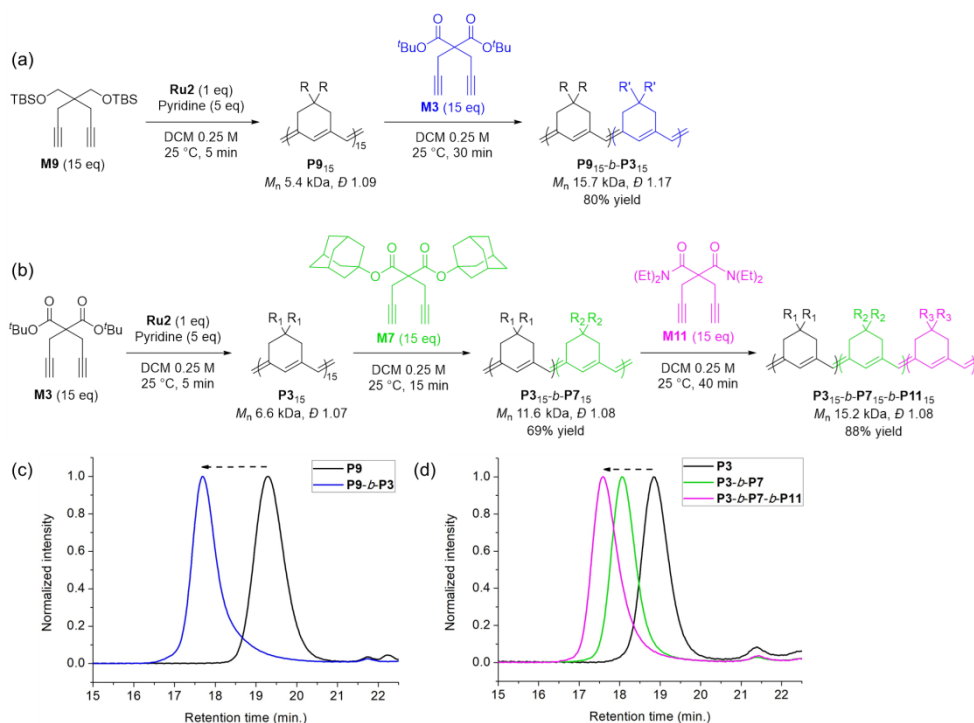
M8	M9	M4	M1	M10	M11

entry	monomer	M/I/Add	time (h)	conv (%) ^a	yield (%) ^b	M_n (kDa) ^c	\mathcal{D}^c	β -selectivity (%) ^d
1	M8	30/1/10	0.5	>99	83	8.1	1.36	93
2		50/1/15	1	>99	85	9.4	1.65	
3	M9	30/1/10	1	>99	82	15.4	1.11	
4		50/1/15	2	>99	73	26.5	1.17	>99
5	M4	30/1/10	2	>99	66	16.3	1.11	
6		50/1/15	3	97	60	26.2	1.35	>99
7	M1	30/1/10	1	>99	61	7.8	1.20	>99
8		50/1/15	3	>99	77	14.2	1.18	
9	M10	30/1/10	2	>99	75	11.3	1.11	
10		50/1/15	4	>99	78	21.7	1.18	74
11 ^e	M11	30/1/10	1.5	>99	99	8.4 ^e	1.18	84
12 ^{e,f}		50/1/15	2	74	65	7.7	1.37	

^aDetermined by ¹H NMR. ^bPrecipitated in methanol at -78°C. ^cDetermined by THF SEC calibrated using polystyrene standards. ^dDetermined by ¹³C NMR. ^ePrecipitated in hexane at -78°C. ^fConducted at 15 °C.

To broaden the monomer scope, we tested CP using Ru2 and monomers containing various non-malonate functional groups for M/Is of 30 and 50 (Table 4.4). CP of M8, containing the small ethyl ether group, showed high reactivity with complete conversion, and a high β -selectivity of 93%, but uncontrolled M_n with relatively broad dispersities (entries 1 and 2). Bulky M9 and M4, containing silyl ether groups, showed not only excellent reactivity and β -selectivity (99%) but also great controllability with narrow \mathcal{D} s, except for a slight broadening in the CP of M4, with a M/I of 50

(entries 3–6). **M1** was another successful example with excellent conversion for both M/Is of 30 and 50, producing **P1** with a controlled M_n and narrow dispersity (<1.20), along with an excellent β -selectivity of 99% (entries 7 and 8). Furthermore, **M10**, with a pivaloyl group, reacted efficiently with excellent conversion, controlled M_n , and narrow dispersity (<1.20) for both M/Is of 30 and 50, despite showing a moderate β -selectivity of 74% (entries 9 and 10). Lastly, amide group-containing **M11** showed complete conversion for an M/I of 30 with a narrow \mathcal{D} and a good β -selectivity of 84%, but the reactivity decreased at higher M/I resulting in only 74% conversion and uncontrolled M_n and \mathcal{D} (entries 11 and 12).



Scheme 4.3 Diblock and triblock copolymerization for synthesizing exclusively β -selective conjugated polyenes (a, b), and THF-SEC traces of the polymers (c, d). Based on the successfully controlled polymerization, we tried another block

copolymerization to determine if living polymerization was feasible with Ru2. Initially, **M9** was used as the first monomer to form **P9** with an M_n of 5.4 kDa and \mathcal{D} of 1.09, after which 15 equiv of **M3** was added to successfully produce **P9-*b*-P3** (M_n 15.7 kDa, \mathcal{D} 1.17), detected by SEC analysis with a complete shift of the traces (Scheme 4.3a, c). Using the same procedure, we synthesized another diblock copolymer using **M3** as the first monomer, followed by the addition of 15 equiv of **M7** as the second monomer, to form **P3-*b*-P7** with an M_n of 11.6 kDa and a narrow dispersity of 1.08 (Scheme 4.3b). To this living polymer end, we further added 15 equiv of a third monomer, **M11**, which resulted in complete conversion to produce **P3-*b*-P7-*b*-P11**, showing a complete shift of SEC trace, with M_n of 15.2 kDa and \mathcal{D} of 1.08 in a good yield of 88% (Scheme 4.3d). This remarkable success with diblock and triblock copolymerizations with a broad monomer scope and narrow \mathcal{D} suggests the superior versatility of Ru2 in β -selective living/controlled polymerization, compared with Ru1, which had a narrower scope.

4.4 Conclusion

In conclusion, we successfully performed β -selective living/controlled CP using two Ru dithiolate catalysts to prepare various conjugated polyenes, bearing mostly six-membered-ring repeat units. The high controllability was achieved by maximizing the steric demands on either the monomer or the catalyst, which improved the stability of the propagating species with the aid of pyridine additives. **Ru1** containing less bulky NHC ligands required the extremely bulky monomer **M2** for controlled polymerization. On the other hand, **Ru2**, already containing a bulky ligand, demonstrated much faster initiation and intrinsically greater stabilization of the propagating species, whereby a versatile living polymerization with a broader monomer scope was possible. Furthermore, we systematically studied the effect of pyridine additives and changing the catalyst by *in situ* ^1H NMR kinetic experiments. In particular, we found that ligands which coordinate more strongly to **Ru2** better stabilized the propagating species and promoted better living/controlled CP. More significantly, we achieved several β -selective diblock and triblock copolymerizations, for the first time, to the best of our knowledge. In short, we achieved a rare β -selective living CP by analyzing the mechanistic details and kinetic parameters, and we expect this study to increase the insight into and versatility of Ru-catalyzed polymerizations.

4.5 Experimental Section

Materials

All reagents which are commercially available from Sigma–Aldrich®, Tokyo Chemical Industry Co. Ltd., Acros Organics, Alfa Aesar®, without additional notes, were used without further purification. Dichloromethane for the polymerization was purified by Glass Contour Organic Solvent Purification System and degassed further by Ar bubbling for 10 minutes before performing reactions. Thin–layer chromatography (TLC) was carried out on MERCK TLC silica gel 60 F254, and flash column chromatography was performed using MERCK silica gel 60 (0.040~0.063 mm).

Characterization

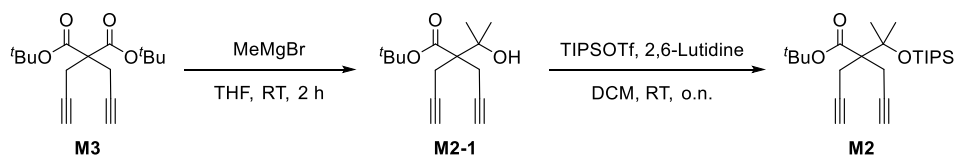
^1H -NMR and ^{13}C -NMR were recorded by Varian/Oxford As-500 (500 MHz for ^1H and 125 MHz for ^{13}C) and Agilent 400-MR (400 MHz for ^1H and 100 MHz for ^{13}C) spectrometers. ^{13}C NMR for the polymers was mainly recorded by Bruker (600 MHz for ^1H and 150 MHz for ^{13}C) spectrometers in the National Instrumentation Center for Environmental Management (NICEM) at SNU. High-resolution mass spectroscopy (HRMS) analyses were performed by the ultrahigh resolution ESI Q-TOF mass spectrometer (Bruker, Germany) in the Sogang Centre for Research Facilities. Size exclusion chromatography (SEC) analyses were carried out with Waters system (1515 pump, 2414 refractive index detector) and Shodex GPC LF-804 column eluted with THF (GPC grade, Honeywell Burdick & Jackson®) and filtered with a 0.2 μm PTFE filter (Whatman®).

The flow rate was 1.0 mL/min, and the temperature of the column was maintained at 35 °C.

Experimental procedures for the preparation of the monomers

Ru1,¹ Ru2,⁶ M1, M3–M6, M8–M11² were prepared by literature methods.

M2 (*tert*-butyl 2-(prop-2-yn-1-yl)-2-(2-((triisopropylsilyl)oxy)propan-2-yl)pent-4-ynoate)

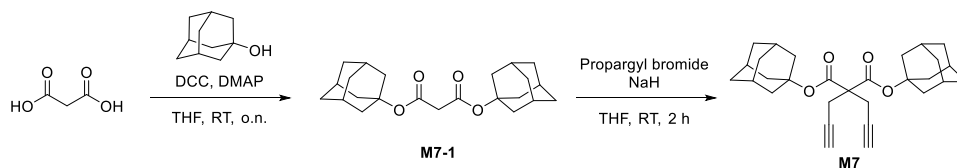


To a solution of **M3** (880 mg, 3.0 mmol) in THF (9 ml), methylmagnesium bromide (3 M in ether, 12 mmol, 4 ml) was slowly added at 0 °C. and The mixture was stirred for 2 hr at room temperature then quenched by saturated NH_4Cl aqueous solution at 0 °C. The organic layer was washed with NaCl aqueous solution, extracted by EtOAc , dried with MgSO_4 , and concentrated. The product was purified by flash column chromatography on silica gel ($\text{EtOAc}:\text{Hexane}=1:20$) to afford **M2-1** as a colorless liquid (510 mg, 68% yield). $^1\text{H-NMR}$ (500 MHz, CDCl_3): δ 3.28 (s, 1H), 2.83 (q, J = 61.0, 17.2 Hz, 4H), 2.05 (s, 2H), 1.49 (s, 9H), 1.31 (s, 6H).; $^{13}\text{C-NMR}$ (125MHz, CDCl_3): δ 172.7, 82.9, 81.9, 74.1, 71.3, 56.2, 28.1, 26.6, 21.8.; HR-MS (ESI) m/z for $\text{C}_{15}\text{H}_{22}\text{NaO}_3$ $[\text{M}+\text{Na}]^+$, calcd. 273.1461, found: 273.1460.

To a solution of **M2-1** (750mg, 3.0 mmol) in DCM (9 mL), 2,6-lutidine (1.4 mL, 12 mmol) was added, and the mixture was cooled down to 0 °C, followed by the addition of triisopropylsilyl trifluoromethanesulfonate (1.1

mL, 6 mmol). After stirring overnight at room temperature, the mixture was quenched by the saturated NH_4Cl aqueous solution. The organic layer was washed with NaCl aqueous solution, extracted by EtOAc , dried with MgSO_4 , and concentrated. The product was purified by flash column chromatography on silica gel (hexane only) to afford **M2** as a colorless liquid (650 mg, 53% yield). ^1H -NMR (400 MHz, CDCl_3): δ 2.83 (q, J = 16.8 Hz, 4H), 1.98 (s, 2H), 1.47 (s, 9H), 1.44 (s, 6H), 1.09 (s, 21H).; ^{13}C -NMR (150MHz, CDCl_3): δ 171.8, 82.7, 81.7, 77.0, 70.4, 57.6, 28.1, 22.4, 18.6, 13.8.; HR-MS (ESI): m/z for $\text{C}_{24}\text{H}_{42}\text{NaO}_3\text{Si}$, $[\text{M}+\text{Na}]^+$, calcd. 429.2795, found: 429.2797.

M7 (di(adamantan-1-yl) 2,2-di(prop-2-yn-1-yl)malonate)



Malonic acid (310 mg, 3.0 mmol) and 1-adamantanol (1.0 g, 6.6 mmol) were solvated in THF (15 ml). A mixture of N,N' -dicyclohexylcarbodiimide (1.4 g, 6.6 mmol) and 4-dimethylaminopyridine (36 mg, 0.30 mmol) in THF (15 mL) was slowly added at 0°C . The mixture was stirred overnight at room temperature then quenched by acetic acid. After partially removing dicyclohexylurea (generated as a byproduct) by filtering, the organic layer was washed with water and extracted by DCM , dried with MgSO_4 , and concentrated. The product was purified by flash column chromatography on silica gel ($\text{EtOAc}:\text{Hexane} = 1:10$) to afford **M7-1** as white solid (740 mg, 66% yield). ^1H -NMR (500 MHz, CDCl_3): δ 3.18 (s, 2H), 2.17 (s, 6H),

2.13 (s, 12H), 1.66 (s, 12H). ^{13}C -NMR (150 MHz, CDCl_3): δ 166.09, 81.83, 44.78, 41.33, 36.28, 30.97. HR-MS (ESI) m/z for $\text{C}_{23}\text{H}_{32}\text{NaO}_4$ $[\text{M}+\text{Na}]^+$, calcd. 395.2193, found: 395.2196.

Sodium hydride (60%, dispersion in mineral oil) (88 mg, 2.2 mmol) in THF (2 mL) was prepared at 0 °C in RBF purged with argon, and a solution of M7-1 (370 g, 1.0 mmol) in THF (1 mL) was added drop-wisely. After 10 minutes of stirring, propargyl bromide (80 wt%, in toluene) (0.50 mL, 2.5 mmol) was added and stirred for 2 hr. The reaction was quenched by adding NH_4Cl aqueous solution, and the organic layer was extracted with EtOAc, dried with MgSO_4 , and concentrated. The product was purified by flash column chromatography on silica gel (EtOAc:Hexane = 1:30) to afford M7 as a white solid (410 mg, 91% yield). ^1H -NMR (500 MHz, CDCl_3): δ 2.88 (d, J = 2.6 Hz, 4H), 2.18 (s, 6H), 2.11 (d, J = 2.9 Hz, 12H), 2.02 (t, 2H), 1.66 (s, 12H). ^{13}C -NMR (150 MHz, CDCl_3): δ 167.7, 82.3, 79.2, 71.5, 57.2, 41.2, 36.3, 31.0, 22.5.; HR-MS (ESI) m/z for $\text{C}_{29}\text{H}_{36}\text{NaO}_4$ $[\text{M}+\text{Na}]^+$, calcd. 471.2506, found: 471.2509.

General procedure for the cyclopolymerization

A 5-mL sized screw-cap vial with a septum was flame dried and charged with monomer and a magnetic bar. The vial was purged with argon four times, and degassed anhydrous DCM was added. After the Ar-purged catalyst (Ru1 and Ru2) and pyridine additive in another 5-mL vial were dissolved in DCM, the solution was rapidly injected to the monomer solution at an experimental temperature under vigorous stirring. The

reaction was quenched by excess ethyl vinyl ether after desired reaction time and partially precipitated in hexane or methanol at $-78\text{ }^{\circ}\text{C}$, remaining small amount of crude mixture ($\sim 10\%$). Obtained solid was filtered and dried in vacuo. Monomer conversion was calculated from the ^1H NMR spectrum of the remaining crude mixture.

In situ NMR experiment: procedure and data

(i) Initiation experiment of Ru1

To an NMR tube was added a solution of Ru1 (2.3 mg, 0.003 mmol) in 0.6 mL DCM- d_2 . The tube was then sealed with a rubber septum, taken out of the glovebox, and placed in a dry ice/acetone bath. Butyl vinyl ether (12 μL , 0.090 mmol) was injected into the tube, and the reaction was monitored by observing the disappearance of the benzyldiene signal by ^1H NMR using an array at the appropriate temperature.

(ii) Kinetic experiments using Ru1 or Ru2

Ru1 or Ru2 (0.003 mmol, 1 eq) and hexamethyldisilane (internal standard, 3 μl) were dissolved in DCM- d_2 (400 μL). Initial benzyldiene was measured by the integral ratio of Ru1 or Ru2 to hexamethyldisilane in ^1H NMR spectrum. (After the addition of 4–7 eq of the pyridine additive,) Monomer (0.06 mmol, 20 eq) solution in DCM- d_2 (200 μl) was added to the catalyst solution and mixed by shaking the NMR tube for 5 seconds. The reaction was monitored by ^1H NMR over time. The k_i or k_p values were obtained from the slope of linear $-\ln [\text{Ru}]/[\text{Ru}]_0$ or $-\ln [\text{M}]/[\text{M}]_0$ vs. time graphs, respectively.

^1H and ^{13}C NMR characterization of polymers

The ^1H NMR and ^{13}C NMR of P1, P3–6, P8–11 are described in the literature.²

P2

^1H (500 MHz, CDCl_3): δ 7.04 – 5.62 (br m, 2H), 3.68 – 2.40 (br m, 4H), 1.42 (br s, 6H), 1.29 (br s, 9H), 1.11 (br s, 21H); ^{13}C (150 MHz, CDCl_3): δ 172.9, 140.3, 137.5, 136.9, 134.0, 131.4, 80.3, 75.9, 57.8, 33.2, 30.6, 27.8, 18.8, 13.8.

P2₁₅–*b*–P3₁₅

^1H (500 MHz, CDCl_3): δ 7.04 – 5.62 (br m, 4H), 3.68 – 2.40 (br m, 8H), 1.42 (br s, 24H), 1.29 (br s, 9H), 1.11 (br s, 21H); ^{13}C (150 MHz, CDCl_3): δ 172.9, 170.1, 137.4, 134.6, 133.2, 131.7, 128.1, 81.5, 80.3, 75.92, 57.8, 55.6, 35.3, 32.5, 30.7, 28.0, 18.8, 13.8.

P2₁₅–*b*–P4₁₅

^1H (500 MHz, CDCl_3): δ 7.04 – 5.62 (br m, 4H), 3.88 – 2.07 (br m, 12H), 1.39 (br s, 6H), 1.29 (br s, 9H), 1.11 (br s, 21H), 1.04 (br s, 42H); ^{13}C (150 MHz, CDCl_3): δ 172.9, 140.4, 137.4, 135.9, 133.4, 132.3, 80.3, 75.9, 66.0, 57.8, 41.3, 33.6, 27.8, 18.8, 18.3, 13.8, 12.2.

P7

^1H (500 MHz, CDCl_3): δ 6.90 – 5.70 (br m, 2H), 3.50 – 2.59 (br m, 4H), 2.14 (br s, 6H), 2.08 (br s, 12H), 1.64 (br s, 12H); ^{13}C (150 MHz, CDCl_3): δ 169.9, 134.8, 134.3, 133.4, 131.9, 81.4, 55.7, 41.1, 36.3, 31.0.

P9₁₅–*b*–P3₁₅

^1H (500 MHz, CDCl_3): δ 6.92 – 5.66 (br m, 2H), 3.39 (br s, 4H), 3.16 – 2.06 (br m, 8H), 1.42 (br s, 18H), 0.88 (br s, 18H), 0.00 (br s, 12H); ^{13}C (150 MHz, CDCl_3): δ 170.2, 135.6, 134.7, 134.4, 133.4, 132.0, 128.0, 81.4, 65.7, 65.3, 55.7, 47.7, 40.6, 35.3, 33.5, 32.4, 30.9, 28.0, 26.1, 18.4, –5.4.

P3₁₅–*b*–P7₁₅

^1H (500 MHz, CDCl_3): δ 6.90 – 5.70 (br m, 4H), 3.50 – 2.59 (br m, 8H), 2.14 (br s, 6H), 2.08 (br s, 12H), 1.64 (br s, 12H), 1.42 (br s, 18H); ^{13}C (150 MHz, CDCl_3): δ 170.1, 169.9, 134.7, 134.4, 133.4, 132.0, 81.4, 55.7, 55.6, 41.2, 36.3, 35.3, 32.4, 31.0, 28.0.

P3₁₅–*b*–P7₁₅–*b*–P11₁₅

^1H (500 MHz, CDCl_3): δ 6.90 – 5.63 (br m, 6H), 3.50 – 2.46 (br m, 20H), 2.14 (br s, 6H), 2.08 (br s, 12H), 1.64 (br s, 12H), 1.42 (br s, 18H), 1.08 (br s, 12H); ^{13}C (150 MHz, CDCl_3): δ 170.1, 169.9, 134.9, 134.3, 133.4, 132.0, 81.4, 55.7, 55.6, 53.6, 41.1, 36.3, 35.3, 32.4, 30.9, 27.9, 14.0, 12.9.

4.6 Supporting Information

Calculation of the regioselectivity for P5 using ^1H NMR

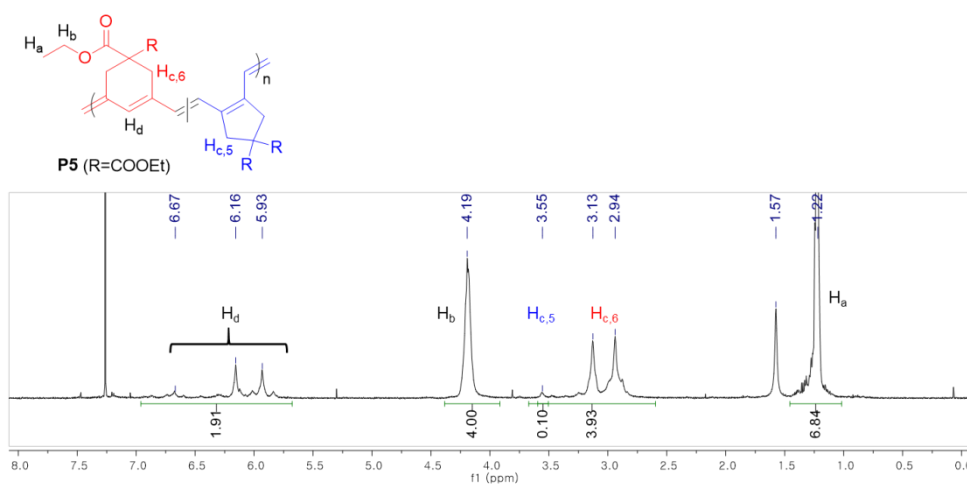


Figure S4.1 ^1H NMR spectrum of the crude mixture of entry 1 in Table 4.2

The composition of five-membered ring = $\frac{2 * \text{H}_{c,5}}{\text{H}_{\text{originated from propargylic}}}$

e.g. (entry 1 in Table 4.2)

Composition of five-membered ring = $\frac{2 * 0.10}{3.93} = 0.051$ ($\therefore \beta$ -selectivity=95%)

Supporting kinetic experiments using Ru1 and Ru2

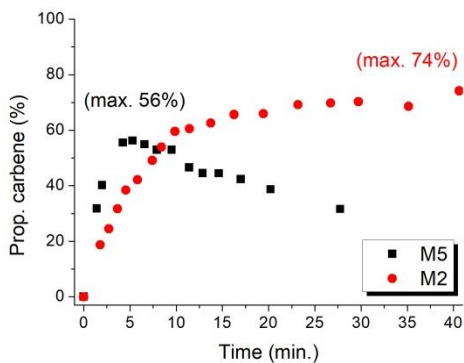


Figure S4.2 Plot of the propagating carbene vs. reaction time for M5 and M2 using Ru1 under 3-ClPy as an additive

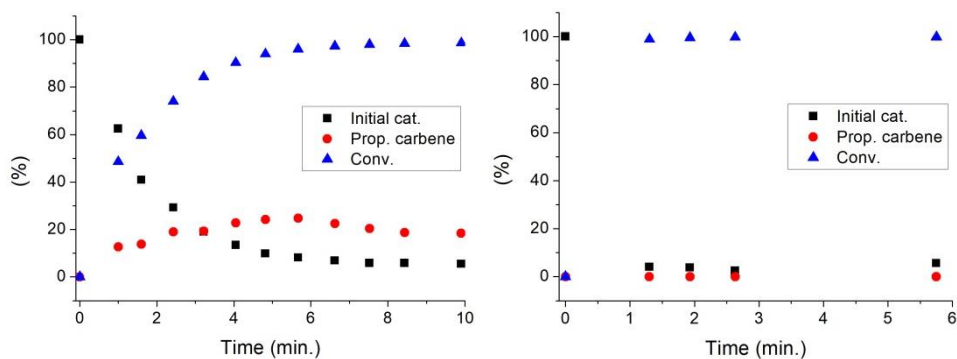


Figure S4.3 Plots of the conversion and initial Ru catalysts vs. reaction time for M5 using Ru1 (left) and Ru2 (right) under 3,5-Cl₂Py as an additive

Table S4.1 Calculated k_p and k_i/k_p values for CP of M5 using Ru2 with various pyridine additives

	No additive (-20 °C)	3-ClPy (0 °C)	Pyridine (0 °C)	4-MeOPy (0 °C)
k_p	1.49	0.193	0.0892	0.0139
k_i/k_p	4.12×10^{-3}	1.25×10^{-2}	2.71×10^{-2}	17.4×10^{-2}

SEC traces of the polymers

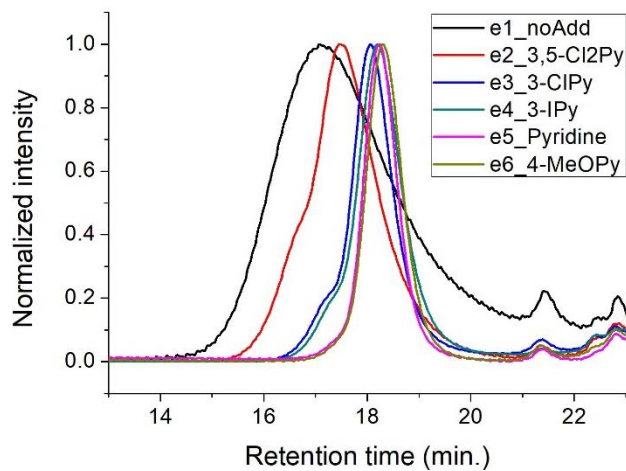


Figure S4.4 SEC traces of P5s in Table 4.2

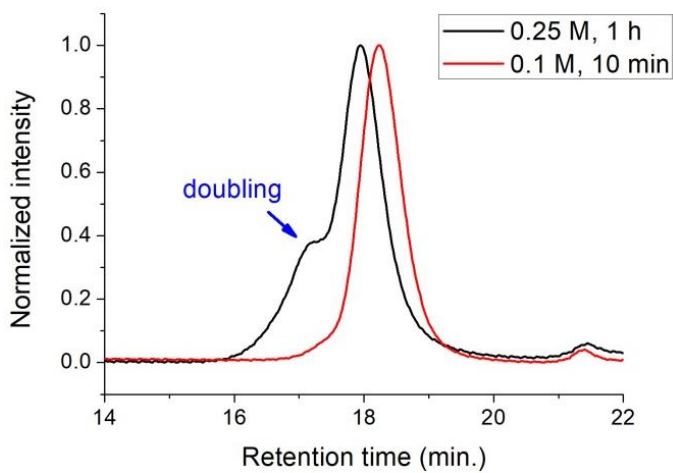


Figure S4.5 SEC traces of P5s synthesized in different conditions

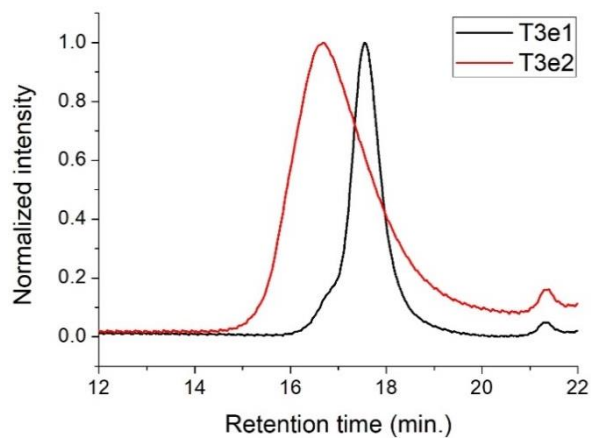


Figure S4.6 SEC traces of P5s in Table 4.3, entries 1 and 2

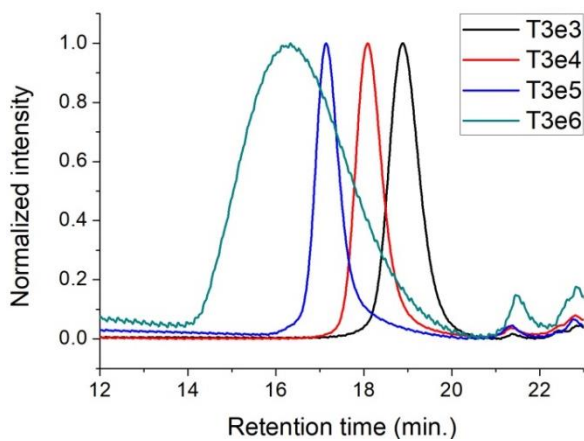


Figure S4.7 SEC traces of P6s in Table 4.3, entries 3–6

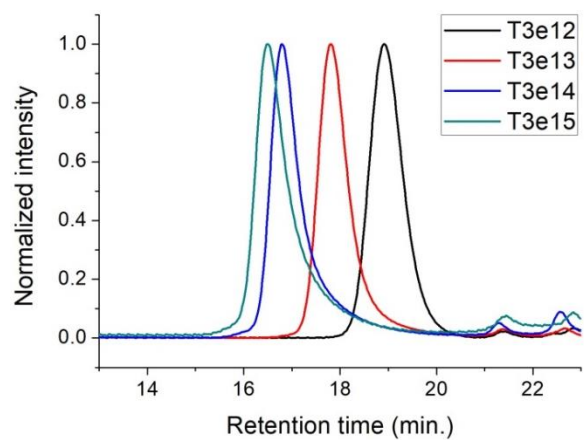
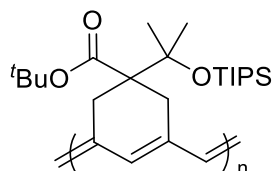


Figure S4.8 SEC traces of P7s in Table 4.3, entries 12–15

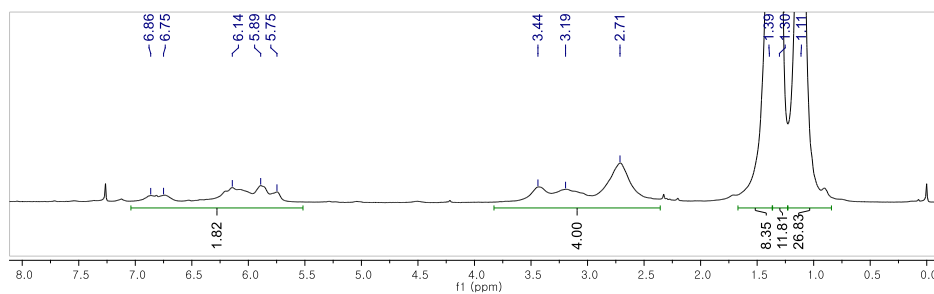
^1H and ^{13}C NMR spectra of the polymers

^{13}C NMR spectra were used for the determination of the ratio between five- and six-ring on the polymer backbone.

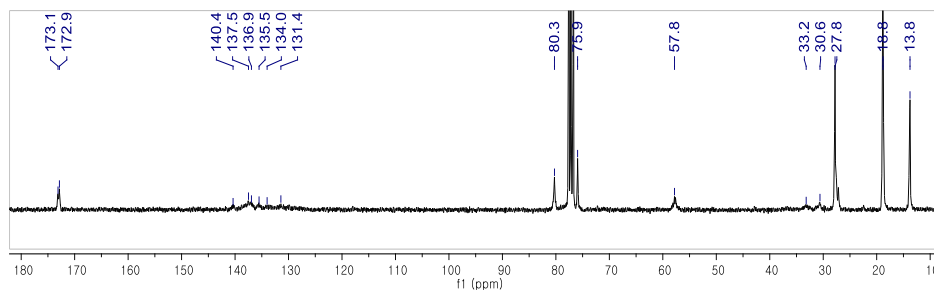
⟨P2 from Table 4.1⟩



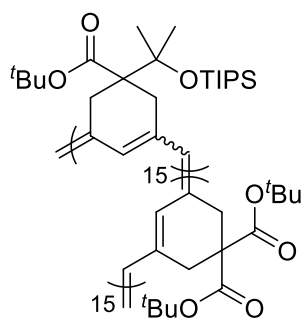
^1H NMR (500 MHz, CDCl_3)



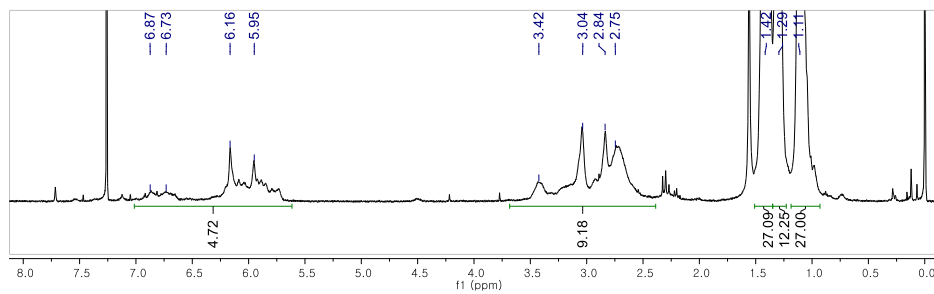
^{13}C NMR (150 MHz, CDCl_3)



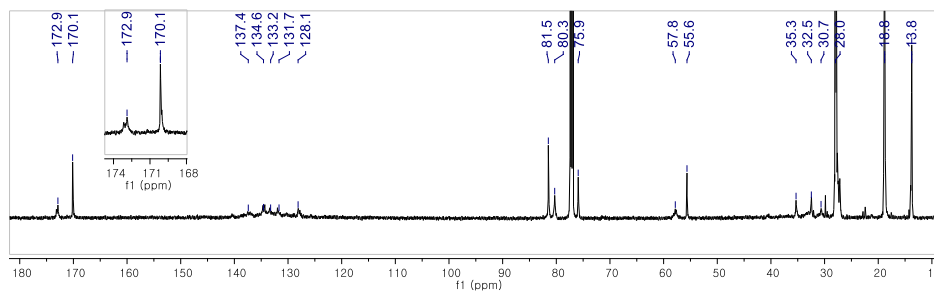
⟨P2-*b*-P3 from Scheme 4.2⟩



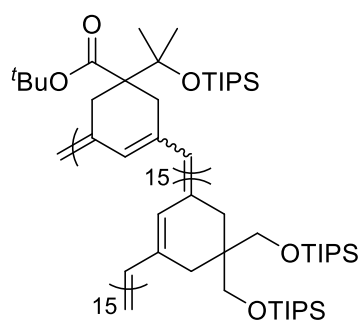
^1H NMR (500 MHz, CDCl_3)



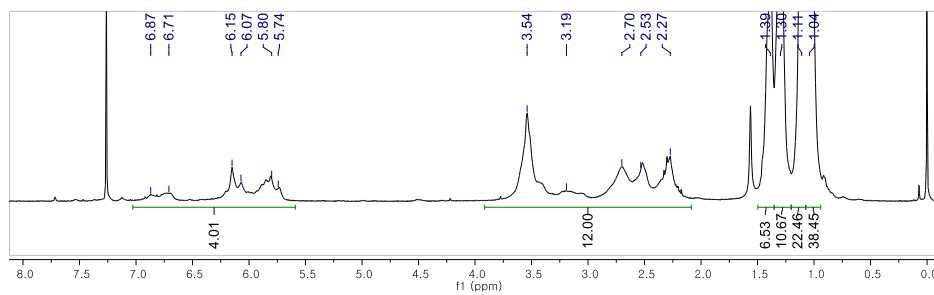
^{13}C NMR (150 MHz, CDCl_3)



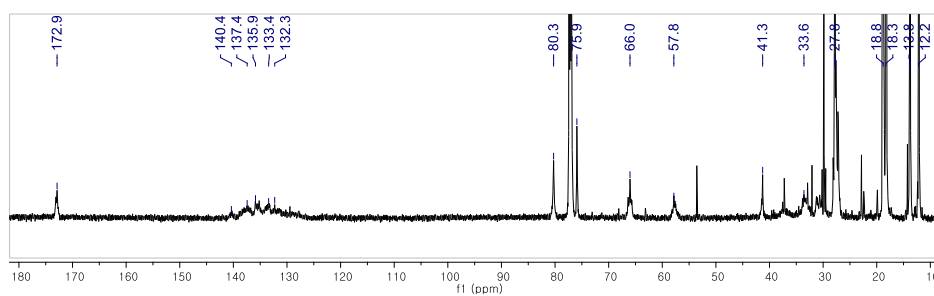
⟨P2-*b*-P4 from Scheme 4.2⟩



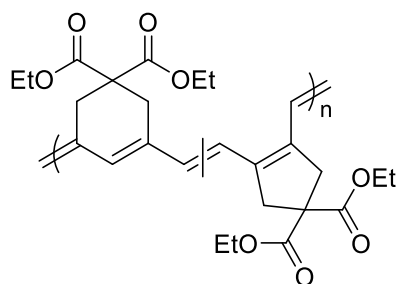
^1H NMR (500 MHz, CDCl_3)



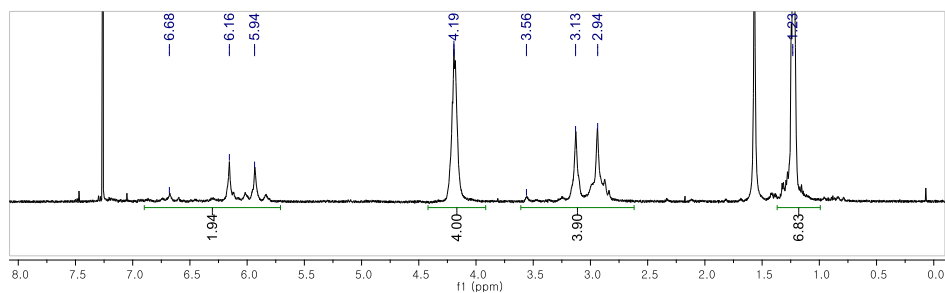
^{13}C NMR (150 MHz, CDCl_3)



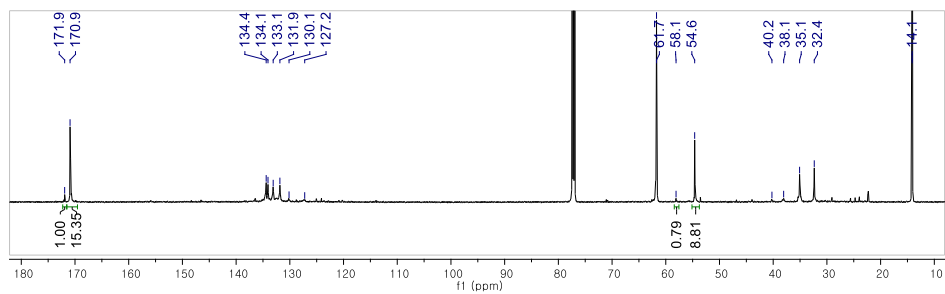
⟨P5 from Table 4.3, entry 1⟩



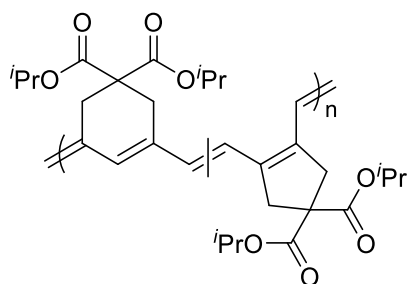
^1H NMR (500 MHz, CDCl_3)



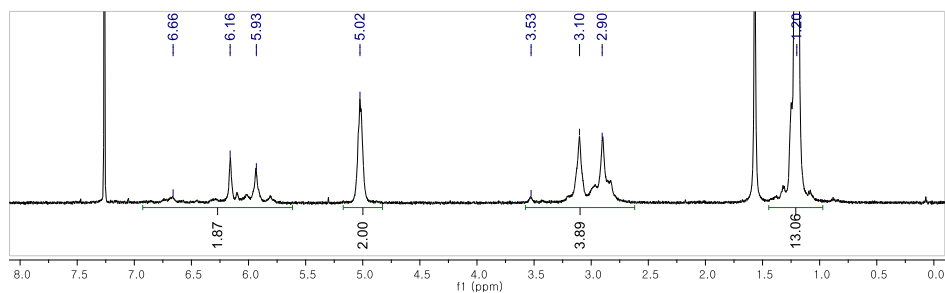
^{13}C NMR (150 MHz, CDCl_3)



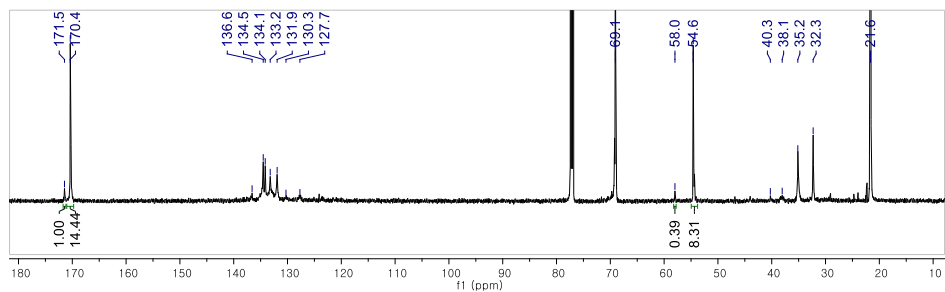
⟨P6 from Table 4.3, entry 5⟩



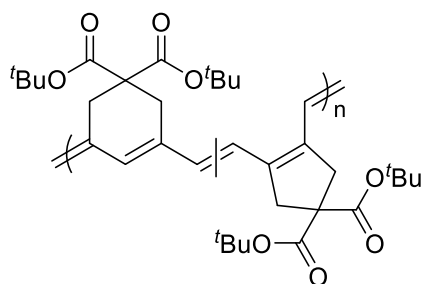
^1H NMR (500 MHz, CDCl_3)



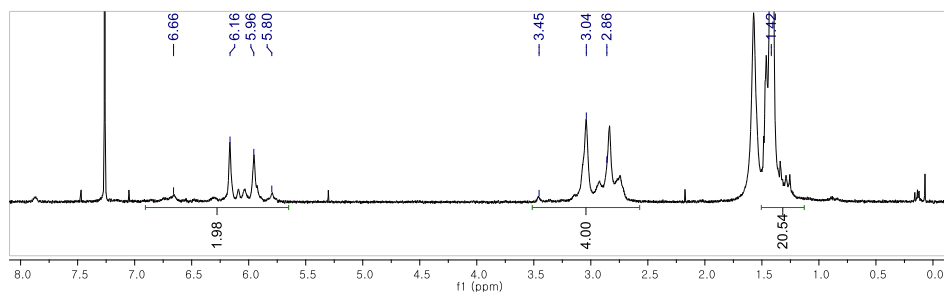
^{13}C NMR (150 MHz, CDCl_3)



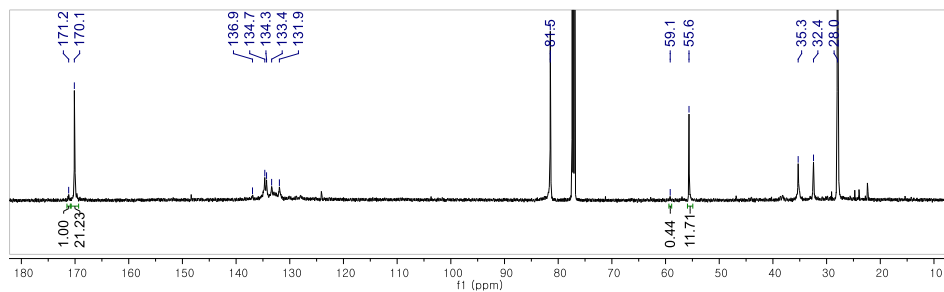
⟨P3 from Table 4.3, entry 9⟩



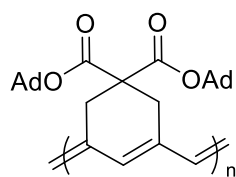
^1H NMR (500 MHz, CDCl_3)



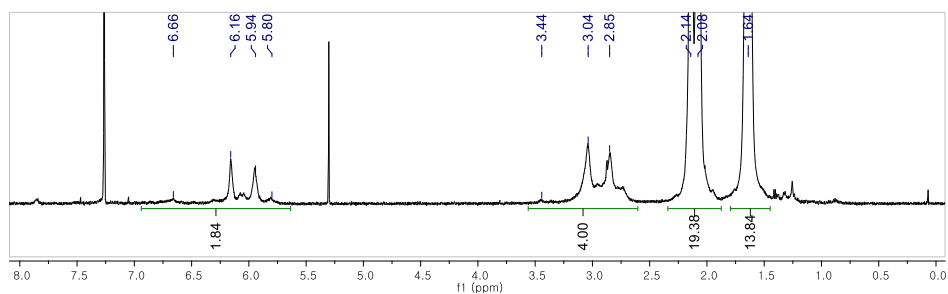
^{13}C NMR (150 MHz, CDCl_3)



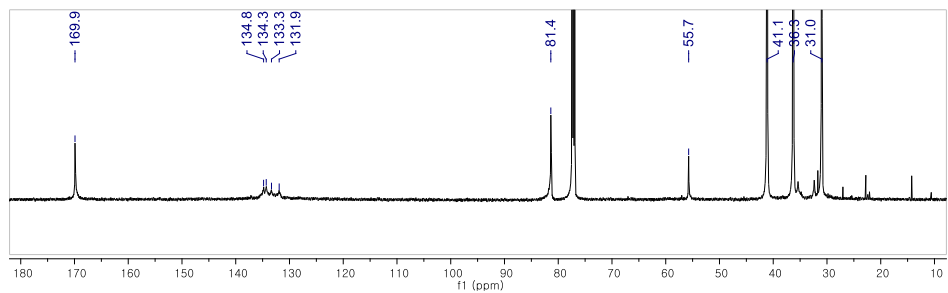
⟨P7 from Table 4.3, entry 14⟩



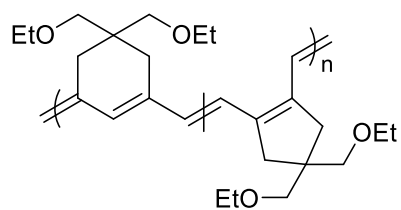
^1H NMR (500 MHz, CDCl_3)



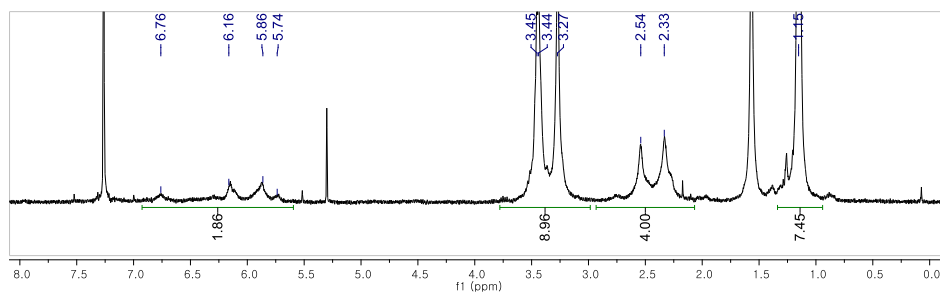
^{13}C NMR (150 MHz, CDCl_3)



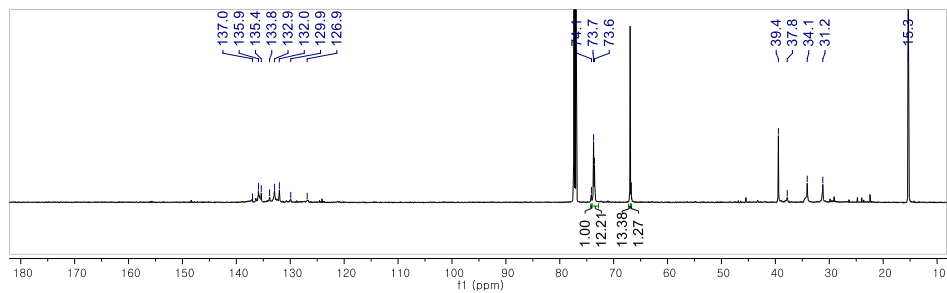
⟨P8 from Table 4.4, entry 1⟩



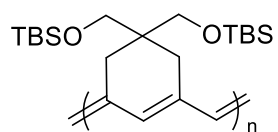
^1H NMR (500 MHz, CDCl_3)



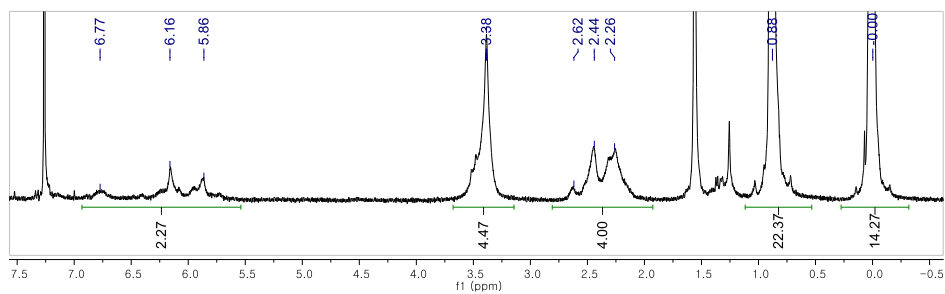
^{13}C NMR (150 MHz, CDCl_3)



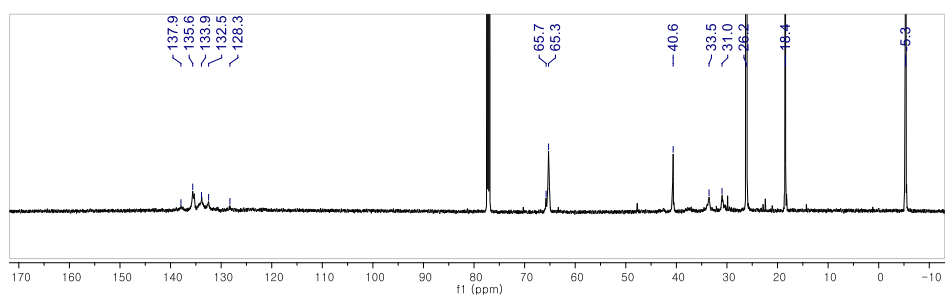
⟨P9 from Table 4.4, entry 4⟩



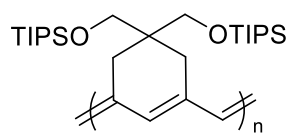
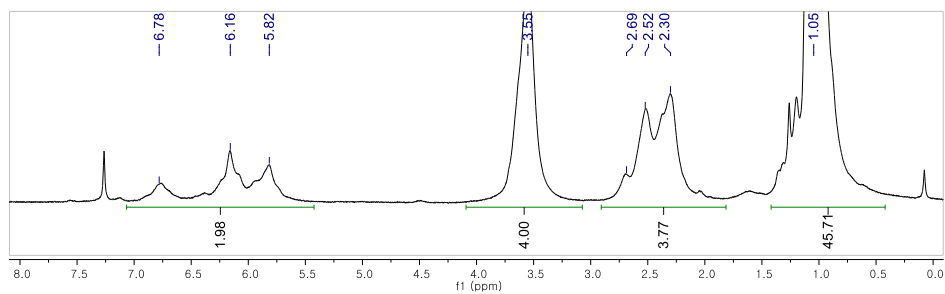
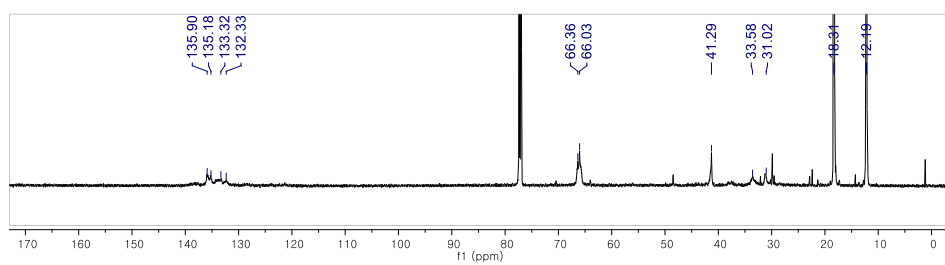
^1H NMR (500 MHz, CDCl_3)



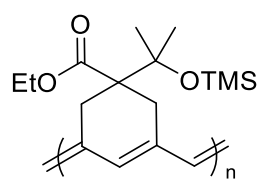
^{13}C NMR (150 MHz, CDCl_3)



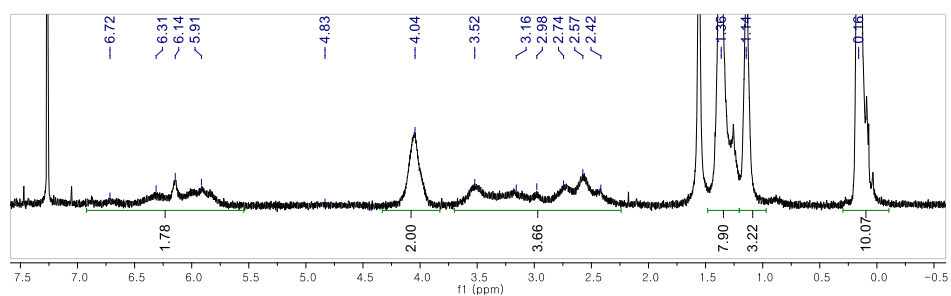
⟨P4 from Table 4.4, entry 6⟩

¹H NMR (500 MHz, CDCl₃) ^{13}C NMR (150 MHz, CDCl_3)

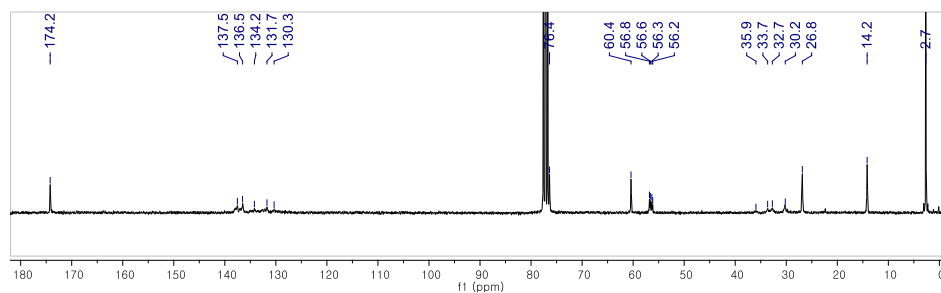
⟨P1 from Table 4.4, entry 7⟩



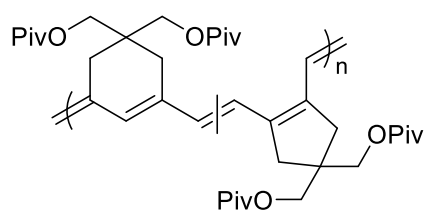
^1H NMR (500 MHz, CDCl_3)



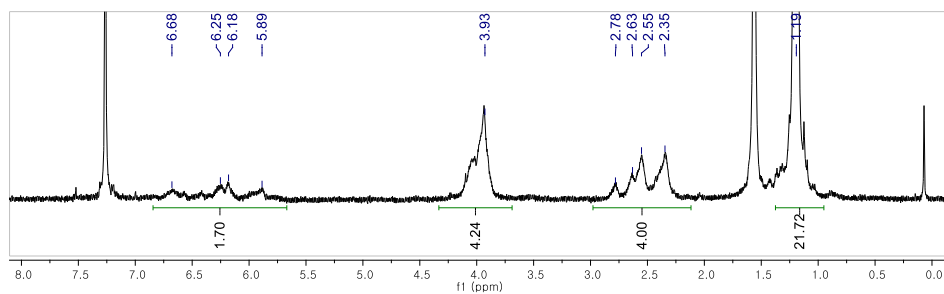
^{13}C NMR (150 MHz, CDCl_3)



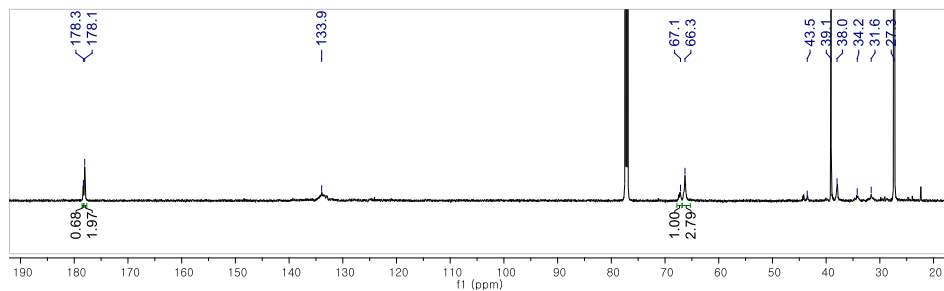
⟨P10 from Table 4.4, entry 10⟩



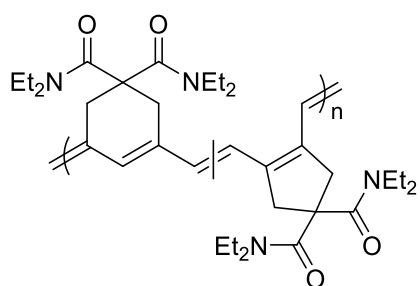
^1H NMR (500 MHz, CDCl_3)



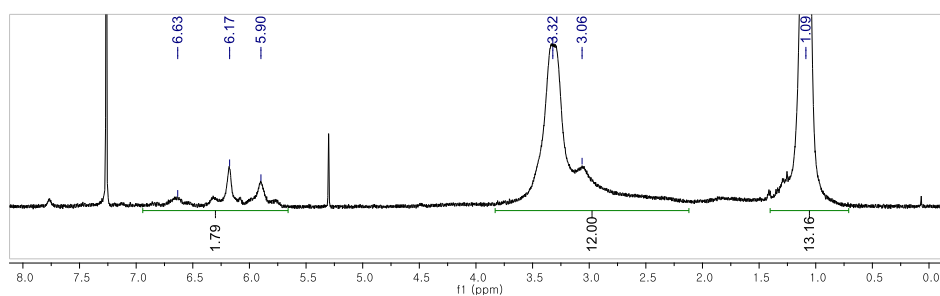
^{13}C NMR (150 MHz, CDCl_3)



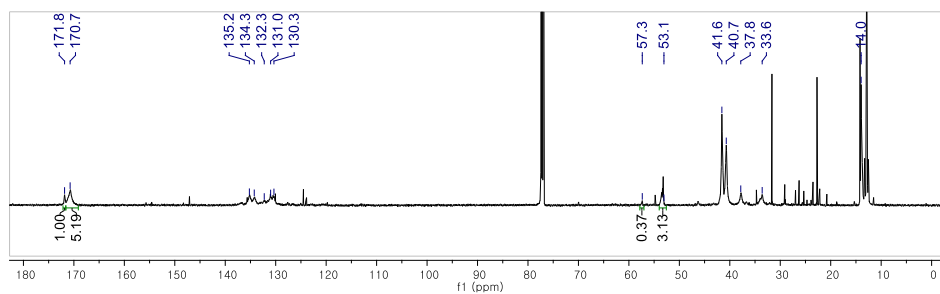
⟨P11 from Table 4.4, entry 11⟩



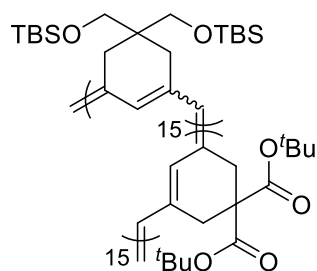
^1H NMR (500 MHz, CDCl_3)



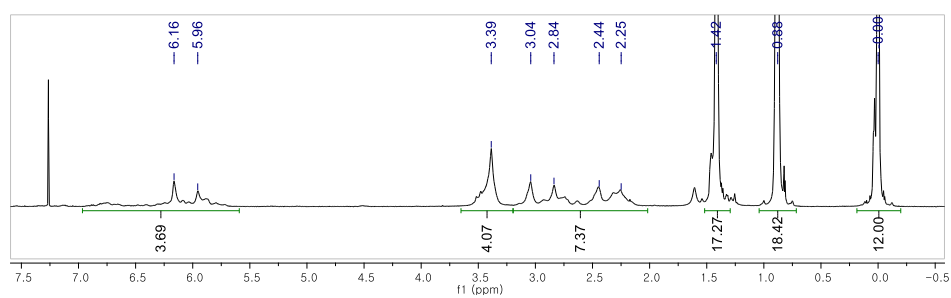
^{13}C NMR (150 MHz, CDCl_3)



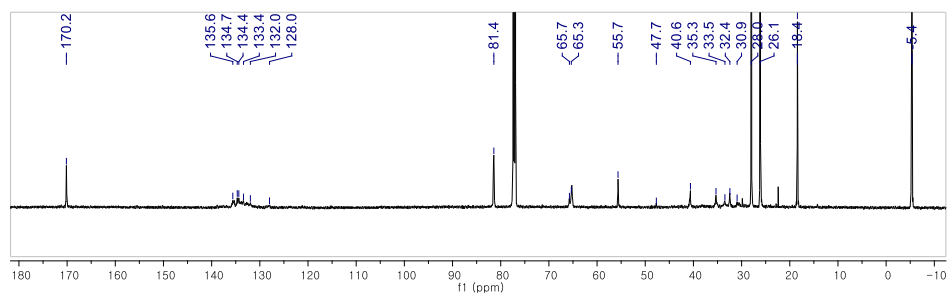
⟨P9-*b*-P3 from Scheme 4.3⟩



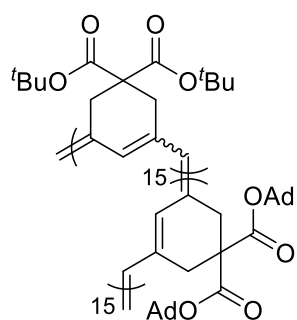
^1H NMR (500 MHz, CDCl_3)



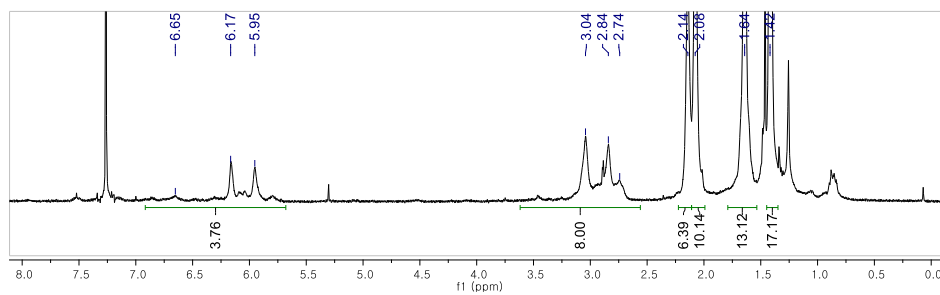
^{13}C NMR (150 MHz, CDCl_3)



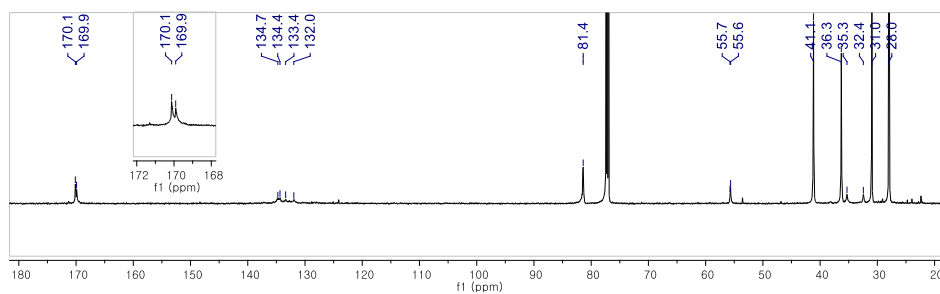
⟨P3-*b*-P7 from Scheme 4.3⟩



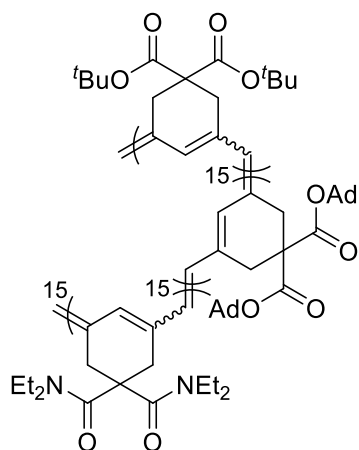
^1H NMR (500 MHz, CDCl_3)



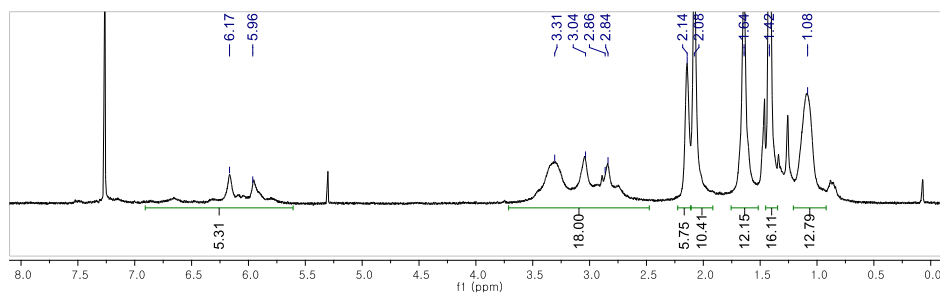
^{13}C NMR (150 MHz, CDCl_3)



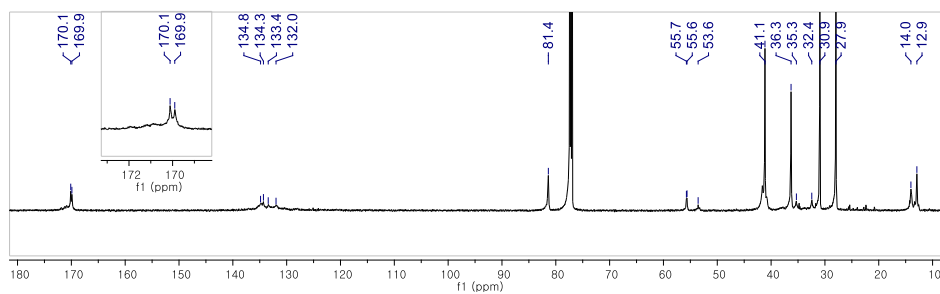
⟨P3-*b*-P7-*b*-P11 from Scheme 4.3⟩



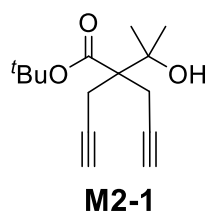
^1H NMR (500 MHz, CDCl_3)



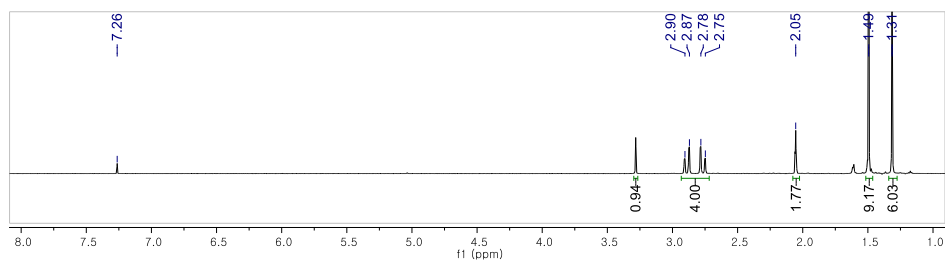
^{13}C NMR (150 MHz, CDCl_3)



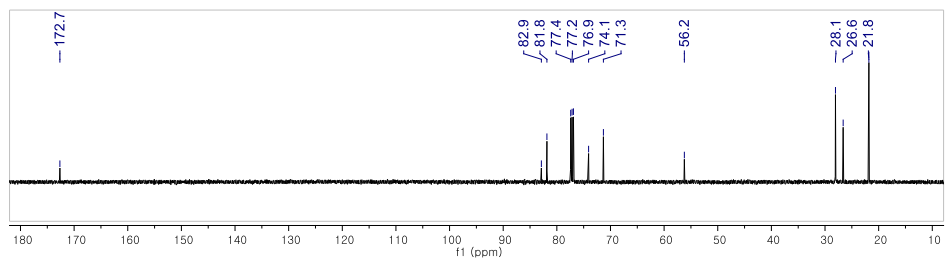
^1H and ^{13}C NMR spectra of the monomers



^1H NMR (500 MHz, CDCl_3)

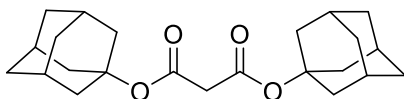


^{13}C NMR (125 MHz, CDCl_3)



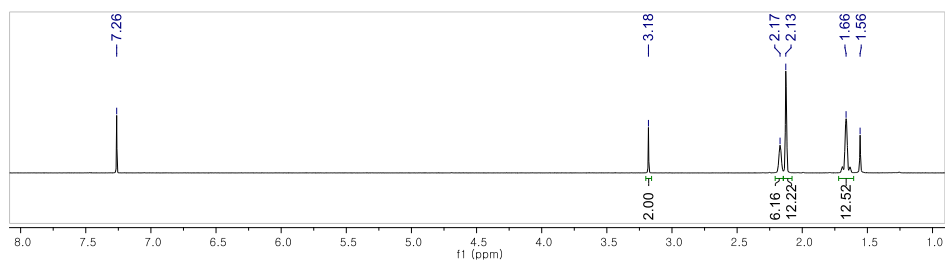


¹H NMR spectrum of compound **1** in CDCl₃. The spectrum shows peaks at 7.26 (s, 1H), 5.30 (s, 1H), 2.89, 2.85, 2.80, 2.76 (m, 4H), 1.97 (s, 3H), 1.47, 1.43 (m, 4H), 1.00 (t, 3H), and -0.00 (s, 3H). Integration values are 4.19, 1.82, 9.18, 6.00, 21.00, and 0.00 respectively.

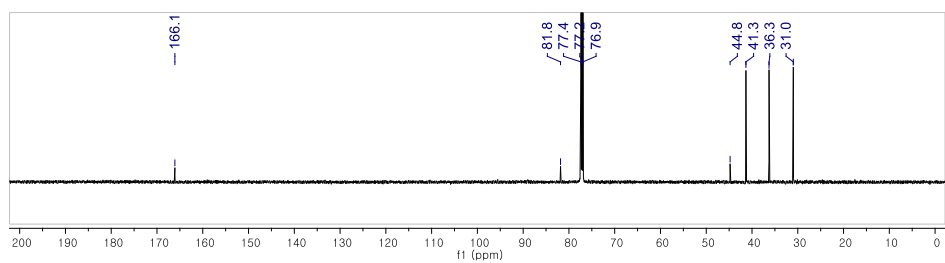


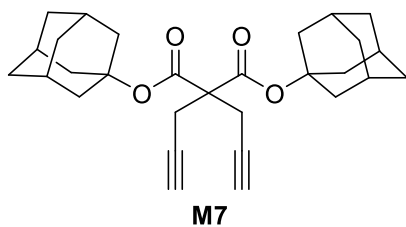
M7-1

^1H NMR (500 MHz, CDCl_3)

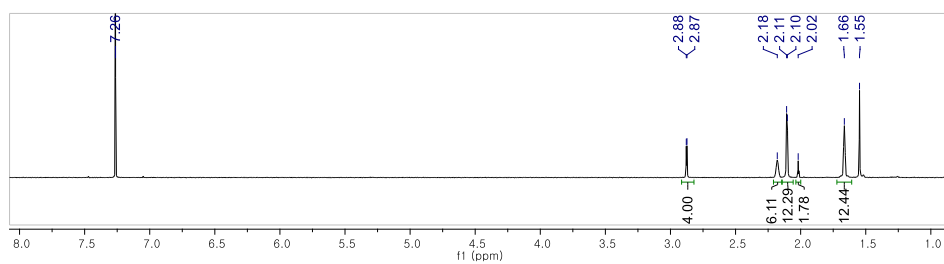


^{13}C NMR (150 MHz, CDCl_3)

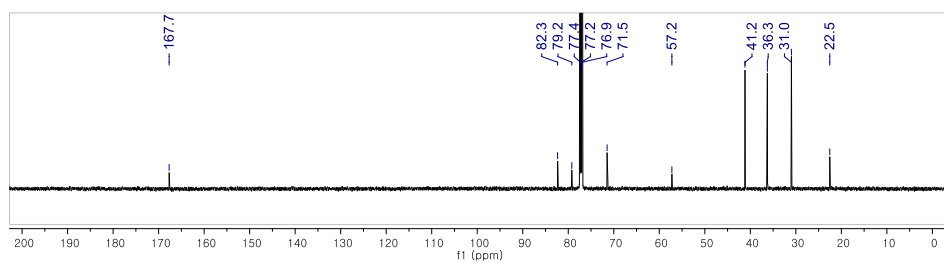




^1H NMR (500 MHz, CDCl_3)



^{13}C NMR (150 MHz, CDCl_3)



4.7 References

1. Koh, M. J.; Khan, R. K.; Torker, S.; Yu, M.; Mikus, M. S.; Hoveyda, A. H., *Nature* **2015**, *517*, 181.
2. Jung, K.; Kim, K.; Sung, J.-C.; Ahmed, T. S.; Hong, S. H.; Grubbs, R. H.; Choi, T.-L., *Macromolecules* **2018**, *51*, 4564.
3. Jung, H.; Jung, K.; Hong, M.; Kwon, S.; Kim, K.; Hong, S. H.; Choi, T. L.; Baik, M. H., *J. Am. Chem. Soc.* **2018**, *140*, 834.
4. (a) Schattenmann, F. J.; Schrock, R. R.; Davis, W. M., *J. Am. Chem. Soc.* **1996**, *118*, 3295; (b) Schattenmann, F. J.; Schrock, R. R., *Macromolecules* **1996**, *29*, 8990.
5. Courchay, F. C.; Sworen, J. C.; Wagener, K. B., *Macromolecules* **2003**, *36*, 8231.
6. Ahmed, T. S.; Grubbs, R. H., *Angew. Chem., Int. Ed.* **2017**, *56*, 11213.
7. Bailey, G. A.; Foscatto, M.; Higman, C. S.; Day, C. S.; Jensen, V. R.; Fogg, D. E., *J. Am. Chem. Soc.* **2018**, *140*, 6931.

Chapter 5. Cyclopolymerization of 1,5-Hexadiyne Derivatives to Form Four-Membered Rings

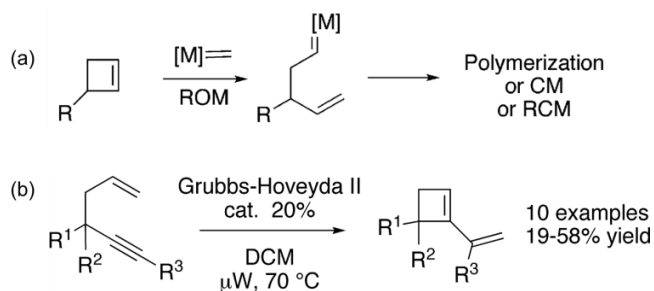
5.1 Abstract

In this chapter, we report cyclopolymerization (CP) of 1,5-hexadiynes to prepare the conjugated polyenes containing four-membered rings as a repeat unit. This new field of CP was explored by a thorough screening of the monomers and catalytic systems, enabling preparation of the ground. Preliminary results in this chapter show the possibility of this study and way to proceed.

5.2 Introduction

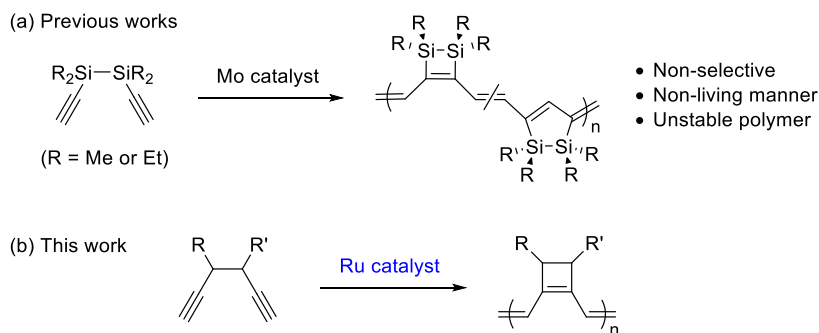
Studies on CP have been focused on the formation of five- or six-membered rings as a repeat unit, which bear relatively low ring strains (4.1 and 0.7 kcal/mol, respectively). As described in Chapter 1, our group have successfully demonstrated CP of 1,6-heptadiynes¹ and 1,7-octadiynes,² generating variously functionalized polyenes with five- or six-membered ring as a repeat unit (by selective α -addition) in living and controlled manners. However, the area of CP to form four-membered-ring has been rarely developed, because it is generally considered that four-membered cycles cannot be formed by ring-closing metathesis (RCM), due to their high ring strain (28.4 kcal/mol). Indeed, such cyclobutene rings could be easily reopened by metal carbene catalysts, the driving force being the relief of ring strain. There are reports on ring-opening metathesis polymerizations (ROMP),³ ring-opening metathesis/cross-metathesis,⁴ and ring-opening metathesis/ring-closing metathesis reactions⁵ using cyclobutene-ene

substrates (Scheme 5.1a). In 2007, the Campagne group disclosed groundbreaking results in this field, by developing a 1,5-enyne metathesis reaction using Ru-based Hoveyda–Grubbs 2nd generation catalyst (HGII) under microwave irradiation, to synthesize various functionalized cyclobutenes in low to fair yields (19–58%, Scheme 5.1b).⁶



Scheme 5.1 (a) Ring-opening metathesis of cyclobutene and (b) 1,5-Enyne Metathesis

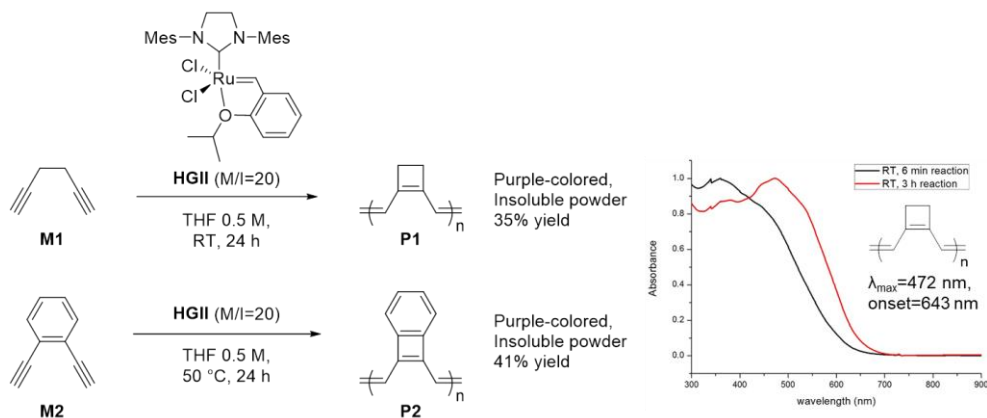
Inspired by this literature, we sought some possibility of CP of 1,5-hexadiyne derivatives. There are two reports on CP of Si-containing 1,5-hexadiyne derivatives using Mo-based catalysts, but these methods showed no regioselectivity or living manner, and the resulting polymers were highly unstable (Scheme 5.2a). In this chapter, we report trials for CP of 1,5-hexadiyne derivatives using various Ru-based olefin metathesis catalysts (Scheme 5.2b).



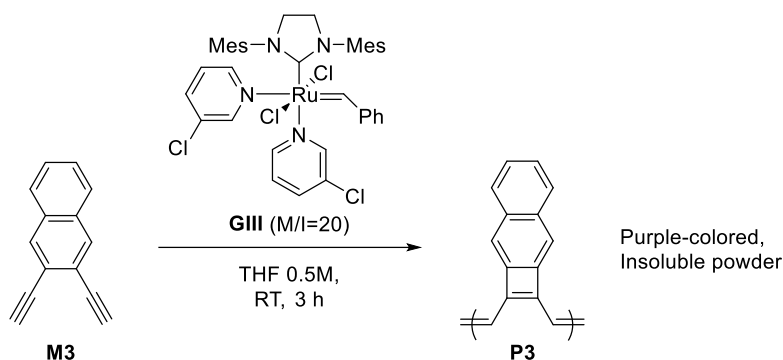
Scheme 5.2 (a) CP of Si-containing 1,5-hexadiynes and (b) Purpose of this work

5.3 Results and Discussion

As our initial attempt, a linear and un-substituted 1,5-hexadiyne **M1** was treated with **HGII**, in the monomer-to-initiator ratio (M/I) of 20 (Scheme 5.3). After 24 h reaction, about 50% of **M1** was converted to give purple-colored powder in 35% yield, but it was insoluble in common organic solvents. However, UV-Vis absorption at 472 nm implied that a conjugated polymer was generated. We also tested CP of a phenyl-containing **M2** in similar reaction condition but obtained a purple-colored insoluble powder, which made us difficult to conduct further characterizations (Scheme 5.3).



Scheme 5.3 Initial results for CP of **M1** and **M2** using **HGII**



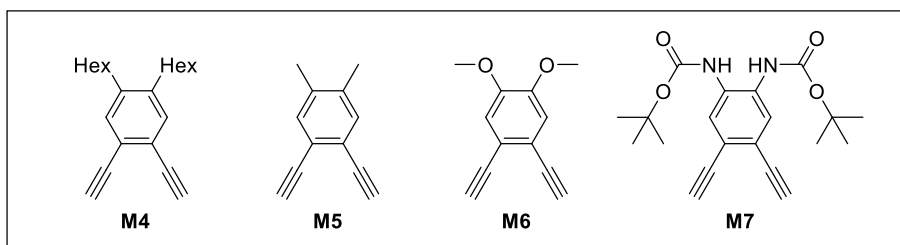
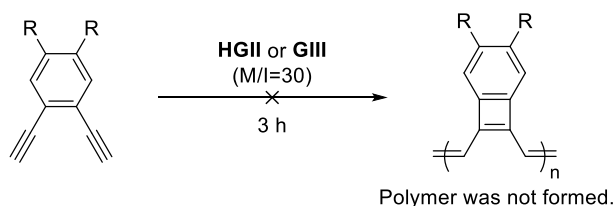
Scheme 5.4 Initial result for CP of **M3** using **GIII**

We prepared another monomer **M3**, a naphthalene derivative, but this monomer showed no reactivity toward **HGII**. Instead, with the treatment of more reactive **GIII**, the color of the reaction mixture turned to purple rapidly, generating an insoluble **P3** (Scheme 5.4).

To improve the solubility of the resulting polymers, we designed several phenyl-type monomers (**M4–M7**). Regarding the literature about the acceleration of metathesis reaction by electron-withdrawing groups on the aryl group of Ru benzylidene,⁷ we planned to differentiate the electronic properties of the aryl substituent. First, the reactivity of **M4** containing dihexyl substituents was examined under the optimized condition for CP of 1,6-heptadiynes (**GIII**, THF solvent), but very low conversion was observed regardless of the reaction concentration (Table 5.1, entries 1 and 2). Change of the solvent to DCM, with used of 3,5-dichloropyridine additives, didn't improve the polymerization efficiency, showing only 26% of conversion (entry 3). To apply a higher temperature, we employed thermal-stable **HGII**, and reaction at 70 °C resulted in an improved conversion in 0.5 M of THF (entry 4). However, the colors of the reaction mixtures from all entries were

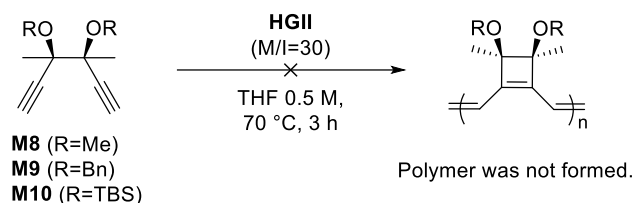
brown, which implied that no conjugated polymer was generated. Using the reaction condition in entry 4 as the optimized one, we tried CP of various tetra-substituted monomers, **M5–M7**, but could not get any promising results at all (0–39% conversion, entries 6–8). The low polymerization efficiencies can be attributed to the antiaromaticity, which presumably generates in the expected polymer structure, and this may reduce the favorable aromatic stabilization energy.⁸

Table 5.1 CP of phenyl monomers **M4–M7**



entry	monomer	catalyst	solvent	temp (°C)	conc. (M)	conv (%) ^a
1	M4	GIII	THF	RT	0.5	27
2	M4	GIII	THF	RT	0.05	33
3 ^a	M4	GIII	DCM	RT	0.5	26
4	M4	HGII	THF	70 °C	0.5	50
5	M4	HGII	THF	70 °C	0.05	23
6	M5	HGII	THF	70 °C	0.5	~0
7	M6	HGII	THF	70 °C	0.5	~0
8	M7	HGII	THF	70 °C	0.5	39

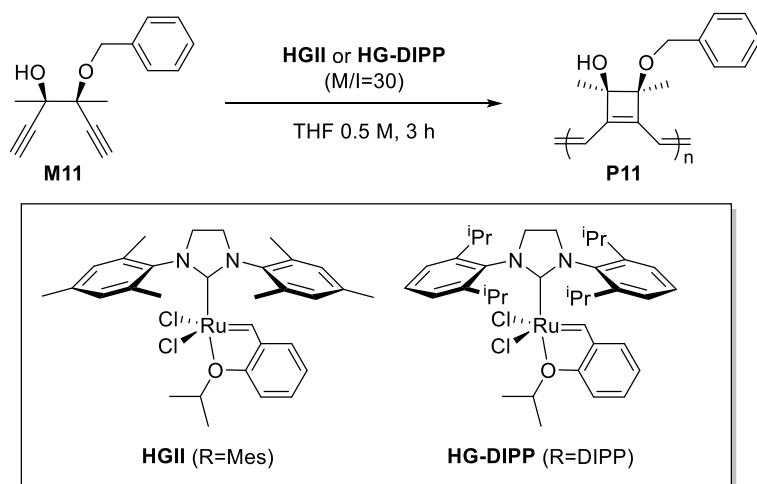
^aDetermined by ¹H NMR, ^b6 equiv of 3,5-Cl₂Py was used as an additive.



Scheme 5.5 Unsuccessful CP of tetra-substituted monomers M8–M10

Speculating that too much steric bulkiness on the side chains suppressed the polymerization, we prepared an analogous tetra-substituted monomer **M11**, which contains one benzyl substituent (its stereochemistry is thought to be (*3R,4S*) or (*3S,4R*), because the synthesis was starting from *meso* compound). This less-substitution was expected to facilitate the catalyst approach to monomers. As depicted in Table 5.2, a reaction of **M11** with HGII at 70 °C resulted in 25% conversion, but the reddish-purple color of the reaction mixture indicated the formation of the conjugated polyene (entry 1). Lowering the reaction temperature from 70 to 50 °C led to a slight improvement on the conversion (entry 2, 35%), which was still not efficient. Taking a lesson from the results of Chapter 4, where introducing a sterically bulkier 2,6-diisopropylphenyl (DIPP) group on the NHC ligand helped to improve the reaction efficiency by faster initiation of the Ru catalyst, we employed a new catalyst, HG-DIPP, in this system. Although the 70 °C reaction didn't give rise to any better result, a trial at 50 °C, to our delight, resulted in 54% conversion of **M11**, which was the highest value so far (entries 3 and 4). A Scale-up reaction in M/I 20, we could obtain the soluble polymer **P11** in a quantitative yield, with M_n of 2.0 kDa with a broad dispersity (entry 5).

Table 5.2 CP of M11 using Hoveyda–Grubbs catalysts



entry	catalyst	temp (°C)	conv (%) ^a	yield (%) ^b	M_n (kDa) ^c	\bar{D} ^c
1	HGII	70	25	nd	nd	nd
2	HGII	50	35	nd	nd	nd
3	HG-DIPP	70	29	nd	nd	nd
4	HG-DIPP	50	54	nd	nd	nd
5 ^d	HG-DIPP	50	71	70%	2.0	1.78

^aDetermined by ¹H NMR, ^bPrecipitated in hexane at -78 °C. ^cDetermined by THF SEC calibrated using polystyrene standards. ^dM/I=20.

The resulting polymer was characterized using ¹H NMR including broad polymeric signals (Figure 5.1a), and UV–Vis spectroscopy with λ_{max} of 632 nm, which showed a slight red-shift compared to the previous HGII case (627 nm, Figure 5.1b).

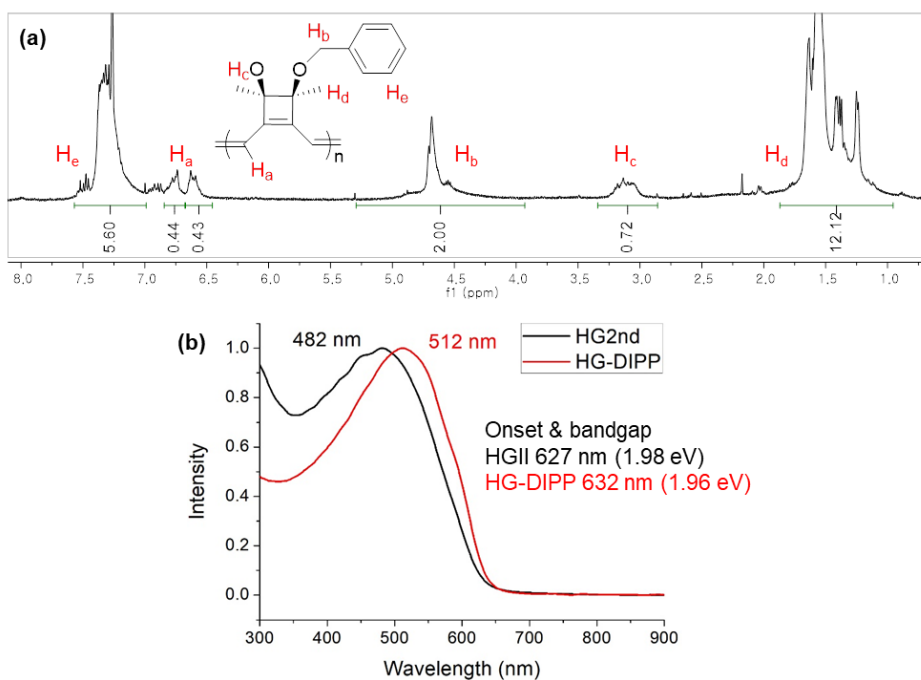
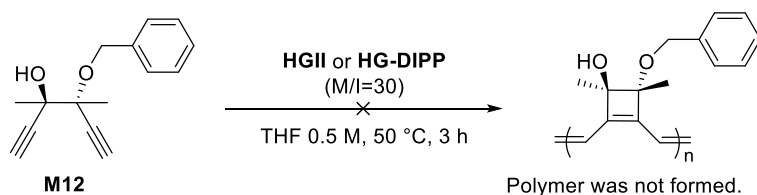


Figure 5.1 (a) ^1H NMR and (b) UV-Vis absorption spectra of P11

To broaden the monomer scope, we synthesized **M12** (an isomeric form of **M11**) and treated with HGII or HG-DIPP in the optimized condition. However, both reactions gave no conversion with any color change, but only brownish color appeared right after the addition of the catalyst solution, implying decomposition of the catalyst.



Scheme 5.6 CP of **M12** using Hoveyda-Grubbs catalysts

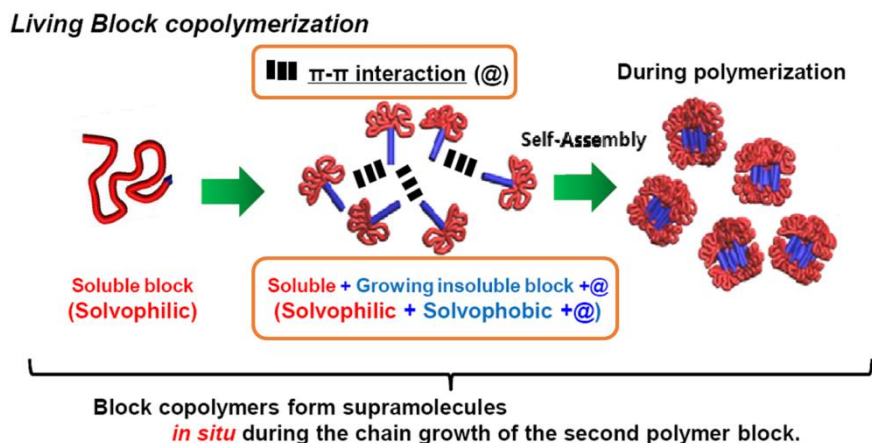
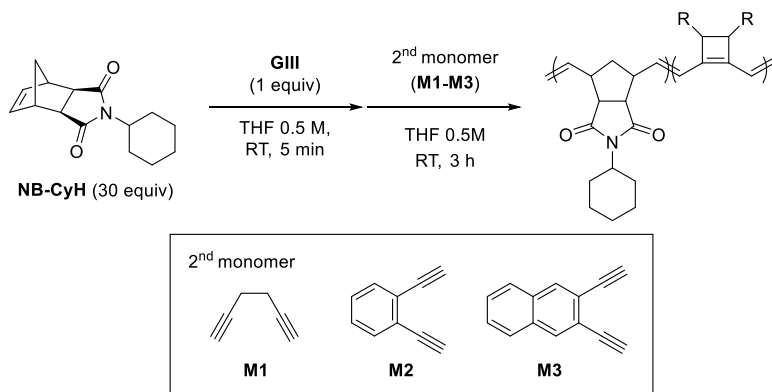


Figure 5.2 *In situ* nanoparticlization of conjugation polymers (INCP)

Using the poor solubility of P1–P3, we anticipated a possibility of *in situ* nanoparticlization of conjugation polymers (INCP), introducing the P1–P3 as the second block. INCP is one of the efficient methods for preparing nanostructures composed of block copolymers in solution without post-treatment (Figure 5.2),⁹ taking advantages of the strong $\pi - \pi$ interactions and insolubility of the conjugated polymer as the driving forces for self-assembly. Our group demonstrated the utility of this strategy, synthesizing the insoluble conjugated second block by living polymerization methods, such as ROMP,^{9–10} CP,^{1c} and catalyst-transfer polycondensation.^{11,12}

Since ROMP of NB derivatives using GIII is well-known to proceed in a living manner, we tried several diblock copolymerizations of a norbornene derivative (NB–CyH) as the first monomer, and M1–M3 as the second monomers (Table 5.3).

Table 5.3 Block copolymerization to induce INCP



entry	2 nd monomer	conv (%) ^a	yield (%) ^b	λ_{\max} (nm) ^c	E_g (eV) ^c	size (nm) ^d
1	M1 (30 equiv)	100, 10	72	416	2.14	nd
2	M2 (30 equiv)	100, 10	75	426	2.21	60.6
3	M2 (15 equiv)	100, 30	65	407	2.44	nd
4	M3 (15 equiv)	100, 53	79	490	2.13	nd

^aDetermined by ¹H NMR. ^bPrecipitated in methanol at -78 °C. ^cDetermined by UV-Vis spectroscopy. ^dDetermined by DLS in chloroform solution (0.1 mg/ml).

First, 30 equiv of **M1** was added as the second monomer after complete consumption of the same equivalent of NB-CyH, but ¹H NMR analysis revealed that the conversion of **M1** was only 10% (entry 1). The resulting polymer showed λ_{\max} of 416 nm in UV-Vis spectrum, but nanoparticle was not detected in dynamic light scattering (DLS) measurement. When the phenyl monomer **M2** was used, the resulting polymer showed red-shifted λ_{\max} and higher optical bandgap (E_g of 2.21 eV, entry 2) compared to the polymer obtained from entry 1 (Figure 5.3a). DLS analysis of this polymer implied that 61 nm of nanoparticle was formed (Figure 5.3b). TEM images of PNB-*b*-P2 suggested some particles with the corresponding size with DLS profile, but the conversion of **M2** seemed to be improved for more

accurate characterization (Figure 5.3b).

Lowering the equivalent of **M2** for the higher polymerization efficiency was not effective for the nanoparticlization, and the use of **M3** as the second monomer was also not successful (entries 3 and 4).

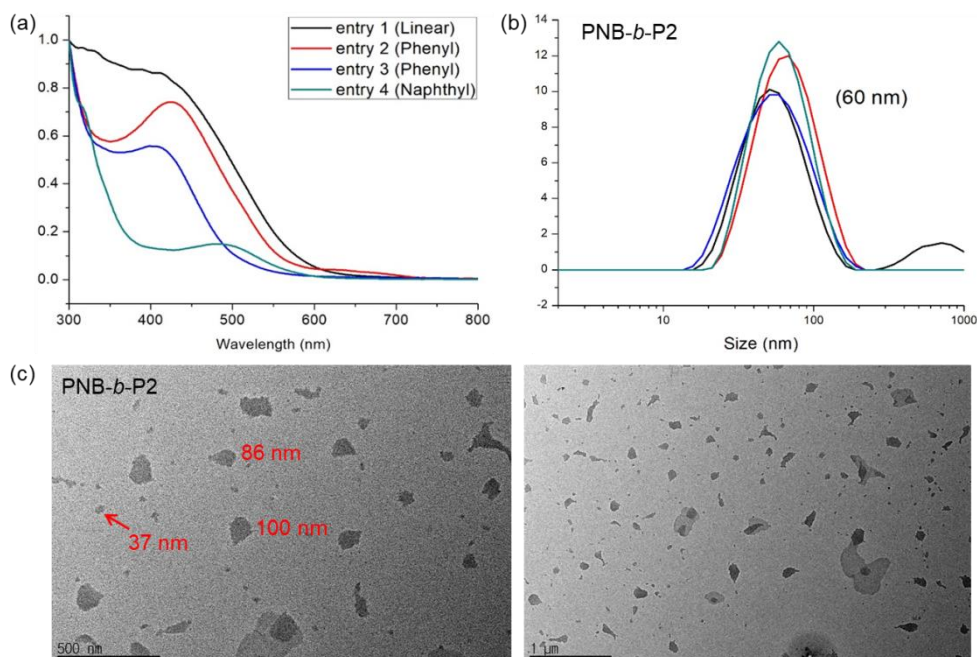


Figure 5.3 Results of the block copolymerization: (a) UV-Vis absorption spectra of the resulting polymers from entries 1–4, (b) DLS profiles and (c) TEM images of PNB-*b*-P2 from entry 2 in Table 5.3

5.4 Conclusion

In short, we have attempted to achieve CP of 1,5-hexadiyne derivatives using various Ru-based catalysts. Although we were not able to establish this system with broad monomer scope, because four-membered rings formation via olefin metathesis is hard to realize, a promising result was obtained with **M11** and **HG-DIPP** containing a sterically bulky NHC ligand. Through further research including the rational design of monomers and extensive optimization of the reaction condition, we will finally demonstrate an unprecedented, challenging CP for preparation of a new class of conjugated polyenes, containing four-membered rings as a repeat unit.

5.5 References

- (a) Kang, E.-H.; Lee, I. S.; Choi, T.-L., *J. Am. Chem. Soc.* **2011**, *133*, 11904; (b) Kang, E.-H.; Lee, I.-H.; Choi, T.-L., *ACS Macro Lett.* **2012**, *1*, 1098; (c) Kim, J.; Kang, E.-H.; Choi, T.-L., *ACS Macro Lett.* **2012**, *1*, 1090; (d) Kang, E.-H.; Choi, T.-L., *ACS Macro Lett.* **2013**, *2*, 780; (e) Kang, E.-H.; Yu, S. Y.; Lee, I. S.; Park, S. E.; Choi, T.-L., *J. Am. Chem. Soc.* **2014**, *136*, 10508; (f) Kang, C.; Kang, E.-H.; Choi, T.-L., *Macromolecules* **2017**, *50*, 3153.
- (a) Lee, I. S.; Kang, E.-H.; Park, H.; Choi, T.-L., *Chem. Sci.* **2012**, *3*, 761; (b) Park, H.; Lee, H. K.; Choi, T. L., *Polym. Chem.* **2013**, *4*, 4676; (c) Song, J.-A.; Park, S.; Kim, T.-S.; Choi, T.-L., *ACS Macro Lett.* **2014**, *3*, 795; (d) Park, H.; Lee, H.-K.; Kang, E.-H.; Choi, T.-L., *J. Polym. Sci. A* **2015**, *53*, 274.
- (a) Maughon, B. R.; Grubbs, R. H., *Macromolecules* **1997**, *30*, 3459; (b) Bielawski, C. W.; Grubbs, R. H., *Prog. Polym. Sci.* **2007**, *32*, 1.

4. Randall, M. L.; Tallarico, J. A.; Snapper, M. L., *J. Am. Chem. Soc.* **1995**, *117*, 9610.
5. (a) Zuercher, W. J.; Hashimoto, M.; Grubbs, R. H., *J. Am. Chem. Soc.* **1996**, *118*, 6634; (b) Weatherhead, G. S.; Ford, J. G.; Alexanian, E. J.; Schrock, R. R.; Hoveyda, A. H., *J. Am. Chem. Soc.* **2000**, *122*, 1828; (c) Nicolaou, K. C.; Vega, J. A.; Vassilikogiannakis, G., *Angew. Chem., Int. Ed.* **2001**, *40*, 4441; (d) Mori, M.; Wakamatsu, H.; Tonogaki, K.; Fujita, R.; Kitamura, T.; Sato, Y., *J. Org. Chem.* **2005**, *70*, 1066.
6. Debleds, O.; Campagne, J.-M., *J. Am. Chem. Soc.* **2008**, *130*, 1562.
7. (a) Adlhart, C.; Hinderling, C.; Baumann, H.; Chen, P., *J. Am. Chem. Soc.* **2000**, *122*, 8204; (b) Park, H.; Kang, E.-H.; Müller, L.; Choi, T.-L., *J. Am. Chem. Soc.* **2016**, *138*, 2244.
8. (a) Jin, Z.; Teo, Y. C.; Zulaybar, N. G.; Smith, M. D.; Xia, Y., *J. Am. Chem. Soc.* **2017**, *139*, 1806; (b) Jin, Z.; Teo, Y. C.; Teat, S. J.; Xia, Y., *J. Am. Chem. Soc.* **2017**, *139*, 15933.
9. Yoon, K.-Y.; Lee, I.-H.; Kim, K. O.; Jang, J.; Lee, E.; Choi, T.-L., *J. Am. Chem. Soc.* **2012**, *134*, 14291.
10. (a) Shin, S.; Yoon, K.-Y.; Choi, T.-L., *Macromolecules* **2015**, *48*, 1390; (b) Yoon, K.-Y.; Shin, S.; Kim, Y.-J.; Kim, I.; Lee, E.; Choi, T.-L., *Macromol. Rapid Commun.* **2015**, *36*, 1069; (c) Shin, S.; Gu, M.-L.; Yu, C.-Y.; Jeon, J.; Lee, E.; Choi, T.-L., *J. Am. Chem. Soc.* **2018**, *140*, 475.
11. Lee, I.-H.; Amaladass, P.; Yoon, K.-Y.; Shin, S.; Kim, Y.-J.; Kim, I.; Lee, E.; Choi, T.-L., *J. Am. Chem. Soc.* **2013**, *135*, 17695.
12. Lee, I.-H.; Amaladass, P.; Choi, T.-L., *Chem. Commun.* **2014**, *50*, 7945.

국문 초록

올레핀 복분해 반응을 기반으로 하는 다이아인의 고리화 중합반응은 사이클로알킨 반복 단위를 포함하는 공액 고분자를 손쉽게 합성할 수 있는 방법 중 하나이다. 이 반응에서 전이금속 촉매는 단량체의 알카인에 대해 α (알파) 혹은 β (베타) 방식의 두 가지 배향으로 접근이 가능하다. 고리화 중합 반응에 관해 진행된 다양한 연구결과로부터 루테튬 기반의 올레핀 복분해 촉매, 특히 그럽스 촉매는 위 반응을 알파 방식만으로 매개함이 알려져 있다. 하지만, 이러한 강한 위치선택성을 이해하기 위한 직관적인 모델은 아직까지 보고된 바 없다. 본 논문에서는 루테튬 기반의 올레핀 복분해 촉매의 위치선택성을 결정하는 요소들에 관한 포괄적인 탐구를 통해 1,6-헵타다이아인의 베타 선택적인 고리화 중합반응을 달성한 과정 및 결과를 소개하고자 한다.

제 1장에서는 올레핀 복분해 반응 및 고리화 중합반응의 유용성 및 역사를 소개하고, 루테튬 기반의 올레핀 복분해 촉매 하의 고리화 중합반응에 대한 기존 연구 결과를 살펴본다.

제 2장에서는 그럽스 Z -선택적 촉매를 이용해 베타 선택적인 고리화 중합반응에 성공한 루테튬 시스템에서의 첫 예시를 보고한다. 이 촉매를 이용하여 1,6-헵타다이아인 유도체의 고리화 중합반응에서 육각 고리를 주요한 반복 단위로 갖는 공액 고분자를 합성하였다. 고리단합 엔아인 복분해 반응을 기반으로 한 예시 연구로부터, 이러한 특이한 위치선택성에 대한 입체화학적 모델 제시하였다.

제 3장에서는 루테튬 기반의 다이싸이올레이트 촉매를 활용하여 보다 많은 단량체 종류 및 향상된 반응성과 함께, 완벽하게 베타 선택적인 고리화 중합반응에 성공한 연구를 서술한다. 친전자성 피셔 카빈 모델에 기반한 개념 이론을 이용하여 고리화 중합반응에서 관찰된 위치선택성의 근원을 밝히고, 나아가 약한 배위 결합을 할 수 있는 리간드를 첨가제로 활용한 경우 활성 촉매의 안정성이 증가하여 중합 효율 역시 높아진다는 점을 알아냈다.

제 4장에서는 루테튬 다이싸이올레이트 촉매 하의 리빙 및 베타 선택적인 고리화 중합반응을 달성한 결과를 소개한다. 단량체 혹은 촉매 구조의 입체 효과의 합리적인 변화를 통해 조절된 분자량과 좁은 분포도를 갖는 폴리아세틸렌을 합성할 수 있었다. 또한, 이러한 리빙 중합 특성을 이용해 이중 및 삼중 블록 공중합체를 성공적으로 합성하였다. 활성 촉매의 카빈을 관찰하여 다양한 결합 친화성을 보이는 피리딘 첨가제가 고리화 중합반응에 미치는 영향을 해석하였다.

제 5장에서는 사각 고리를 반복 단위로 포함하는 공액 고분자를 형성할 수 있는 1,5-헥사다이아인의 고리화 중합반응에 대한 연구를 설명한다. 다양한 종류의 단량체 및 촉매를 활용한 광범위한 실험을 통해 루테튬 촉매 시스템에서의 첫 번째 예시로서, 폴리아세틸렌의 주요 사슬에 사각 고리를 도입할 수 있었다.

주요어: 고리화 중합, 폴리아세틸렌, 그럽스 촉매, 루테튬 촉매, 위치선택적 고분자 중합, 리빙 중합

학번: 2013-20281